UMBILICAL ARTERIAL FLOW ANALYSIS TO DETERMINE AN INDEX OF PLACENTAL IMPEDANCE

ANDREW WILLIAM WRIGHT

B.Sc.(ELEC ENG)

Submitted to the University of Cape Town in partial fulfilment of the requirements for the degree of Master of Science in Medicine, Biomedical Engineering.

Supervisor: Dr. WL CAPPER

MARCH 1994

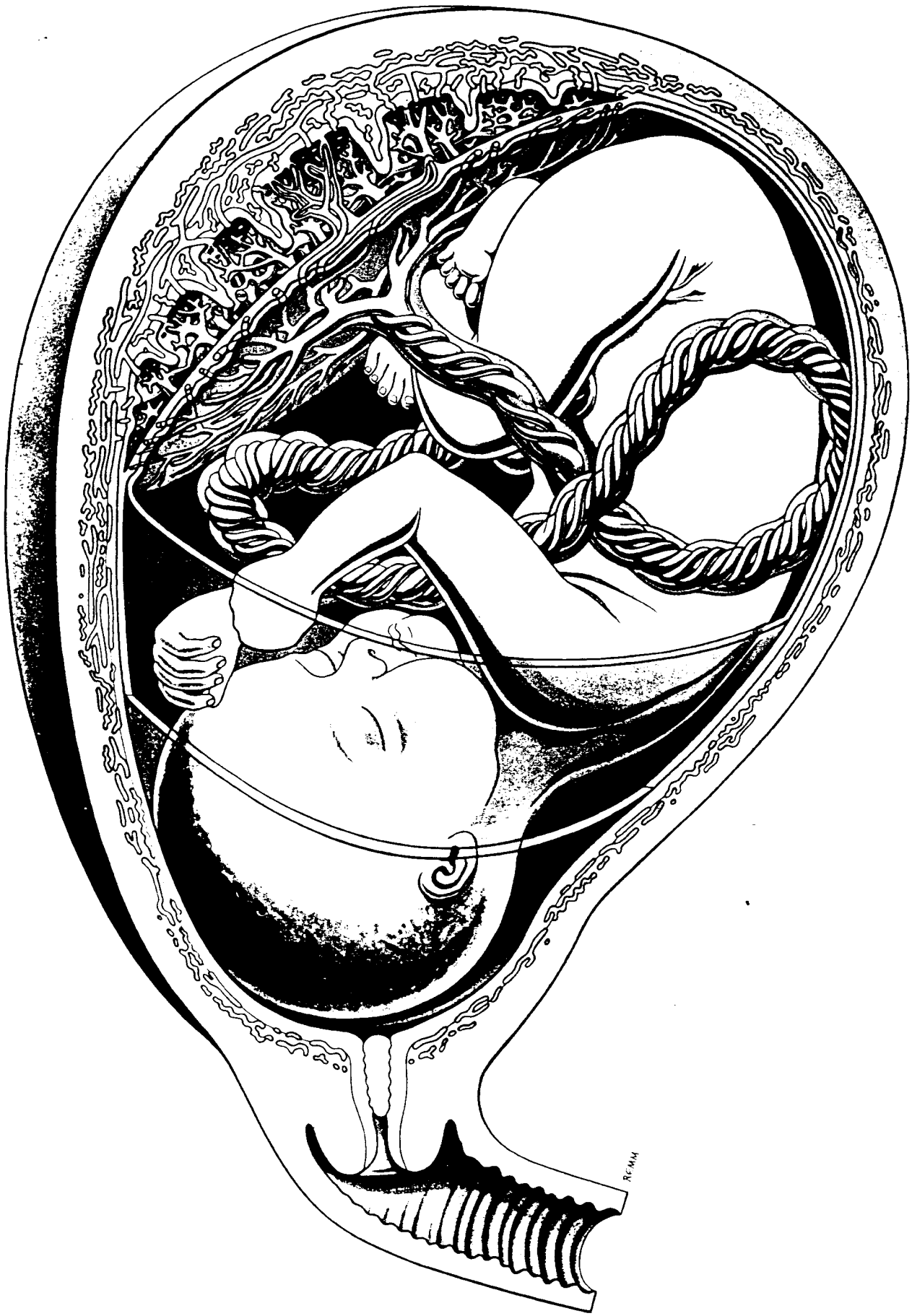

THE FOETOPLACENTAL UNIT

(Gray's Anatomy 1980, 36th Edition, Williams & Warwick, Churchill Livingstone, p132.)

SIGNED DECLARATION

I, ANDREW WILLIAM WRIGHT, declare that this dissertation is my own, unaided work. It is being submitted for the degree of Master of Science in Biomedical Engineering at the University of Cape Town. It has not been submitted before for any degree or examination at any other University.

Signed by candidate

ANDREW WILLIAM WRIGHT

17th MARCH 1994

ACKNOWLEDGEMENTS

I would sincerely like to thank Dr. Wayne Capper for his guidance and encouragement as my supervisor. I would also like to thank the staff of the Biomedical Engineering Department for the interest they have shown in the project.

I am also sincerely grateful for the input provided by the following people:

My father, Dr. Michael Wright, for his encouragement and insight regarding Obstetric theory.

Dr. H. Odendaal, Dr. K. Norman, Dr. A Szentkuti and Sister A. Theron for their support in the preliminary stages of the project.

Dr. H. Wainwright for her assistance with post-mortem experiments.

Professor F.X. Omlin for his advice on Histological matters.

Finally I would like to thank the South African Foundation for Research Development and the University of Cape Town for their financial support.

PRESENTATIONS AND PUBLICATIONS

Work from this thesis has already been published and further publications are under preparation. In addition, it has also been presented in both verbal and poster form at international conferences.

PUBLICATIONS

1) Szentkuti A., Capper W.L., Norman K., Wright A.W., Theron A., Odendaal H.

(Abstract) 1993.

The High Resistance State Index: A New Method of Rapid Assessment of Foetal Compromise in Absent Umbilical Artery Flow.

Journal of Maternal-Fetal Investigation, Vol 3 No.3 pp 177.

2) Capper W.L., Wright A.W., Szentkuti A., Norman K., Theron A., Odendaal H.

(Abstract) 1993.

The High Resistance State Index: Modelling High Placental Resistance and Absent End Diastolic Flow.

Journal of Maternal-Fetal Investigation, Vol 3 No.3 pp 177.

PRESENTATIONS

VERBAL

1) Szentkuti A., Capper W.L., Norman K., Wright A.W., Theron A., Odendaal H.

September 1993.

The high resistance state index: a new method of rapid assessment of foetal compromise in absent umbilical artery flow.

6th Congress of The International Perinatal Doppler Society. Rome.

2) Capper W.L., Wright A.W., Szentkuti A., Norman K., Theron A., Odendaal H.

September 1993.

The high resistance state index: modelling high placental resistance and absent end diastolic flow.

6th Congress of the International Perinatal Doppler Society. Rome.

POSTER

1) Wright A.W., Capper W.L., Szentkuti A.

April 1994.

Modelling the foetal circulation to simulate umbilical blood flow waveforms.

Medical Engineering and Computing in Sub-Saharan Africa. Somerset West, Cape Town, South Africa.

FUTURE PUBLICATIONS

1) Szentkuti A., Capper W.L., Norman K., Wright A.W., Theron A., Odendaal H.

To Submit in June 1994.

The high resistance state index: a new method to assess foetal compromise in absent umbilical arterial flow.

2) Wright A.W., Capper W.L., Szentkuti A.

To submit in June 1994.

Modelling the umbilical arterial flow waveforms to test a new index of placental resistance.

ABSTRACT

INTRODUCTION

Umbilical flow velocity waveforms (FVW's) can be measured non-invasively using Doppler ultrasound. Changes in the FVW's occur long before the warning signs from other conventional monitoring methods. Correct interpretation of the changes in the FVW has the potential of providing the clinician with an early warning of foetal distress. A number of indices have been described in the literature to characterise the FVW including the Pulsatility Index (PI), the Resistance Index (RI) and more recently, the High Resistance State Index (HRSI). Researchers have shown a dependence of the FVW, and thus the indices which describe it, on factors such as the placental resistance (Muijsers et al 1990a) blood pressure pulsatility (Mulders et al 1986), and the foetal heart rate (Downing et al 1991). In order to model the foetal circulation, the dimensions of the foetal vessels were required. These were taken from the literature when available, but had to be supplemented by measurements on post mortem specimens. This information, together with blood pressures and flow rates taken from the literature, was used to design electrical analogous models of the foetal arterial circulation (model 1 and model 2), which were implemented using PSpice, which is an electronic circuit simulator package. The Flow Velocity Waveforms (FVWs) simulated were stored and then analyzed using MATLAB, which is a mathematical package to calculate the waveform indices and both the blood pressure and percentage blood flow to the different anatomical regions of the foetus. Model 1 is

a simple model of the umbilical placental unit only, which assumes a rectified sine wave with a D.C. offset as an input waveform while Model 2 is a distributed element model of the complete foetal arterial system, including a realistic representation of the foetal heart.

AIM

Simulations of the FVW were used to examine the effects of placental obliteration (raised placental resistance), placental size, foetal heart rate (FHR), blood pressure pulsatility (BPPI), mean blood pressure (BP), and site of measurement of the FVW along the umbilical artery and thus on the waveform indices which are used to describe it (RI, PI and HRSI).

RESULTS / DISCUSSION

The investigations using models 1 and 2 showed that the indices were significantly dependent on the placental resistance, the size of the placenta and the type of placental obliteration. Model 1 was also used to investigate the effect of FHR variations on the indices under the original assumption that the input waveform to the umbilical/placental unit was a rectified sinusoid offset by a constant voltage (D.C.) (Thompson and Trudinger 1990). The result obtained, that is, the FHR does not affect the indices (in particular the PI) needed further investigation because the assumption for the input waveform is not true under all conditions. For this reason the simulations were repeated using model 2, with the interesting result that there is a difference between short

term FHR variations and long term FHR variation. Short term FHR variations had a pronounced effect on the indices. The blood pressure pulsatility and the indices concerned varied by large amounts in this case, which indicated a link between the blood pressure pulsatility and all the indices. Long term FHR variations had an inconsistent but small effect on the blood pressure pulsatility and in turn had a small effect on the RI and PI. The mean blood pressure in these simulations decreased with increasing FHR which resulted in a pronounced increase in the HRSI which indicated the dependency of this index on the mean blood pressure rather than on the blood pressure pulsatility.

It was found that the HRSI is a good index of placental resistance and may be particularly useful in evaluating high placental resistance in cases of absent flow during diastole, since, in these cases it is only slightly affected by the FHR. A value of greater than 34 percent is the recommended HRSI value to indicate severe foetal distress.

The results also indicate that the FVW shape varies along the umbilical artery and is far more pulsatile at the aortic (proximal) end than the placental end. This is reflected in the indices which thus have worst case values at the placental end. It is thus recommended that, where possible, the indices are measured at the placental end of the umbilical artery.

A clinical study of the HRSI is concurrently in progress. A pilot study has been published (Szentkuti et al 1993), but since a complete statistical evaluation will not be possible until sufficient data has been accumulated, this study will not be included in this thesis.

GLOSSARY

Commonly used symbols and abbreviations in the design of the models are listed below.

A : mean flow (ml/min)

AA : aortic arch

A.C. : alternating current (amps)

AEDV : absent end diastolic velocity

AGA : appropriate for gestational age

BP : average blood pressure (mmHg)

bpm : beats per minute

BPPI : blood pressure pulsatility index

C : compliance of the arterial walls per unit length (cm^3sec^2/g)

|catecholamines| : catecholamine concentration (mM)

CTG : cardio-tocograph

D : diastolic minimum of flow velocity waveform (ml/min)

DA : ductus arteriosus

D.C. : direct current (amps)

DIST. : distributed obliteration

E : Young's modulus (g/sec^2cm)

Et : ejection time

FFT : fast fourier transform

FHR : foetal heart rate (bpm)

FVW : flow velocity waveform

h : arterial wall thickness (mm)

HRSI : High Resistance State Index

L : inertance of blood flow per unit length (g/cm^5)

l : arterial length (cm)

LA : left atrium

LTV : long term foetal heart rate variation

LV : left ventricle

M' : amplitude of flow with respect to the pressure gradient

M : amplitude of pressure gradient

m : number of lobules per lobe

n : number of lobes in the placenta

$|O_2|$: oxygen concentration (mM)

PA : pulmonary artery

PEt : post ejection time

PI : Pulsatility Index

PM : post mortem

PROG. : progressive obliteration

PV : pulmonary vein

ΔP : change in pressure (mmHg)

q : fractional placental obliteration

R : resistance to blood flow per unit length (g/cm^5sec)

r : arterial lumen radius (mm)

RA : right atrium

RDS : respiratory distress syndrome

Re : Reynold's number

RI : Resistance Index

RP : resistance profile

Rp : placental resistance (Ohms)

RV : right ventricle

Δr : change in radius (mm)

S : systolic maximum of flow velocity waveform (ml/min)

S/D : Systolic to Diastolic ratio

SGA : small for gestational age

STV : short term foetal heart rate variation

SV : stroke volume (ml)

Td : diastolic time (sec)

Ts : systolic time (sec)

U.A. : Umbilical artery

α : alpha is a dimensionless quantity describing the type of flow present in a tube

ϵ : phase lag of flow with respect to pressure gradient (deg)

ρ : density of blood (g/cm^3)

μ : viscosity of blood (g/cmsec)

Φ : phase of pressure gradient (rad)

ω : angular frequency (radians/sec)

σ : Poisson ratio

1 Poise = 1 g/cmsec

1 Dyne = 1 gcm/sec^2

1 $Dyne/cm^2$ = 0.1 N/m^2

1 mmHg = 133 N/m^2

AIMS OF THE THESIS

The aim of this thesis was to model the foetal umbilical placental circulation in the following stages:

1) reproduce the mathematical model (model 1) developed by Thompson and Trudinger (1990) which simulated the blood flow in the umbilical arteries and placenta.

2) develop a more complex mathematical model (model 2) to represent the foetal arterial and umbilical placental circulation. This model was based on the Thompson and Trudinger model.

3) use model 1 and model 2 to investigate the following effects on the foetal umbilical velocity waveform and the indices which describe it (in particular the resistance index, the pulsatility index and the high resistance state index were investigated):

a) placental resistance

b) placental size

c) type of placental obliteration

d) umbilical blood pressure pulsatility

e) mean umbilical blood pressure

f) foetal heart rate variation

4) use model 2 to investigate the effect of the site of measurement of the flow velocity waveform along the umbilical artery on the indices.

TABLE OF CONTENTS

CHAPTER TWELVE

LIST OF ILLUSTRATIONS

FIGURES

TABLES

CHAPTER ONE

INTRODUCTION

The foetus pumps its blood via the umbilical artery into the placenta where gaseous and nutrient exchange occurs with maternal blood. The maternal and foetal circulations are separated by membranes across which diffusion takes place.

Figure 1.1: A Photograph of the Umbilical Placental Unit

The foetus is totally dependent on a healthy placental circulation in order for it to oxygenate its blood, receive nutrients and

dispose of waste products. Certain pathological conditions can result in an increase in placental resistance and a decrease in placental blood flow which will threaten the life, or normal development, of the foetus. Timeous detection of the problem allows the clinician the option of delivering the baby in order to prevent further damage. Common signs of foetal compromise and abnormal foetal development include:

1: Abnormal foetal heart rate patterns which can be detected using a cardio-tocograph (CTG);

2: Small foetal size for gestational age as assessed using ultrasound imaging;

3: A reduction in the volume of amniotic fluid surrounding the foetus. For a normal (healthy) foetal circulation the fluid should increase in volume as the foetus excretes urine. Under unfavourable conditions this fluid does not increase in volume. This can be monitored using ultrasound imaging.

4: A decrease in placental blood flow which results in a reduction of the diastolic component of the umbilical arterial blood flow waveforms. These are measured using either pulsed or continuous wave Doppler ultrasound (Rochelson 1989). Normally, continuous forward blood flow exists in the Umbilical artery throughout the foetal cardiac

cycle and is depicted in a positive diastolic component in the FVW. Flow waveforms in abnormal situations can have periods of reduced, absent or even reversed diastolic flow. This is an indication of increased placental resistance and leads to foetal compromise. It is reported that there is a strong correlation between absent end diastolic velocity (AEDV) and an abnormal pregnancy (Johnstone et al 1988). McCowan et al (1987) and Muijsers et al (1990b) also report that a decrease in diastolic flow is related to increased placental resistance or a decrease in the number of patent small vessels in the placenta. The chances of the AEDV reverting back to positive end diastolic flow (EDV) is reported to be only 15% (Brar et al 1989). Thus only a small percentage of these cases have a good prognosis if left unattended. The improvement can be due to a late increase in the compliance of vessels; formation of a collateral circulation; regeneration of the vessels; or a relaxation of the vessels if they were in spasm. Enhancement of one of these states may increase the flow (Brar et al 1989), yet this has been shown to be unlikely.

AEDV, or even reverse flow during diastole , may lead the clinician to terminate the pregnancy as a matter of urgency. As a result monitoring the FVW is of great significance in monitoring foetal well being.

It has been shown that changes in the umbilical flow occur long before any changes can be detected on the CTG, foetal size or volume of amniotic fluid. Schulman et al (1989) report that foetal heart rate monitoring is an end stage test for foetal compromise. Correct interpretation of the changes in the FVW thus provides the clinician with an early warning of foetal distress.

To numerically describe the flow velocity waveform (FVW), clinicians often use the popular pulsatility index (PI) and resistance index (RI), which are defined according to critical points on the FVW (see Chapter 3.1). However, there is no exact mathematical relationship between RI, PI and placental resistance.

Placental embolization or obliteration (associated with increased resistance) was thus simulated using models of the blood flow in the umbilical arteries and placenta, to investigate the effect of increased placental resistance on the FVW. The effects of the FHR, size of the placenta, type of obliteration, mean blood pressure, blood pressure pulsatility and site of measurement of the FVW along the umbilical artery were also investigated. In addition, the models were used to investigate a new index for foetal assessment, that is the High Resistance State Index (HRSI), which incorporates information from the entire whole waveform.

The models were based on clinical and experimental data from the literature, but where data was unavailable, for example the

dimensions of the foetal arteries and their wall properties, simple investigations on post-mortem specimens were performed to obtain the necessary information. Other unknown parameters were estimated and formed part of the assumptions on which the models were based. These are described in chapters 5 and 11.

CHAPTER TWO

THE FOETAL CIRCULATION

This section presents the anatomy and physiology of a foetus in the detail required for the complex modelling the foetal circulation.

2.1 GENERAL DESCRIPTION

The thesis covered foetuses of gestational ages between 28 weeks and full term. The growth of the foetus is illustrated in figure 2.1, where foetal mass is related to gestational age.

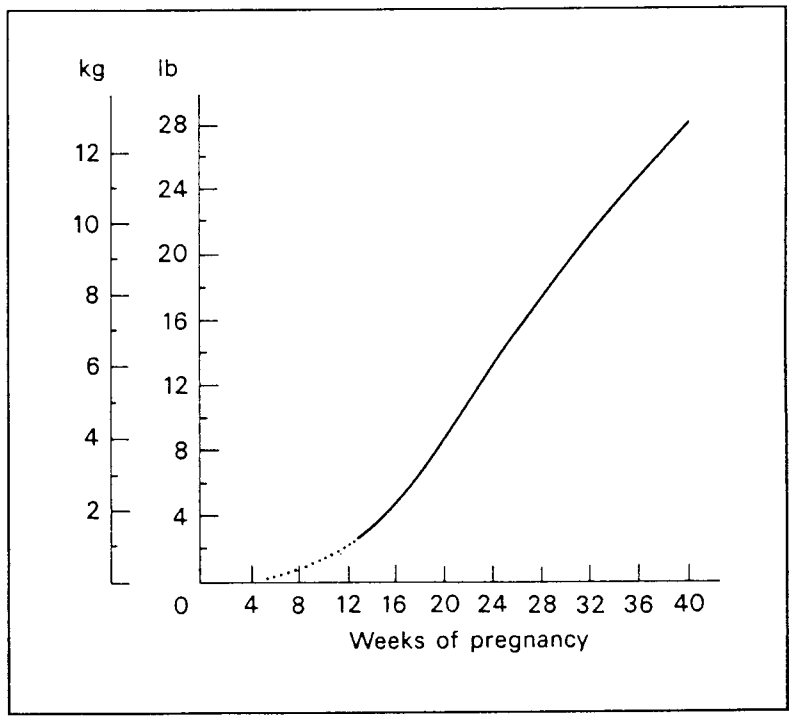

Figure 2.1: Foetal Mass vs Gestational Age (Hytten and Chamberlain 1991)

The major blood vessels in the foetus are the same as those in a small child, however the dimensions of these vessels differ from

the foetus to the young child. In addition a placental unit is present in the foetus resulting in a different circulation. Figure 2.2 illustrates the foetal circulation to be examined. Human foetus's and foetal sheep have very similar circulatory systems which have very similar response characteristics. Due to the lack of data on the human foetal circulation, certain data from the foetal sheep will have to be incorporated into the model of the human foetal arterial circulation. The discussion will thus include information on both to illustrate their similarities.

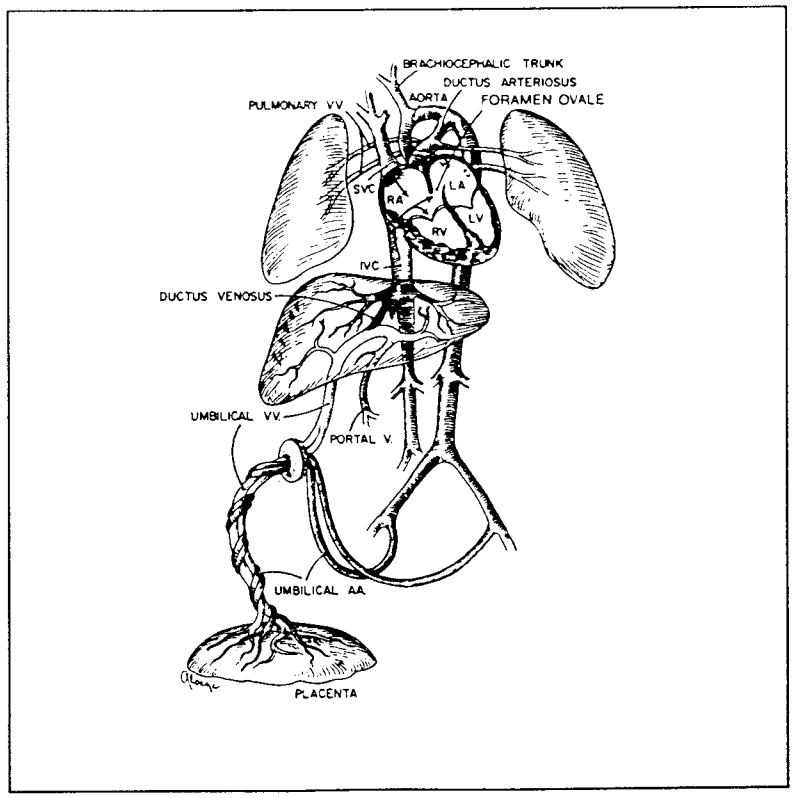

Figure 2.2: The Foetal Circulation (Veth 1976).

The heart of the foetus is also different in structure to a child, and thus has a different haemodynamic performance (figure 2.3).

Firstly the atria are joined by the FORAMEN OVALE. Blood flowing into the atria mix, resulting in equal distribution of the blood between the atria (Polin and Fox 1992). The two ventricles are as "two kernels of a nut" and are considered to act as two halves in parallel (Polin and Fox 1992). They contain the same volume of blood, have nearly identical ejection pressures, and have the same output (Dawes 1968, DeMulder et al 1984).

Figure 2.3: The Foetal Heart (Rudolph 1970a)

(RV - Right Ventricle
LV - Left Ventricle
RA - Right atrium
LA - Left atrium)

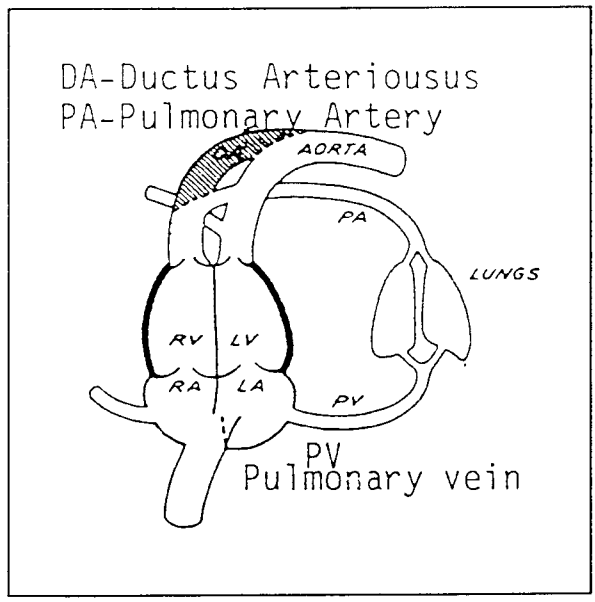

The pulmonary artery is joined to the aorta via the DUCTUS ARTERIOSUS. The lungs are not functional at this stage even though "foetal breathing" movements do occur. The ventricles of the heart expel the same volume of blood, thus the blood which would normally travel to the lungs must now find an alternative route via the ductus arteriosus (DA). The flow rates in the pulmonary vein and the vena cava are also different. This requires the foramen ovale to evenly distribute the blood between the atria and, consequently,

the ventricles (Polin and Fox 1992).

2.2 THE FOETAL HEART

The anatomy of the foetal heart has been described in the previous section. The cardiac output of the foetal heart is simply the product of the stroke volume and the heart rate. The normal range of heart rate is from 120 to 160 bpm (Thompson and Trudinger 1990). The values of cardiac output reported in the literature for foetal sheep vary between 200 and 500 ml/min/kg foetal weight (Assali et al 1968, Dawes 1968, Makowski et al 1968 and Rudolph et al 1970b). Polin and Fox (1992) state that the approximate cardiac output in human foetuses is 450 ml/min/kg, which is much the same as in foetal sheep.

The stroke volume is maintained at a constant value for normal ranges of FHR in a developing foetus (Goodlin et al 1972, Koos et al 1987, Beard and Nathanielz 1976). Thus the only way to vary the cardiac output is by varying the FHR (Polin and Fox 1992). The stroke volume is thus maintained at a value between 1.25 ml/kg and 4.2 ml/kg for a normal FHR of 120 to 160 bpm. There is however a reflex response which will reduce the stroke volume if the FHR goes out of the normal range. It has however been shown by Goodlin et al (1972) and Murata et al (1974) that for a newly born baby, the stroke volume is inversely proportional to the heart rate. This is different from the case in utero. This change in action occurs after birth.

Another important parameter in the mechanics of the foetal heart is the ejection time. It has been reported that the systolic time interval (ejection time) remains constant and the diastolic interval changes as the FHR is varied in foetal sheep (Veth 1976, Downing et al 1991, Thompson 1987). The diastolic interval is thus inversely proportional to the heart rate. A mean ejection time of 180 msec is quoted in the literature and will be used in further calculations (figure 2.4).

With specific reference to this thesis, the three major contributors to the action of the foetal heart were the stroke volume, the heart rate and the ejection time and have thus been described in detail.

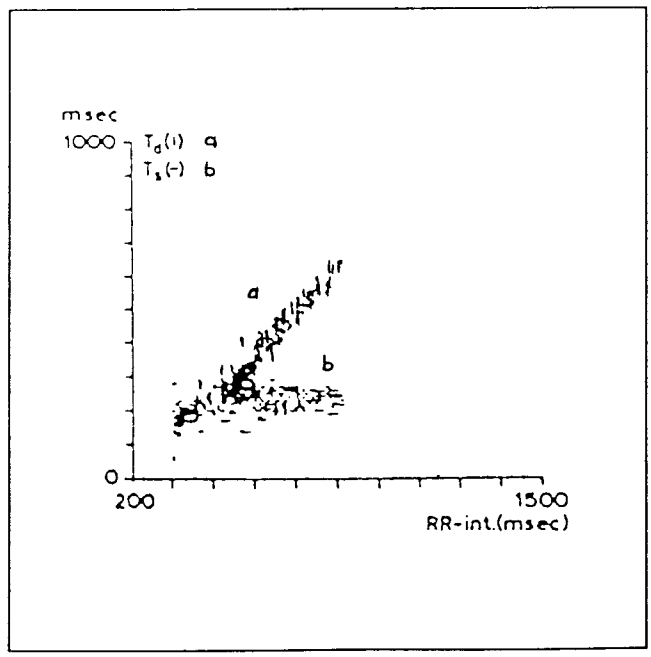

Figure 2.4: Systolic and Diastolic Time Intervals in Two Foetal Sheep (Veth 1976)

Td = Diastolic time

Ts = Systolic Time

2.3 BLOOD PRESSURE AND FHR RESPONSES UNDER NORMAL CONDITIONS

Blood pressure is determined by the stroke volume, the heart rate and the peripheral resistance. In the foetus the stroke volume is constant for normal values of FHR (120 to 160 bpm) and thus does not play a role in controlling blood pressure.

$$BP = SV * FHR * PR \quad (1)$$

where BP = Blood Pressure

SV = Stroke Volume

FHR = Foetal Heart Rate

PR = Peripheral Resistance

The control of the mean blood pressure is initiated by the baro and chemo reflexes which are fully developed in the foetus by the 3rd trimester (Veth 1976). The chemoreflex is considered more important than the baroreflex in cardiovascular regulation (Polin and Fox 1992).

The baroreceptors are located in the carotid sinus and the aortic arch, the same location as that of the chemoreceptors. The chemoreceptors responsible for controlling the foetal circulation are present in the aortic arch. They are probably the only ones operative in the foetus as the chemoreceptors in the carotid sinus are responsible for respiratory regulation (Dawes et al 1969a,b).

The baroreflex is prominent in controlling the FHR, and thus the blood pressure indirectly. The baroreflex causes changes in the FHR, the total peripheral resistance and the ventricular contractility in order to maintain a constant blood pressure. This reflex response acts via sympathetic and parasympathetic activity.

With respect to neural control, the foetal mean arterial pressure depends on the degree of change in the foetal vascular resistance (Muijsers et al 1993, Adamson et al 1989). The peripheral resistance of the foetal carcass (except the placenta as it is not innervated) is thus a control mechanism for blood pressure. The autonomic nervous system is actively involved in controlling the peripheral resistance and is thus also actively involved in controlling the blood pressure. Veth (1976) reports that the parasympathetic nervous system is capable of exerting significant control and that this control increases as the foetus approaches full term. Veth (1976) also states that alpha and beta adrenergic control of the resting heart rate and peripheral circulation is present in early foetal life and increases as the foetus reaches maturity. This however involves hormonal control which has a far slower action than neural control.

The peripheral bed is also able to regulate the blood pressure and the percentage blood flow distribution to itself. This auto regulation is dependent on the metabolic activity and blood flow requirements and is independent of the autonomic nervous system.

The autoregulation mechanism will not be discussed in detail as it is not within the scope of this thesis. It will however be stated that this regulation acts within a longer time span than that for reflex responses. The auto regulation mechanism adjusts blood flow to specific organs with specific metabolic needs and is masked by any reflex response (Liedtke et al 1973, Sagawa et al 1975).

The blood pressure is thus dynamically controlled by the FHR and the peripheral resistances, via the baro and chemo reflexes.

2.4 THE UMBILICAL PLACENTAL UNIT

The umbilical cord consists of two umbilical arteries which spiral around the umbilical vein. The two arteries anastomose at the end of the cord (Thompson and Trudinger 1990, Creasy and Resnik 1989), before branching into the radial branches of the placenta. Literature reports that there are 5 of these arteries (Thompson and Trudinger 1990). The radial branches then branch into smaller arteries which make up the lobes before branching into the lobules or tertiary stem villi (figure 2.5). There are between 15 and 20 lobes in a human placenta and there are as many as 60 to 200 lobules per lobe (Creasy and Resnik 1989, Hibbard et al 1988, Thompson and Trudinger 1990).

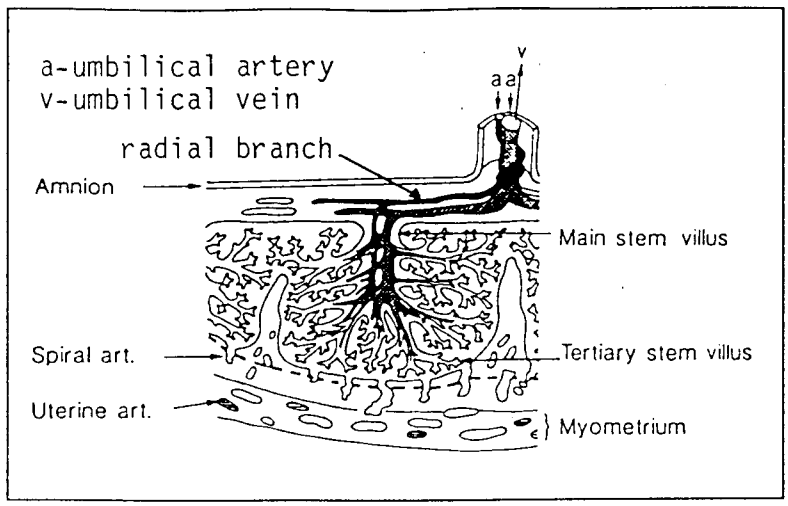

Figure 2.5: A Plan of the Placenta and Umbilical Arteries (Thompson and Trudinger 1990)

The umbilical cord is reported to be between 50 and 70 cm long (Thompson and Trudinger 1990, Danforth 1977, Hibbard 1988). The radial branches are reported to be 10 cm long; the primary and secondary stem villi (lobules) are 10cm long, and the tertiary stem villi (lobes) 1 cm long (Thompson and Trudinger 1990).

The umbilical arteries and the placental bed are not innervated and are thus not controlled by the foetal autonomic nervous system (Veth 1976). The umbilical arteries and larger arteries in the placental bed have been shown to be under hormonal control as they are sensitive to catecholamines (Adamson et al 1989, Dawes 1968, Howard et al 1987). Umbilical placental resistance can thus be varied by the action of hormones but are not under neural control.

The development of the normal foetoplacental circulation depends on the proliferation and maintenance of small vessels in the secondary and tertiary villi. As their numbers increase, so the placental resistance decreases and normal perfusion of the placenta is

maintained.

2.5 FLOW DATA

The umbilical arteries and placenta are not only functional as an exchange organ between mother and foetus, but are also active in the regulation of flow to the foetal organs. The placenta and umbilical arteries are seen as part of the periphery. Thus any change in their resistance or compliance will result in a change in the distribution of blood flow (Assali et al 1962).

Literature reports that normal umbilical blood flow in humans is between 30 and 40 percent of the cardiac output (Giles et al 1986, Polin and Fox 1992, Creasy and Resnik 1989). In sheep, the values range between 40 and 60 percent for an AGA foetus (Jensen et al 1992, Dawes 1968, Beard et al 1976, Rudolph et al 1970b, Jensen et al 1991, Trudinger et al 1987a). The value is greatly reduced to 21 percent for a SGA foetus (Trudinger et al 1987a). The umbilical flow is reported to vary between 100 and 145 ml/min/kg foetal weight in a human foetus (Ounsted 1973, Barnes 1968, Dawes 1968, Gill et al 1981, Trudinger et al 1987a). The umbilical flow in the foetal sheep is reported to be larger at 100 to 244 ml/min/kg foetal weight (Rudolph et al 1970b, Cohn et al 1980, Trudinger et al 1987a, Richardson 1992, Paulick et al 1991, Adamson et al 1992, Jensen et al 1992/1992).

If the mean umbilical flow is assumed to be 120 ml/min/kg, then for

a 36 week old 2.6 kg foetus, the mean umbilical flow will be 312 ml/min. If 40 percent of the cardiac output flows to the placenta, the cardiac output will be 780 ml/min. It has already been described that the cardiac output may vary between 200 and 500 ml/min/kg. Thus for a 2.6 kg foetus the cardiac output may vary between 520 and 1300 ml/min. A normal value of 120 ml/min/kg for umbilical arterial blood flow was thus assumed in this thesis.

The mean arterial blood pressure in human foetuses is reported to be approximately 50 to 53 mmHg (Hibbard 1988, Dawes 1968). In foetal sheep the mean arterial blood pressure is reported to be between 44 and 66 mmHg (Polin and Fox 1992, Beard et al 1976, Dawes 1968, Cohn et al 1980, Paulick et al 1991, Adamson et al 1992, Jensen et al 1991/1992). The mean blood pressure in the umbilical arteries is reported to be almost equal to the mean arterial pressure (Veth 1976) and will be assumed to be from 50 to 60 mmHg.

Thompson and Trudinger (1990) state that the physiologically realizable mean arterial blood pressures range between 30 mmHg and 90 mmHg which supports the assumption made.

2.6 THE FOETAL BLOOD FLOW WAVEFORM

A blood flow waveform can be detected using Doppler ultrasound by the 15th week. Any decrease in blood flow from this time on may indicate foetal distress and results in possible growth retardation.

The blood flow waveform is dependent on the resistance of the system into which the blood is pumped. For example, the greater the placental resistance, the less the blood flow to this area. The main contributors to the shape of the FVW are thus the peripheral outflow resistance, the cardiac pump, the condition of the arterial walls and the blood viscosity (Thompson 1987).

The blood flow waveform may be considered in two time periods, the systolic and the diastolic part. The systolic part (Ts) is defined as the period of time from the bottom of the steep upstroke of the flow waveform after a heart beat to the point where the waveform reaches its maximum value (systolic peak). The diastolic part (Td) is defined from the time from the systolic peak to the beginning of the next waveform (figure 2.6).

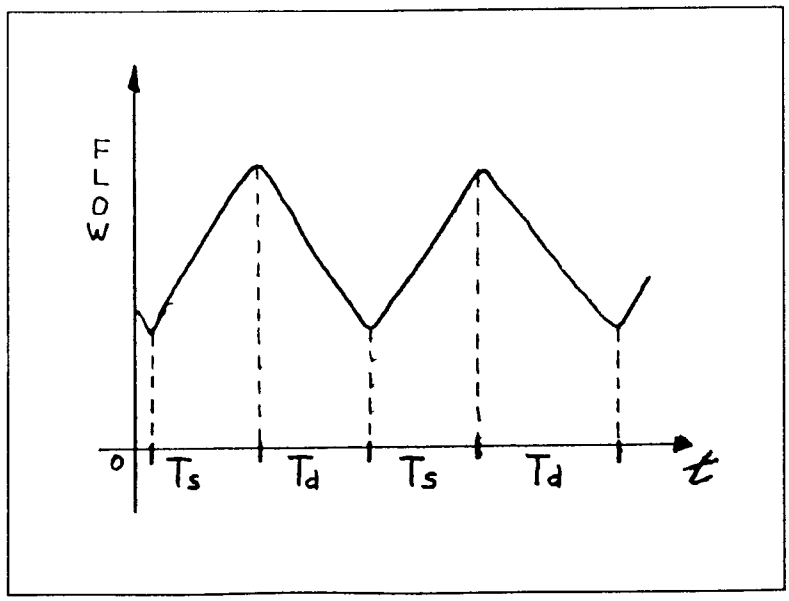

Figure 2.6: The Systolic and Diastolic Intervals of a FVW. (Ts AND Td)

An absence of flow at some stage during the diastolic cycle is a very important indicator of foetal distress or growth retardation.

The absent flow is a result of an increase in peripheral resistance which limits the flow of blood. The persistence of such a condition is a clear sign of foetal distress. Figure 2.7 illustrates the outcome of a pregnancy once absent flow had been persistent in the FVW.

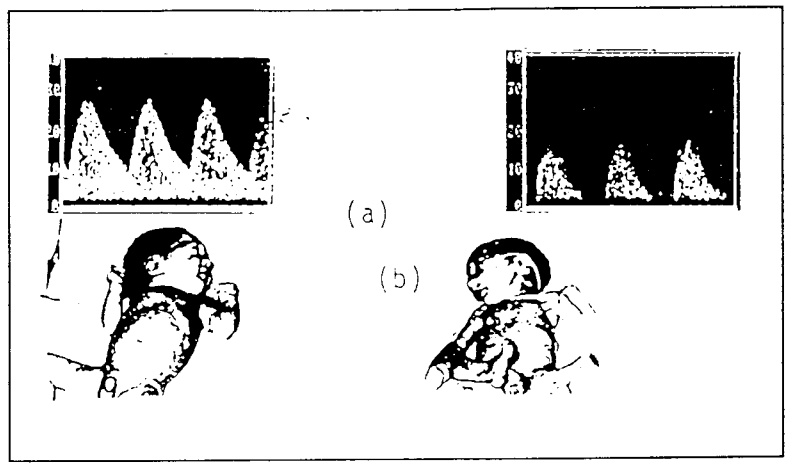

Figure 2.7: (a) A Normal Foetus (2200g) with a normal FVW; (b) A SGA Foetus (1600g) with Absent Flow in the FVW (Rochelson 1989)

As the foetus ages, so the placental resistance should decrease. This is because of the increase in the number and size of the arteries and arterioles supplying the placenta. Therefore, normally, one does not expect to find low or absent flow during end diastole as the foetus ages from 23 weeks on (figure 2.8).

Figure 2.8: Characteristics of the FVW at Different Gestational Ages (Trudinger et al 1987b)

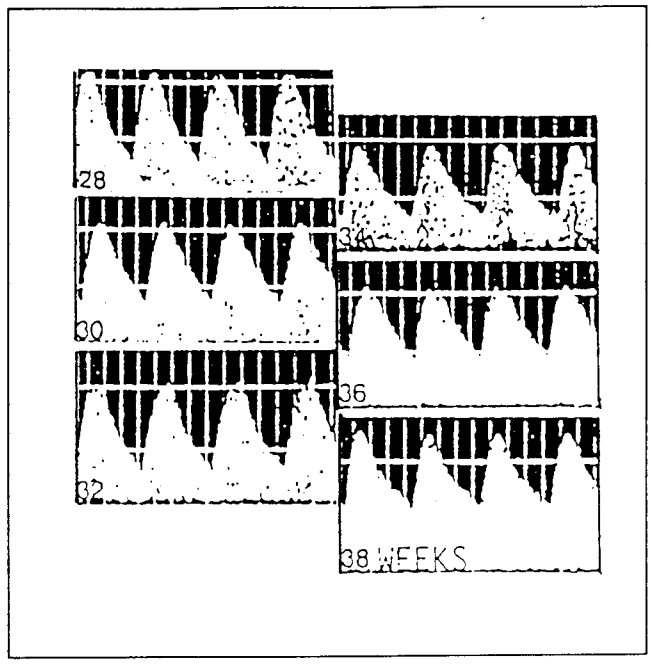

2.7 THE BLOOD FLOW DISTRIBUTION

The circulation was divided into 4 sections: the placenta; the upper carcass which included the brain, adrenals, lungs, heart and upper limbs; the aortic bleed offs, which included all the blood flow to the abdominal and thoracic viscera and finally the lower carcass, which included the lower limbs.

Table 2.1 represents the percentage blood flow distribution as a percentage of the cardiac output in foetal sheep. No references were found which gave the percentage distribution in humans.

Table 2.1: Percentage Blood Flow in Foetal Sheep

	RUDOLPH (1967)	JENSEN (1991)	RUDOLPH (1970b)
PLACENTA	41.2 %	44 %	42.2 %
UPPER CARCASS	28.3 %	34.8 %	30.7 %
LOWER CARCASS	19.9 %	13.8 %	15.9 %
AORTIC BLEED OFFS	10.8 %	8.8 %	11.3 %

2.8 HYPOXIA

The foetal circulation has been shown to be severely affected by hypoxia. Hypoxia in the foetus may be a result of maternal hypoxia, a reduction in umbilical blood flow or a restriction of uterine blood flow. Clinically this includes maternal lung disease, cord compression and severe uterine contractions during the second stage of labour (Jensen et al 1991,1992). The effect may be acute or chronic. Any form of hypoxia may be associated with an increase in placental resistance and will cause a change in foetal circulation and needs to be discussed as placental resistance is to be simulated in the models.

A brief summary of hypoxia is given in figure 2.9.

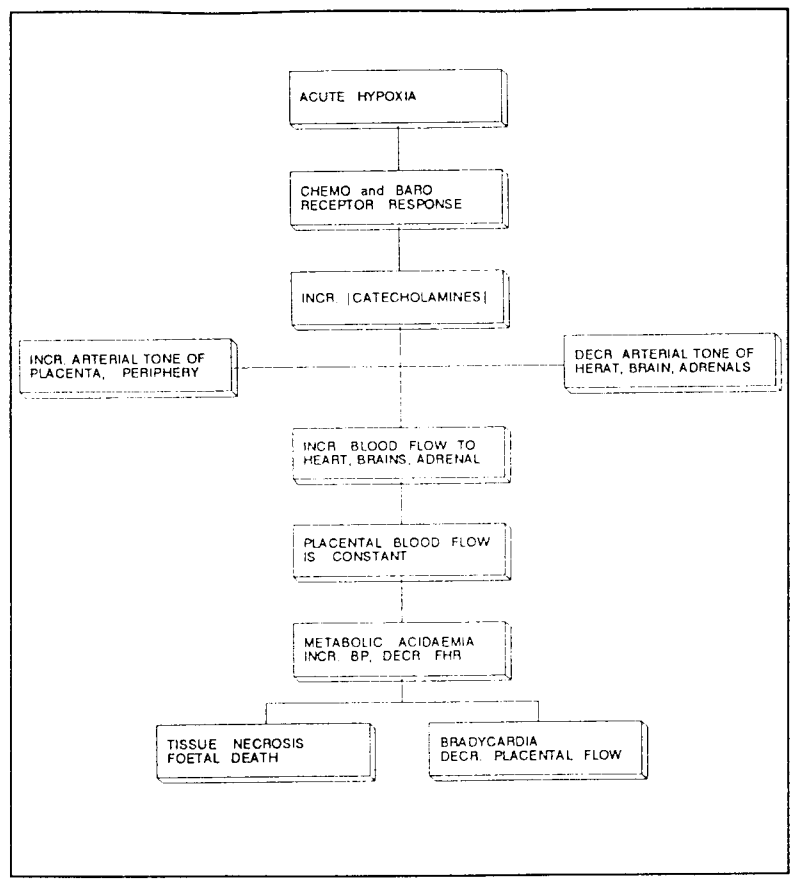

Figure 2.9: A Response to Foetal Hypoxia

2.8.1 ACUTE HYPOXIA

Acute hypoxia may be caused by cord compression, severe uterine contractions and abruptio placenta.

Acute forms of hypoxia have been reported to have little or inconsistent effects on the placenta (Muijsers et al 1990b).
Acute hypoxia causes a redistribution of blood in the foetus. The relative blood flow to the brain, heart and adrenals increase and that to the rest of the carcass decreases (figure 2.10). The blood flow to the placenta remains constant. Kunzel (1986) reported that this redistribution is a result of the increased concentration of catecholamines. In severe cases, foetal bradycardia and foetal

hypertension will result because of acidemia (Campbell et al 1991, Lampe et al 1988, Parer 1983).

It has been shown by Howard et al (1987) that an increase in catecholamine concentration causes foetoplacental vasoconstriction. (Catecholamine concentrations are greatest during severe hypoxia and are fairly low at mild degrees of hypoxia.) Pualick (1987) showed that with progressive deoxygenation, systolic and diastolic pressures as well as pulse pressure increases. They also found that there was no uniform reaction pattern of the basal FHR to progressive deoxygenation. Muijsers et al (1990a,b) showed a similar result. Catecholamines were reported to increase by large amounts which cause vasoconstriction. Thus the increase in blood pressure is a result of the increased placental vasoconstriction resulting from the action of the catecholamines (severe hypoxia). Koos et al (1987) found that changes in FHR only occur in cases of severe hypoxia. They also found that the increase in blood pressure because of hypoxia, only occurs in severe cases where acidemia is produced. They attribute this to the increased circulating concentrations of vasopressin and catecholamines which are present in cases of severe hypoxia and acidemia. This is also reported by Purves et al (1966) and Veth (1976). Any redistribution of blood due to mild hypoxia thus not affect the blood pressure or FHR as the circulating catecholamines are in low concentrations.

Conversely, under different experimental conditions, Pualick et al

(1987) reported that during severe hypoxia the foetal sheep was able to maintain its blood pressure with a falling FHR. The blood pressure is thus controlled by decreasing the FHR as the peripheral resistance increases under catecholamine action.

Both experiments are valuable in understanding the effects of catecholamines and hypoxia on blood pressure and the foetal circulation. FHR is also shown to have a major impact.

At a fixed FHR, it can be concluded that severe hypoxia causes an increase in placental resistance and an increase in blood pressure. This increase in blood pressure is directly related to the increase in placental resistance resulting in a maintained umbilical blood flow. Only in cases of severe acidemia does the FHR decrease in compensating for large increases in blood pressure. In this case the umbilical artery blood flow will be reduced.

A graphic representation of the blood flow re-distribution to the brain, heart and adrenals is given by Polin and Fox (1992). If one assumes that the ratio of blood flow distribution to the organs, not represented on the graph, remains the same as that given in table 2.1, one is able to calculate the respective decrease in blood flow to those organs.

2.8.2 CHRONIC HYPOXIA

Chronic hypoxia is induced by a number of conditions which result

in a persistent reduction in oxygen supply to the foetus. These conditions may include maternal hypertension and maternal lung disease. Chronic hypoxia results in a redistribution of blood and an increase in the hormone secretion as described in acute hypoxia (figure 2.10). The red cell mass increases and the oxygen consumption decreases (Kitanaka et al 1989, Alonso et al 1989). These authors report minimal changes in FHR during chronic hypoxia. Alonso et al (1989) however reported a 20 % increase in blood pressure where Kitanaka et al (1989) reported a constant blood pressure.

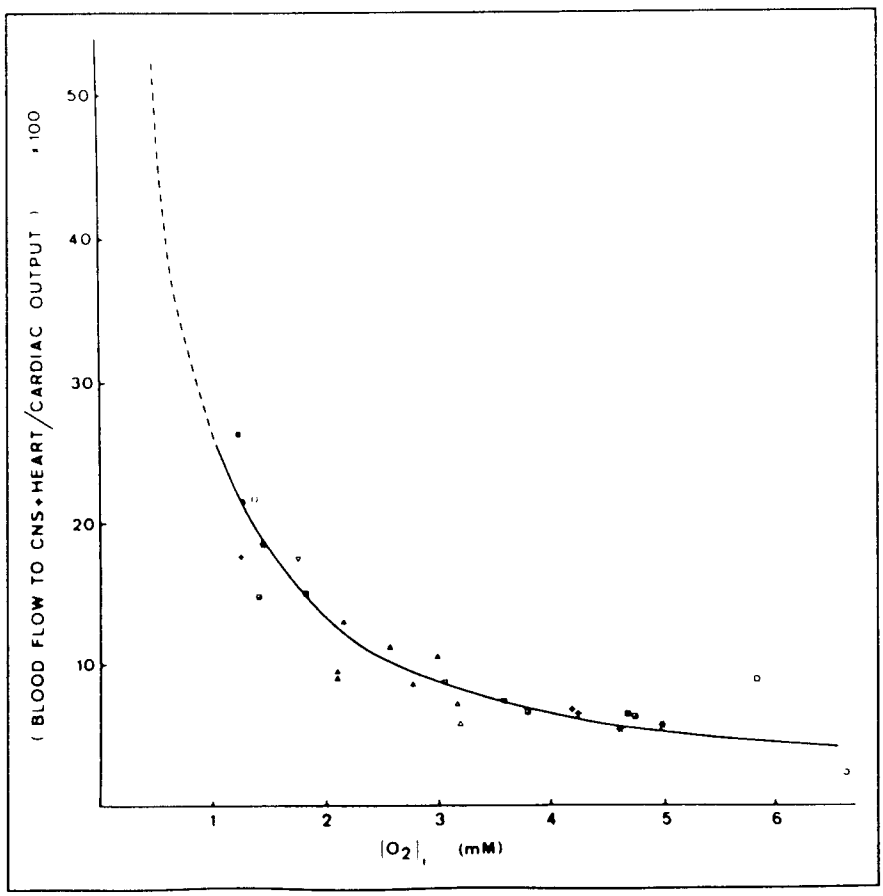

Figure 2.10: The Redistribution of Blood in the Foetus due to Hypoxia (Heart and Brain Percentage Blood Flow, Polin and Fox 1992)

The difference between acute and chronic hypoxia thus lies in the behaviour of the FHR and blood pressure as the foetus compensates or adjusts to the situation over a longer period of time. Chronic cases illustrate the ability of the foetus to adapt to any changes in resistance and blood pressure by adjusting the FHR.

Placental pathologies resulting in increased placental resistance will cause hypoxia. Simulating increased placental resistance thus requires an understanding of the responses to hypoxia in order to realistically simulate the umbilical artery blood flow waveform. For the purpose of modelling the foetal circulation, the effects of hypoxia thus provide valuable guidelines in the simulation of increased placental resistance.

CHAPTER THREE

COMMON INDICES USED TO DESCRIBE THE FVW SHAPE

3.1 THE RESISTANCE INDEX, THE PULSATILITY INDEX AND THE HRSI

Very primitive methods of analyzing the umbilical artery blood flow waveforms are commonly used. Different ratios have been devised in order to describe the blood flow waveform. Amongst these ratios are the 'Resistance index' (RI) and the 'Pulsatility index' (PI). The main indices used are described in figure 3.1 by their formulae. The points used are indicated on the waveform.

Since these ratios are empirical, there is no clear understanding about how differing conditions affect them.

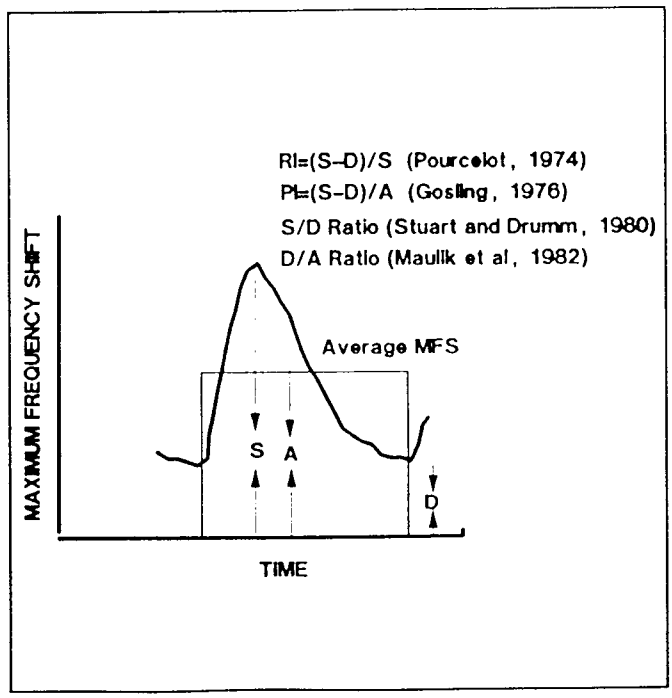

Figure 3.1: A Typical Normal FVW and the Indices which are Used to Describe it.(Maulik 1989)

S: maximum peak systolic velocity.

D: minimum end diastolic velocity.

mean (A): mean value of the waveform.

When absent flow is present for part of the flow waveform the RI=1.0 and this remains constant irrespective of the duration of absent flow. This in itself is an important factor as the length of absent flow is a critical indicator of the degree of foetal distress. The S/D ratio is infinite in absent flow and also remains constant irrespective of the duration of absent flow.

PI has a major drawback during absent flow, since as the peripheral resistance is further increased, the systolic peak decreases in amplitude, thus resulting in a decrease in PI. If the value of PI is considered in isolation, this worsening situation can result in a false sense of security since it is not reflected by the PI (Chudleigh and Pearce 1986). Furthermore, all these indices, except the PI which incorporates the mean, discard a great deal of potentially meaningful information, since they utilize only two points of the whole waveform (the maximum and the minimum).

As a result of these problems, clinical practice does not have well established guidelines regarding the management of the absent flow state. This controversy is well depicted in the book of Chudleigh and Pearce (1986).

The subject has however been tackled by Thompson and Trudinger (1990) and has been backed up by Stevens (1989). They investigated a simple mathematical and physical model of the placental circulation. They proceeded to test the well known and much used

PI, in an attempt to explain the relationship between the index magnitude and the placental resistance. Numerous clinical tests have also been done which investigate the indices in an attempt to quantify foetal distress. It has been shown that there is a positive correlation between elevated index magnitudes and increased placental resistance. The PI and RI thus have potential in indicating possible foetal distress.

An additional index has been formulated by Dr. Andras Szentkuti (Szentkuti et al 1993). Unlike the PI and RI, this index is a representation of the whole flow waveform and not just two or three critical points from the FVW. It is designed to be sensitive to reduced, absent and worsening cases of absent diastolic flow.

From the flow velocity waveform curve, a new curve called the Resistance Profile (RP) is generated by means of the function:

$$RP[t]=(S-X[t])/S \qquad (2)$$

This is based on the classic formula of the Resistance Index (figure 3.2).

X[t]=:value of the flow velocity waveform at any time t.

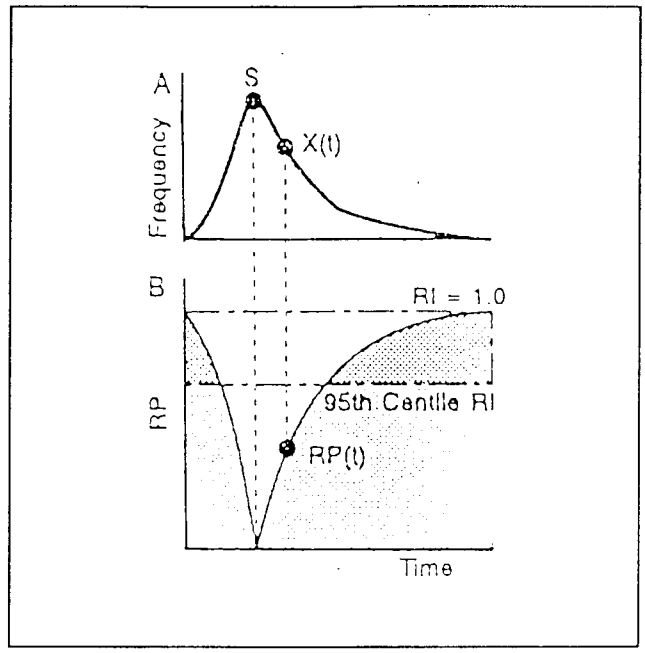

Figure 3.2: The Transformation from the FVW to the Resistance Profile (Szentkuti et al 1993)

The Resistance Profile, as with other indices, is independent of the insonating frequency and probe-vessel angle. It is equal to RI at the end of diastole, and zero at peak systole. The area under the RP curve, called Resistance Profile Area (RPA) is related to the degree of vascular resistance. For the quantification of the elevated resistance the rectangle above the 95th centile RI value and under the RI=1.0 line is chosen as the region of interest. The area under the RP curve that falls into this rectangle is expressed as the percentage of the rectangle area and is called the High Resistance State Index. In cases of reversed flow, the flow velocity magnitudes become negative and the function takes values exceeding 1.0. Therefore the HRSI might theoretically exceed 100%. Note that the HRSI utilizes each and every point of the waveform curve, and that the points are represented with the same weight. Therefore the waveform is comprehensively represented in the HRSI.

The value used to represent the 95th centile value is obtained from a graph of RI versus gestational age (figure 3.4). This was measured at Tygerberg hospital (Pattinson et al 1989). This graph is being used by the clinicians as a tool to assess whether the RI obtained from a given foetus is in the normal range for its gestational age.

The HRSI ratio has been implemented at Tygerberg Foetal Evaluation Clinic. However it is not being used for clinical evaluation as it has not been fully investigated.

3.2 THE EFFECT OF FHR ON THE INDICES

The normal range of FHR is between 120 and 160 bpm (Thompson and Trudinger 1990). This range of FHR needs to be considered when analyzing indices as it could have an effect on the measured index.

It has been reported that in a normal pregnancy, the placental resistance in late third trimester should not change. Thus any change in an index is due to the pulsatility of the blood pressure signal. This in turn implies a dependence on the FHR (Mulders et al 1986). Downing et al (1991) have shown the significant negative correlation between the PI, RI and S/D ratio and FHR. Newnham et al (1990) tested the S/D ratio and came to the same conclusions. Mulders et al (1986) reported that short term FHR variation effects on the PI are because of changes in blood pressure pulsatility.

The effects of factors such as foetal heart rate (FHR), blood pressure and placental resistance on the PI, RI and S/D ratio thus need to be investigated. It has been reported that FHR does affect these indices but can be ignored as the effect is not clinically relevant (Maulik et al 1989, Newnham et al 1990).

In the clinical setting the effect of FHR on PI is assumed to be negligible as long as the FHR remains in the normal range of 120 to 160 bpm (Newnham et al 1990, Low 1991, Thompson et al 1986).

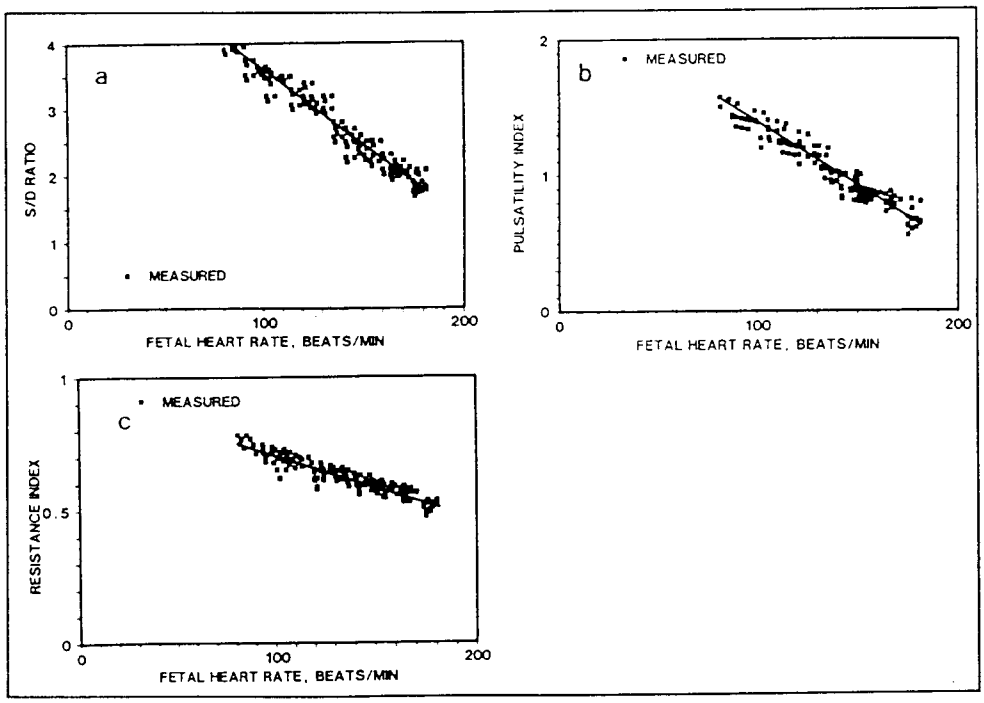

Figure 3.3: The Effect of FHR on the Indices which Describe the FVW (Downing et al 1991)

3.3 NORMAL REFERENCE VALUES FOR THE INDICES

Normal indices for RI, PI and S/D ratios were obtained by Pattinson et al (1991). RI was shown to have the lowest coefficient of variation and the least inter-observer variation. Thompson et al

(1986) found that the three indices gave the same amount of information and that only one needed to be calculated. It was thus concluded that because RI is related to the placental impedance and because it is the most sensitive, it would be the most useful index to use clinically.

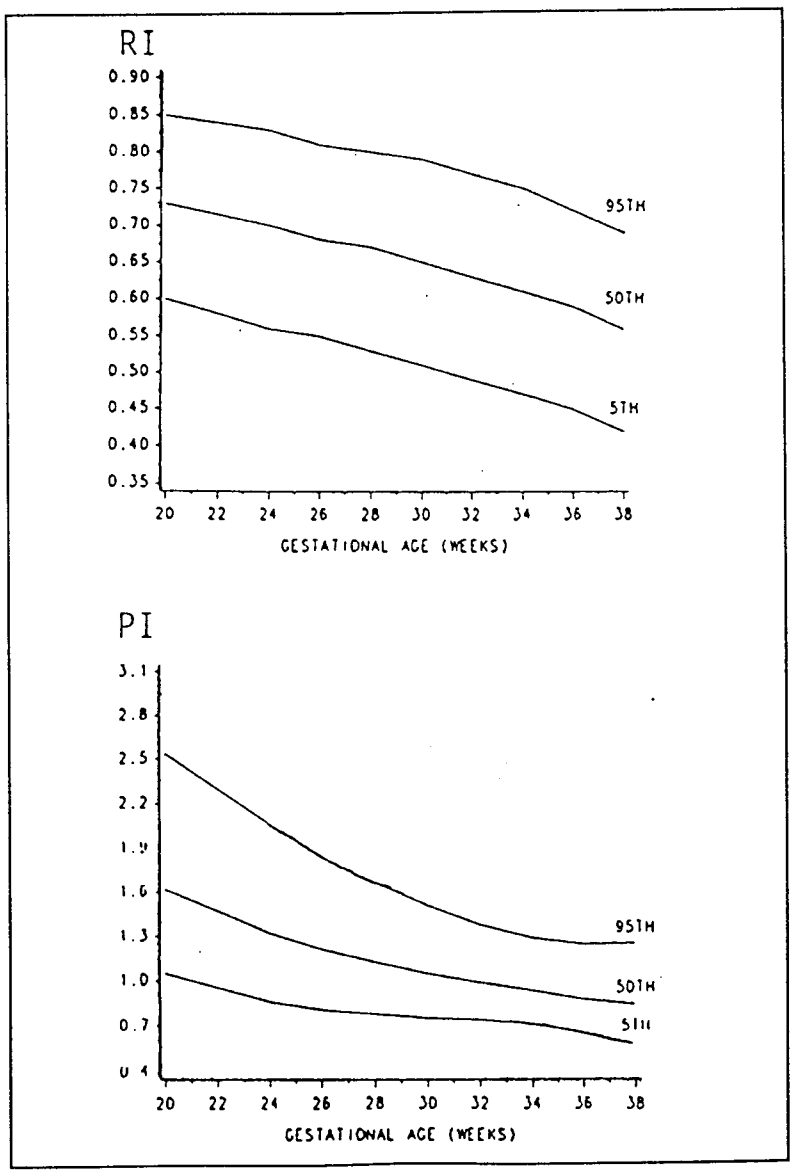

Figure 3.4: The Effect of Gestational Age on the Indices which Describe the FVW (Pattinson et al 1989)

Graphs of normal ranges of the RI and PI given in figure 3.04. They represent the 5th to the 95th centile values and may be used in clinical settings to indicate the status of the foetus.

3.4 THE BEHAVIOUR OF THE INDICES UNDER ABNORMAL CONDITIONS

The literature indicates that the indices are dependent on peripheral resistance. Muijsers et al (1990b) showed that in the case of mild foetal hypoxia, because of the redistribution of blood, the indices of peripheral blood flow change. The blood flow to the placenta did however not change, thus the umbilical flow indices did not change in his experiments. However, in severe cases of hypoxia (as described in section 2.8), it has been shown that the placental resistance is greatly elevated as a result of the action of catecholamines, resulting in a reduction of the umbilical blood flow (Downing et al 1991) (figure 3.5). As illustrated below, the indices will reflect this in their increase. Muijsers et al (1990b) also showed that the embolisation of the umbilical placental circulation resulted in an increase in placental resistance and thus a reduction of blood flow. The indices describing the blood flow to the placenta depict this in their increase (figure 3.6).

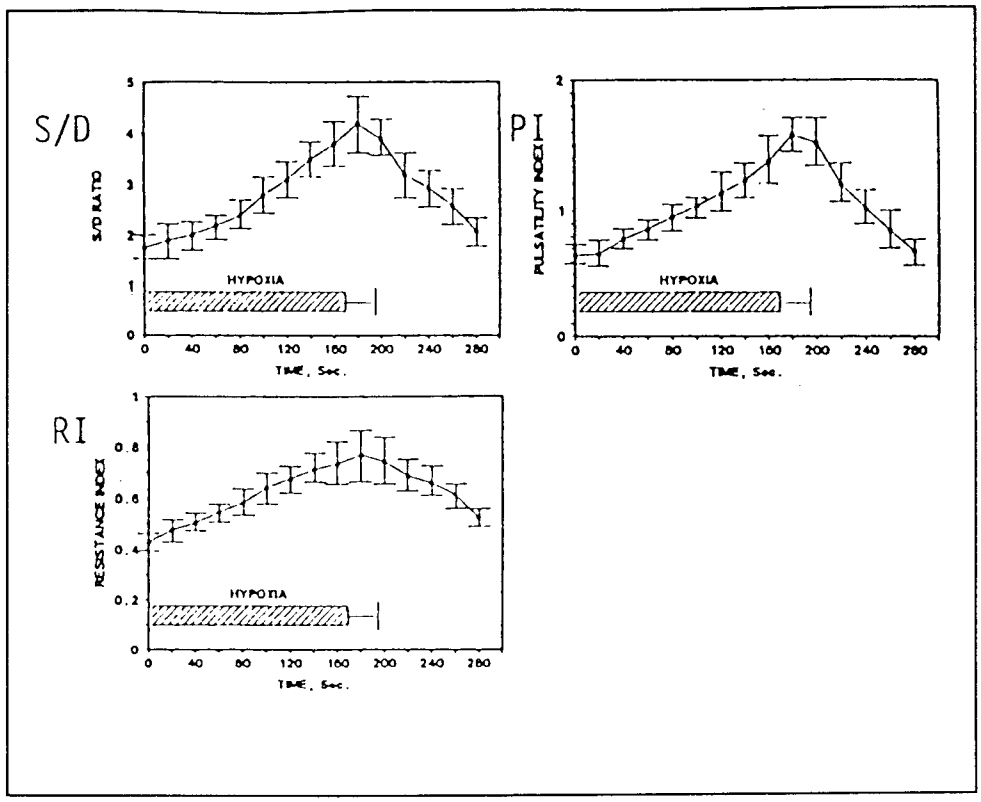

Figure 3.5: The Effect of Maternally Induced Hypoxia on the Indices used to Describe the Umbilical FVW. (Downing et al 1991)

Figure 3.6: The Relationship Between the PI and Placental Resistance (Muijsers et al 1991)

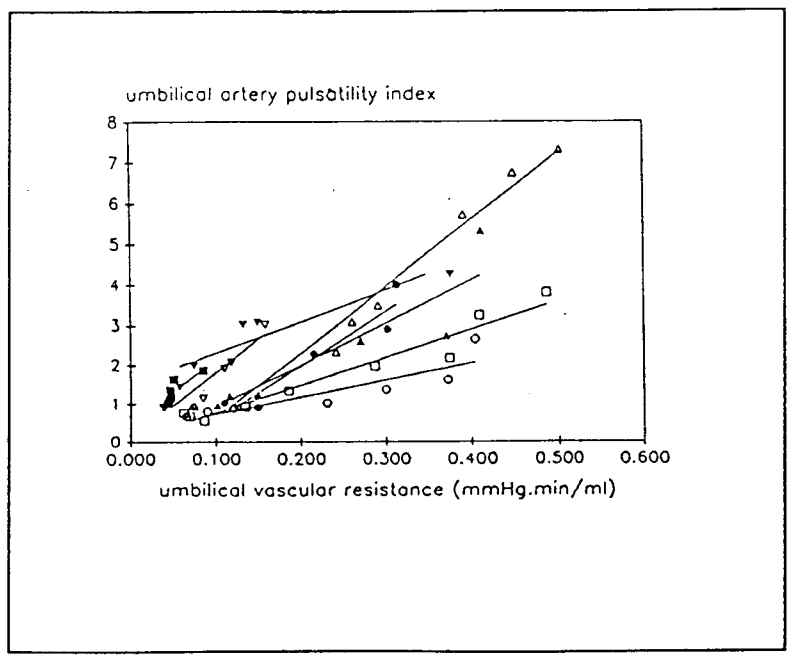

McCowan et al (1987) showed a highly significant negative relationship between the number of small arteries in the placenta and the PI (figure 3.7). As the number of arteries is inversely related to the placental resistance, the PI is positively related to the placental resistance. (The vessel count is done per microscopic field. Five fields from the mid zone are studied and averaged to give a single result. 25 fields per placenta are studied and averaged to give a single result.)

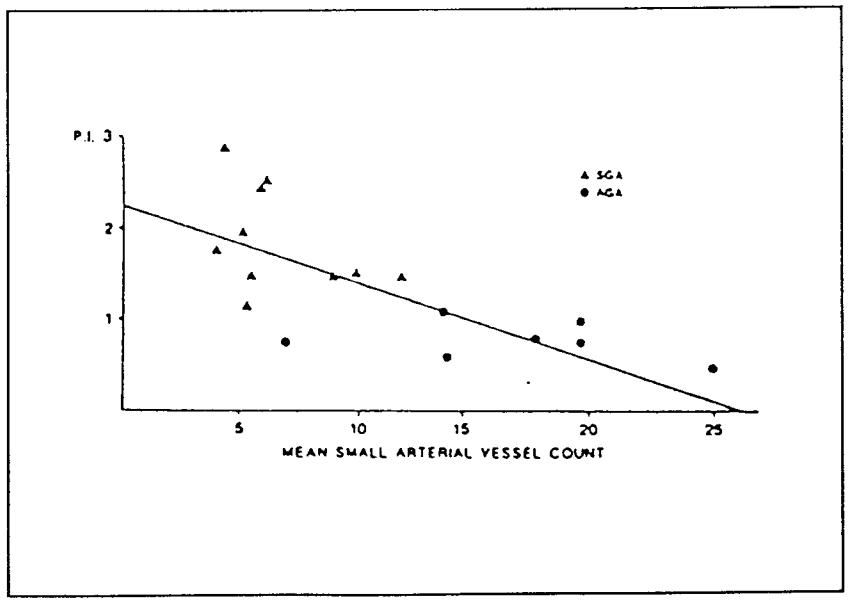

Figure 3.7: Umbilical Artery PI vs Small Vessel Count (McCowan et al 1987)

The reasons for elevated indices and the effect of FHR variations on the indices are to be investigated in this thesis.

CHAPTER FOUR

CLINICAL ASSESSMENT

4.1 INTRODUCTION

It is hoped that the results of this thesis will provide further insight into clinical assessment of foetal distress. Technical problems arise when trying to analyze the blood flow velocity waveform and will thus be described briefly to provide a basic background to clinical assessment.

One such problem is the high pass filter which is present on most commercial ultrasound machines. This filter considerably reduces the amplitudes of the lower frequencies to reduce the effects of vessel wall motion. These lower frequencies contain information on the end diastolic part of the blood flow velocity waveform. The filters range from 80 to 100 Hz. If an AEDV waveform is obtained using the 100 Hz filter, the filter should be reduced to 80 Hz to confirm the finding.

Another problem is that the velocity of the shifted signal is dependant on the angle of insonation. Ratios or indices describing the FVW thus need to be independent of the angle of insonation. This is due to the fact that the angle is not known when using continuous wave Doppler machines. Further complications lie in the site of measurement and the degree of foetal activity.

4.2 THE IMPORTANCE OF THE SITE OF RECORDING OF THE UMBILICAL FVW

The shape of the FVW is altered by the site of recording (Mehalek et al 1989) and changes in shape along the umbilical artery. AEDV's may be obtained at the aortic end of the umbilical artery and a normal FVW at the placental end (figure 4.1). Literature reports that the FVWs are more pulsatile at the aortic end of the umbilical artery. An average of five measurements should thus be collected from different sites along the umbilical artery to obtain an average value for the index. If it were possible to locate the placental end of the umbilical artery, this would be the best place to take the measurements. This is because the magnitudes correlate best with placental resistance at this site (Trudinger 1987b, Abromowicz et al 1989, Mehalek et al 1989).

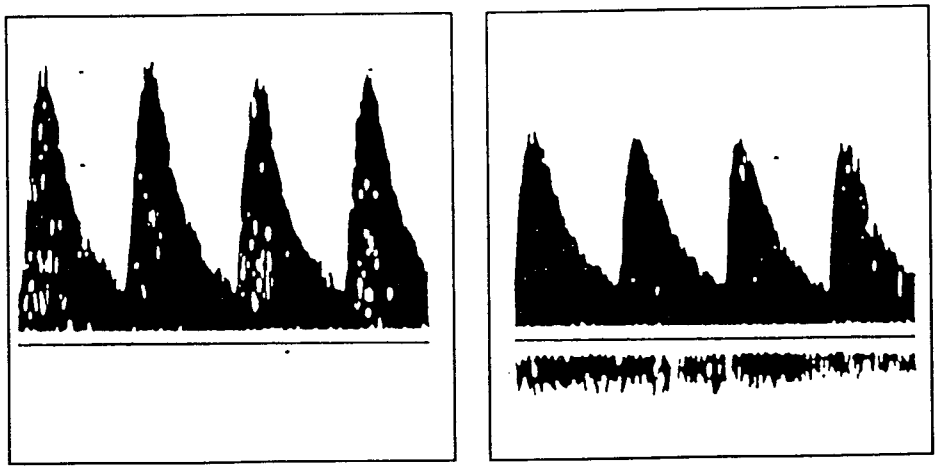

(a) (b)

Figure 4.1: Umbilical FVWs from the Aortic(a) and the Placental End(b) of the Umbilical Artery (Mehalek et al 1989)

The relevance of the recording site has been reported to decrease with gestational age and is minimized near late third trimester (Mehalek et al 1989). This was analyzed in the thesis.

As the umbilical arteries spiral their way around the umbilical vein, it may be possible for the FVW to include the signal from the umbilical vein if the flow is in the same direction. In this case the diastolic component will be shadowed and a false FVW will be present. To avoid this, a flow waveform for the vein must be present but must be represented in the opposite direction to ensure a true FVW (Trudinger 1987b).

The angle at which the reading is taken can have a significant effect on the waveform. It is thus essential that the waveform be read from different angles until the largest and clearest signal is obtained. A signal read at an angle close to 90 degrees will be of low magnitude. The thump filter present in the system will then further attenuate the signal and a non-representative signal will be obtained. Care should thus be taken to obtain the largest and clearest FVW.

4.3 THE EFFECT OF FOETAL MOVEMENTS AND ACTIVITY ON THE UMBILICAL FVW

It is very important that during recording of the FVW the foetus is motionless and not "breathing" (Trudinger 1987b, Mulders et al 1986, Newnham et al 1990). These will lead to fluctuations in the

amplitudes of the FVW as the umbilical artery is moved and intra abdominal pressures are changed. A constant venous signal is used to indicate when the foetus is motionless and not "breathing".

CHAPTER FIVE

POST MORTEM STUDIES

5.1 DISCUSSION

As a result of the lack of data on human foetal arterial dimensions, post mortem specimens of human foetuses were gathered from which the necessary data was measured. The post mortem specimens were gathered from the department of Anatomical Pathology. The foetuses were all delivered in Cape Provincial hospitals and were dissected by a consultant pathologist.

The foetuses all had fully developed hearts and major arterial vessels.

The data collected included :

a) the length of the aorta, ductus arteriosus and common iliac arteries.

b) the diameter of the aorta, ductus arteriosus and common iliac arteries.

c) the wall thickness of the aorta, ductus arteriosus and the common iliac arteries.

Figure 5.1 is a photograph of a typical specimen from which the readings were taken.

The lengths were measured using a vernier calliper. The aortic arch

was measured from the aortic valve to the insertion of the ductus arteriosus into the aorta. The aorta was measured from this point to the aortic bifurcation. The ductus arteriosus was measured from the pulmonary valve to the insertion of the ductus into the aorta. The common iliac artery was measured from the aortic bifurcation to the branch of the umbilical artery.

Figure 5.1: Post-Mortem Specimen

The internal diameters were calculated by measuring the circumference of the vessels. The diameters of the aorta and iliac arteries were measured at mid-length along the vessels. Normal diameters of the human foetal aortas for different gestational ages

are given by Chen et al (1988). The diameters measured were then scaled according to the ratio of the diameters reported by Chen et al (1988) to the diameters measured on the post mortem specimen. The difference between his results and the results obtained from the post-mortems are attributed to the fact that Chen et al (1988) measured the diameters in live foetuses with the aid of ultrasound. Our measurements were however taken from dead specimens which had been treated with 10% formalin which could explain the decrease or shrinkage in diameter.

The wall thicknesses were measured with the aid of a micro-meter screwgauge. The wall specimens were all taken from the mid-length position on the vessels.

No scaling of the lengths or wall thicknesses were possible as there were no reference values to use as guidelines. It is assumed that the length and wall thickness of an artery will not change much from the live to the dead specimen. Diameters are however felt to be dependent on the live or dead state of the specimen and it was thus advantageous to have reference values from which scaling could be done.

The data was collected to provide a guideline for the modelling of the foetal arteries. The birth weight of the foetuses were collected in order to give an idea of how normal the foetal dimensions were for that foetal age. The results from the foetuses

with approximately normal weights for gestational age were used, as the dimensions were assumed to be closely representative of that gestational age.

Table 5.1 illustrates the post mortem results.

Table 5.1: Post-Mortem Results.

PM	AGE	AORTA	ILIACS	AORTA	ILIACS	AORTA	ILIACS	AORT.C ARCH	DUCTUS	DUCTUS	DUCTUS
NUMBER	weeks	l	l	h	h	r	r	l	l	r	h
49	28	?	12	0.19	0.3	1.43	0.64	?	?	?	?
1	30	54	21	0.21	0.16	1.59	0.56	8	7	1.11-1.27	0.22
54	33	?	?	0.26	0.2	1.75	0.8	6	6	1.59	0.25
55	35	?	20	0.25	0.2	1.91	0.8-0.9	?	?	?	?
10	36	77	24	0.28	0.22	1.75	0.8-0.88	11	9	1.67	0.31
44	36	68	25	0.33	0.18	1.59	0.64	7	7	1.43	?
3	40	77	33	0.31	0.26	2.07	0.88	13	?	?	?
5	40	71	23	0.36	0.28	2.23	0.8	18	?	?	?
28	40	77	28	0.34	0.30	2.39	0.8	13	12	2.23	0.41
36	40	?	?	0.37	?	2.07	?	8	8	1.91	0.27
48	40	69	24	0.35	0.18	2.07	0.88	?	?	?	?
67	40	66	24	0.29	0.24	2.23	0.8	7	5	2.07	0.32
66	42	?	25	0.33	0.19	2.39	0.8	9	?	?	0.41

l = LENGTH (mm) r = RADIUS (mm) h = WALL THICKNESS (mm)

5.2 CONCLUSIONS

The results obtained from the post mortem studies were by no means a conclusive representation of the arterial dimensions. It is advised that a further study be conducted in which the dimensions

should be taken from living or recently deceased specimens in order to determine possible ranges of normal dimensions.

As a result of the lack of specimens and lack of time, this study could not be conducted in conjunction with this thesis. The assumptions made were thus based on the data which was available. The radii of all the major arteries were assumed to change in proportion with the change in radii of the aorta from a live to a dead specimen. The wall thickness was assumed to remain unchanged from a live to dead specimen as there was no data on its possible shrinkage. Histologically, there must be a change in its thickness but the change was probably very small. The lengths of the arteries were also assumed to remain unchanged.

For the purpose of this thesis, where an approximation to the foetal arterial circulation is being made, these assumptions have to be made.

CHAPTER SIX

THE EQUATIONS DESCRIBING THE MODEL PARAMETERS

6.1 DISCUSSION

Fluid flow in an elastic tube is described by the resistance to flow, the mass or inertance of the fluid and the compliance of the tube. In the case of this thesis, the tube was an artery and the fluid was blood.

If an electric analogous model is used, electrical resistance is analogous to the resistance to blood flow due to friction. This resistance is highly dependent on the shape or type of the blood flow. For example, plug flow and turbulent flow result in a high resistance whereas parabolic blood flow has a comparatively lower resistance (figure 6.1). The type of flow is dependent on the diameter of the lumen of the artery and the velocity of blood flow. High velocities and large lumens are responsible for turbulent flow.

Inductance is analogous to the inertance of the mass of the blood which is moving. The inertance of the fluid is also dependent on the shape or type of flow. The inertances of the arterial walls (transverse inertance) is not incorporated as it is far smaller than the fluid inertance.

The equations describing resistance (5) and inertance (6) are (McDonald 1974)

$$R=8\mu l/\pi r^4 \tag{5}$$

$$L=\rho lk/\pi r^2 \tag{6}$$

Where k = 1.35 for parabolic flow.

The equation describing resistance was derived from the Poiseulle equation which relates the flow rate between two points to the pressure difference between the two points. The equation describes steady laminar parabolic flow of a viscous fluid in a cylindrical tube. The inertance of the fluid was calculated from the definition of

$$L=MASS/AREA^2 \tag{7}$$

assuming a parabolic profile.

Figure 6.1: Flow Profiles (McDonald 1974)

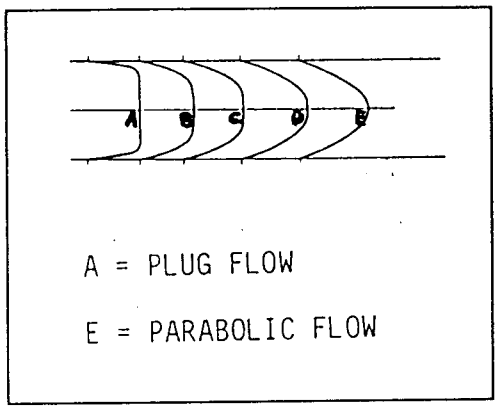

The volume compliance resulting from the expansion of the elastic arterial walls is represented by a capacitance. This is not dependent on the type of flow and only involves the physical properties of the arterial walls. The compression compliance of the fluid (blood) is negligible in comparison with wall compliance.

The compliance of the arterial walls was modelled by a capacitor in the electrical analogous design. The compliance of an artery is dependent on the radius of the lumen of the artery and the thickness and elasticity of the wall. The elasticity of the artery wall is described by the Young's modulus (E). The Young's Modulus was calculated according to equation 3.

$$E=\Delta P r^2/h\Delta r \qquad (3)$$

The magnitudes of the Young's modulus for different arteries are shown in Appendix I. Equation 4 describes the compliance of the artery wall

$$C=2\pi r^3 l(1-\sigma^2)/Eh \qquad (4)$$

(Thompson, Trudinger and Stevens 1990) (Appendix A). σ is the Poisson ratio and is dependent on the change in wall thickness as the length of the pipe or artery is varied. The maximum possible value for this ratio is 0.5 in the case of highly elastic materials and biological material. The ratio was thus set to 0.5 for arterial walls.

The electrical/fluid analogies are described in the following units:

1 mA = 1.33 cm^3/sec

1.33 V = 1330 $gsec^{-2}/cm$

R (Ohm) = R (g/cm^4sec)

C (Farad) = C (cm^4sec^2/g)

L (Henry) = L (g/cm^4)

CHAPTER SEVEN

TURBULENCE OF BLOOD FLOW IN THE FOETAL ARTERIES

7.1 REYNOLD'S NUMBERS

A Reynold's number is a number which is an indicator of the probability of turbulent flow. After careful measurements of the different kinds of flows possible in a tube, Osborne Reynolds (1842-1912) discovered that, in a long smooth tube with a constant average flow rate, the presence of turbulence is a function of the velocity (V) of the fluid flow, the viscosity (μ) and the density (ρ) of the fluid, and the radius of the tube (r).

He defined a dimensionless number called the Reynolds number as

$$Re=2Vr\rho/\mu \qquad (8)$$

Turbulent flow is not easily described mathematically. This is due to the fact that the motion of one fluid particle is not exactly repeated by any other particle. Thus, all the data on turbulence is based on experimental observation. These experiments revealed that for a Reynolds number less than 2000, laminar flow remained laminar and any turbulent flow settled down to laminar flow. The converse is true for a Reynolds number greater than 2000.

Turbulent flow is not of any definite frequency and has no ordered

pattern. Turbulence is thus seen as fluctuations of velocity superimposed on the main velocity. The root mean square of the fluctuations is proportional to the intensity of the turbulence. The frequency of sign change of the fluctuations is proportional to the size of the eddies in the turbulence.

It is also noted that the energy dissipation increases in cases of turbulent flow. Thus the resistance to flow increases at higher flow rates (MASSEY B.S. 1976).

7.2 FOETAL REYNOLDS NUMBERS

Modelling the blood flow in the foetus requires an understanding of the type of flow present. In blood flow, turbulence has been shown to set in at Reynolds numbers below 2000 (McDonald 1974). This is due to the non-Newtonian properties of blood.

Very noisy clinical FVW's have often been recorded from the umbilical arteries and are believed to be a result of turbulence.

The aorta and umbilical arteries have the largest flow rates of all the foetal arteries. The Reynold's numbers were thus calculated in order to assess the probability of turbulence occurring. These arteries were considered to be circular when calculating the Reynolds numbers.

The viscosity of blood varies with the haematocrit. In normal adults the haematocrit can vary between 40 and 45 percent. In a foetus the haematocrit is closer to 40 percent and values as low as 37 percent are normal. The viscosity of blood for a normal haematocrit is between 3×10^{-2} and 4×10^{-2} Poise for vessels of radius >= 0.1mm (McDonald 1974) and will be used to calculate the range of Reynold's numbers.

7.2.1 THE AORTA

Reed et al (1986) reports mean and maximum flow velocities of 18 and 70 cm/sec. Additional results of mean velocities between 26 cm/sec and 30 cm/sec are given for human foetus's by Chen et al (1988). The Aortic diameter is 0.63cm , the density is unity and the viscosity is between 3×10^{-3} and 4×10^{-2} Poise.

The maximum Reynolds numbers occurred for low viscosity values. Thus for viscosity equal to 3×10^{-2} Poise, the Reynolds numbers were: Re(mean flow) = 378 to 630 (velocity = 18 to 30 cm/sec) Re(max flow) = 1470 (velocity = 70 cm/sec). Thus even near peak flow, turbulence, as a result of waveform pulsatility should quickly settle to laminar flow.

7.2.2 THE UMBILICAL ARTERY

The umbilical blood flow is approximately 40 percent of the cardiac output and approximately 50 percent of the aortic blood flow. The umbilical blood flow is thus approximately 15 cm/sec.

The mean and maximum magnitudes of normal FVWs were calculated from clinical waveforms. The maximum flow in the umbilical artery was calculated to be of the order of 3 to 4 times greater than the mean (This was also true for abnormal FVW waveforms which have a greatly reduced diastolic flow.). Reynolds numbers of 137 were obtained for the mean, and Re ranges from 411 to 548 as the velocity was increased from 3 to 4 times the average. In normal circumstances the maximum velocity was far lower than 4 times the average. In abnormal cases, due to the increased pulsatility of the flow, the maximum was as great as 4 times the normal mean.

Therefore, the noisy FVW's that are often seen in clinical practice are unlikely to result from turbulence, since the calculated Reynold's numbers are so low for the foetal vessels. Another possible cause of this noise could be the spectral estimation technique employed, and this should be investigated further in future work.

7.3 DESCRIBING THE TYPE OF FLOW

The equations describing R and L in the previous chapter assume parabolic flow. However due to the pulsatile nature of the waveform, parabolic flow is only established late in the cycle. For most of the cycle plug flow exists. A dimensionless parameter, alpha, was used to describe the type of flow and was thus used as a scaling factor of the resistance to flow and the inertance of the fluid. Alpha is a function of the radius (r) of the artery, the

frequency of flow (ω) and the viscosity (μ) of the fluid. Alpha increases linearly with the radius of the tube or artery and as the square root of the frequency of flow (McDonald 1974).

$$\alpha = r\sqrt{(\omega/\mu)} \tag{9}$$

The relationship between alpha and the type of flow is shown in figure 7.1. As alpha increases so the flow becomes more plug-like. Thus as alpha increases so the resistance to flow increases and the inertance of the fluid decreases. This is shown in figure 7.3(a). Note that alpha is dependent on the frequency of the signal and was usually calculated for the fundamental frequency.

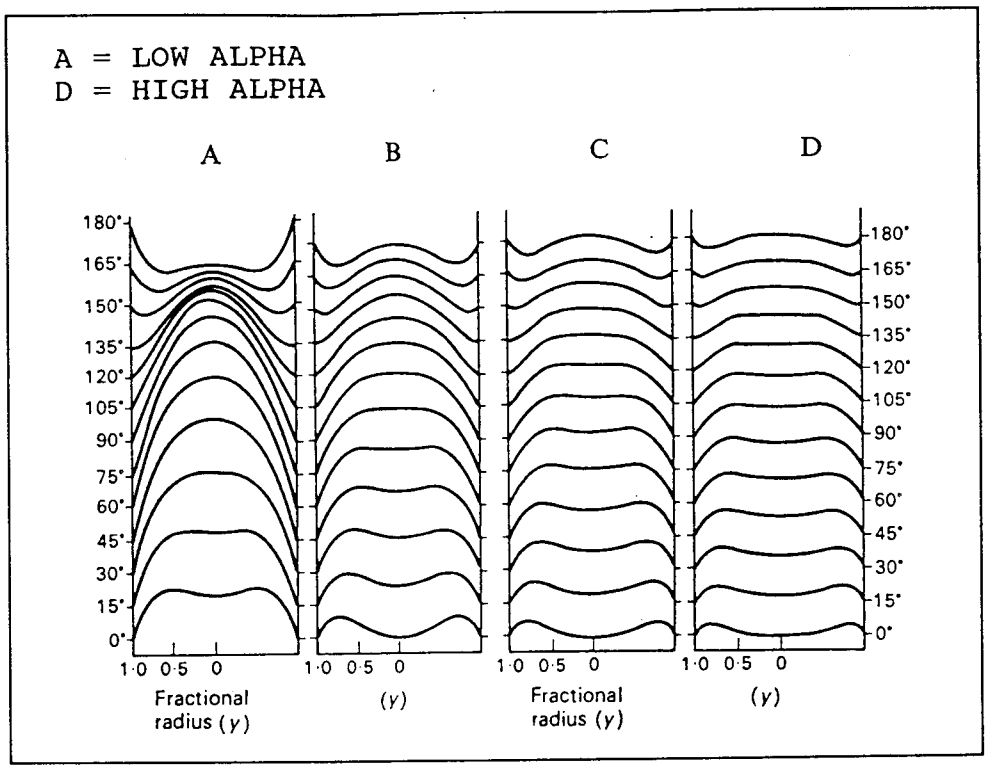

Figure 7.1: Velocity Profiles for Different alpha Values (McDonald 1974)

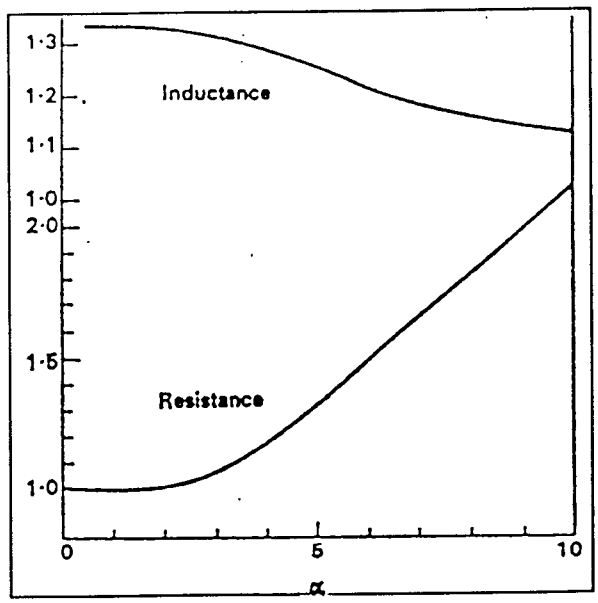

Figure 7.2(a): Resistance and Inductance Scaling Factors for Different alpha Values (McDonald 1974)

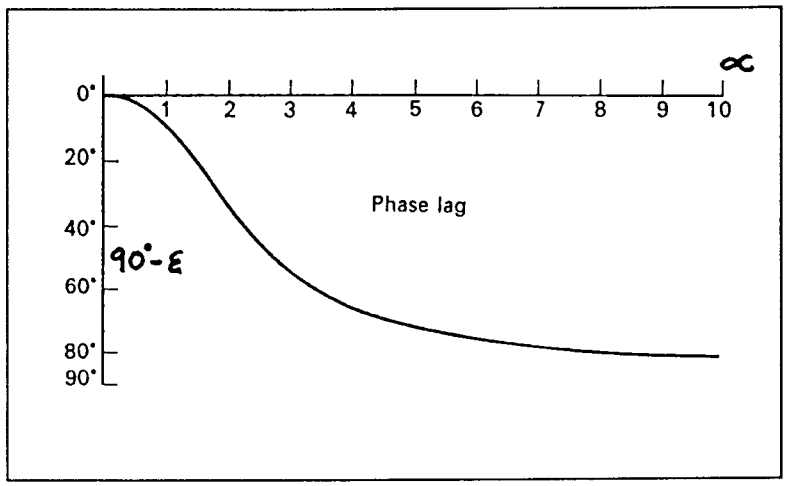

Figure 7.2(b): Phase Scaling Factor (90°-ϵ) (McDonald 1974)

Calculating alpha for a specific artery enabled the scaling of the resistance and inertance. This in turn accommodated any type of flow. The resistances and inductances were scaled according to the amplitude and phase lag (figure 7.2(b)) of the flow present with respect to the pressure gradient. The equations of resistance and inertance are described by equations 10 and 11 respectively.

$$R=(\mu\alpha^2 l\sin(\epsilon))/(\pi r^4 M') \qquad (10)$$

$$L=(\rho l\cos(\epsilon))/(\pi r^2 M') \qquad (11)$$

The scaling factors for amplitude (M') and phase (ε) are given in Appendix F. (For parabolic flow the overall scaling factor for R is 8, and for L is 1.35. This is presented in equations 5 and 6)

7.3 CONCLUSIONS

Turbulent flow was not a major factor in the blood flow in the foetus even though there was an indicator for turbulence in the aorta. As far as the umbilical artery Doppler signal was concerned, it was very unlikely that any "noise" on the signal was from turbulence. A noisy umbilical FVW which was often seen clinically, was probably because of the errors in the Fast Fourier Transform (FFT) calculations and not as a result of turbulence of the blood flow. The ultrasound machine performs a FFT on the raw data to produce the maximum velocity signal which was used to calculate the indices. Fluctuations (noise) on the signal may thus be as a result of the FFT (Kaluzynski et al 1993 and Hoskins et al 1991).

Thompson and Trudinger (1990) also concluded that no turbulence was present in either the umbilical arteries or placenta. Modelling the foetal circulation however requires the inclusion of different types of flow. The scaling of R and L for this purpose has been described in this chapter.

CHAPTER EIGHT

MODELLING THE FOETAL CIRCULATION

8.1 INTRODUCTION

Thompson, Trudinger and Stevens (1989,1990) investigated the effects of placental resistance, FHR, mean blood pressure and blood pressure pulsatility on the PI by modelling the umbilical arteries and placenta. The electrical analogous model described by them was used in this thesis in its exact form. It was called 'model 1' and was used to investigate the PI, RI and HRSI.

Model 1 was a very simple representation of the umbilical placental circulation. A very simple pressure input to the umbilical arteries, which was not dependent on the foetal arterial circulation, was assumed and the model was a lumped equivalent circuit which did not represent the arteries spatially.

A second improved model (model 2) was thus designed in which some of the representations described in model 1 were incorporated. In model 2 the umbilical arteries were represented as a transmission line, and the foetal circulation was modelled around the umbilical placental unit. Model 2 provided a pressure input to the umbilical placenta unit which was physiologically more realistic than the simple input implemented in model 1. Model 2 had the additional advantage that the pressure waveforms were dependent on the

behaviour of the foetal arterial system. Numerous different responses of the foetal arterial circulation to physiological changes can easily be simulated and their effects assessed. Model 2 thus provided scope for the analysis of complex physiological variations on the umbilical FVW and the indices which described it.

The accuracy of the models are limited by the assumptions used in their design. The models were thus used to provide an understanding of the blood flow in the foetal arterial circulation and in understanding the physiological variables which affect the umbilical arterial FVW. The models did not aim to provide precise quantitative information about the umbilical FVW and the indices which describe it.

Modelling the umbilical placental circulation aimed to provide insight into the effects of the following variables on the umbilical FVW and in turn the RI, PI and HRSI :

1) placental resistance
2) placental size
3) type or site of obliteration
4) FHR variations and the foetal physiological response to it
5) blood pressure pulsatility and mean blood pressure
6) blood flow distribution
7) the site of measurement of the FVW on the umbilical artery

The scope of the modelling did not involve every physiological

variable possible in the foetus. It only analyzed the physiological and anatomical variables described above as these are clinically the variables of most interest. The variability of the new HRSI was of particular interest.

8.2 SIMULATOR METHODOLOGY

The models of the umbilical placental and foetal circulation were implemented in PSPICE which is an electronic circuit analysis package. The FVW's obtained from PSPICE were analyzed using a mathematical analysis package called MATLAB.

Actual human umbilical arterial FVWs were recorded from a Sonicaid Vasoflo 3C ultrasound machine at Tygerberg Hospital and were used as a comparison for the FVWs simulated in PSPICE.

CHAPTER NINE

THE THOMPSON, TRUDINGER AND STEVENS MODEL (MODEL 1)

9.1 DESCRIPTION AND METHODOLOGY

Even though a full description of foetal anatomy and physiology was given in chapter two, it will be re-mentioned in this chapter, but with specific respect to its relevance in modelling the foetal circulation.

9.1.1 THE STRUCTURE OF THE MODEL

The anatomy of the placenta and umbilical arteries are fairly simple and as a result were easily modelled as an equivalent analogous electrical circuit. The simplified representation of the umbilical/placental circulation is a s follows: There are two umbilical arteries which anastomose shortly before reaching the placenta. The placenta consists of 5 radial branching arteries which branch into lobes and then lobules ($<90\mu m$), which are the branching networks of the placenta. The model associated 10 lobes (n) and 50 lobules (m) with a small placenta, 20 lobes and 200 lobules with a large placenta. Figure 9.1 depicts the structure of the system. It can be seen that the umbilical arteries branch into radially branching arteries which then branch into the main stem villi. The main stem villi branch into smaller tertiary stem villi where exchange of nutrients, gases and waste products with the maternal circulation takes place.

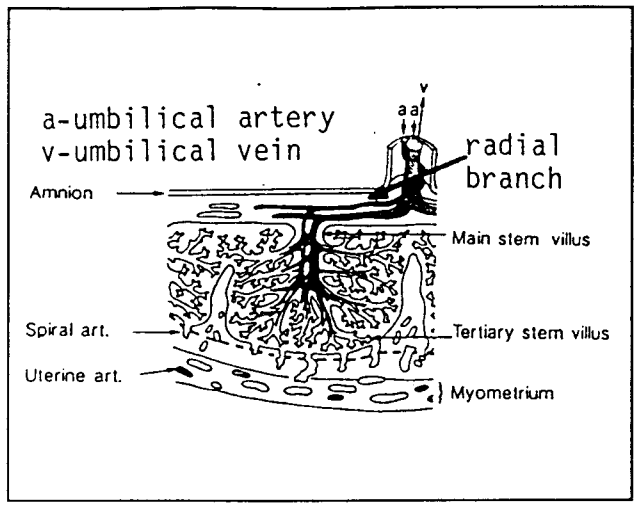

Figure 9.1: Placental Structure (Thompson and Trudinger 1990)

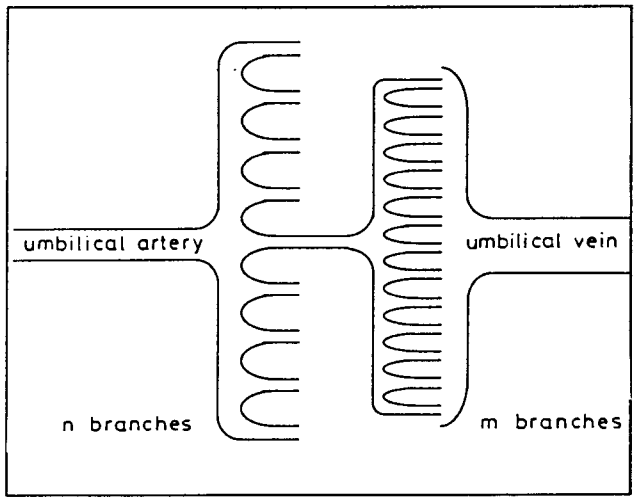

Figure 9.2: Diagrammatic Structure of the Placenta (Thompson and Trudinger 1990)

The model thus consisted of 4 different orders or levels from the umbilical arteries down to the lobules. The umbilical arteries and radial branching arteries were combined to form one umbilical artery and the lobes and lobules were combined to form the placenta. The placenta is illustrated in diagrammatic form in figure 9.2. The branching of the lobules from the lobes is also illustrated in this figure.

The dimensions of the different arteries are given in table 9.1. (The flow parameters of resistance, compliance and inertance are

calculated in MKS units.)

Table 9.1: Dimensions of the Arteries (Thompson et al 1990).

UMBILICAL ARTERY AND PLACENTAL VESSEL DIMENSIONS
DIMENSIONS USED IN THE THOMPSON ET AL MODEL

UMBILICAL ARTERY	UMBILICAL ARTERIES (2)	RADIAL BRANCHES (5)
RADIUS a (mm)	1.00	0.5
LENGTH l (mm)	500	100
WALL THICKNESS h (mm)	0.15	0.075
COMBINED (MKS)	R=0.58E10	C=710E-13
PLACENTA	LARGE BRANCHES	SMALL BRANCHES
RADIUS a (mm)	0.5	0.1
LENGTH l (mm)	100	10
WALL THICKNESS h (mm)	0.1	0.08
RESISTANCE (MKS OHMS)	1.63E+10	1E+12
CAPACITANCE (MKS FARAD)	1.2E-12	1.200E-15
	SMALL PLACENTA	LARGE PLACENTA
No. OF LOBES (n)	10	20
No. OF LOBULES (m)	50	200
YOUNG'S MOD. (N/m ^ 2)	500000	
VISCOSITY (Kg/M/s)	0.004	

9.1.2 THE TYPE OF FLOW

The flow in the umbilical arteries was determined to be quasisteady as the alpha values were calculated to be between 0.89 and 2.5. (For a FHR of between 120 and 160 bpm and an artery diameter of 1 to 2 mm.) This represented the fundamental of the FVW. The first harmonic, which comprised of 42 % (Appendix C) of the fundamental, resulted in alpha values of between 1.25 and 2.89. The second harmonic was of little consequence as it only comprised 16 % of the fundamental. The alpha values were thus taken to be approximately

2 and quasisteady state flow was assumed (Thompson and Stevens 1989).

The Reynolds numbers for the umbilical flow indicates laminar flow as they are below the critical value for turbulence.

9.1.3 THE ELECTRICAL ANALOGY

The quasisteady state flow was assumed to be dominated by viscous rather than inertial forces. Therefore each arterial branch, lobe and lobule was modelled by a resistor and a capacitor. Inertance of the blood flow was ignored (Thompson and Stevens 1989). Figure 9.3 illustrates how the placenta is modelled as a branching structure. The resistance is given in equation 5. The compliance of the vessels is calculated from equation 4. Sigma (σ) is the Poisson ratio and was equal to 0.5 for highly elastic tubes.

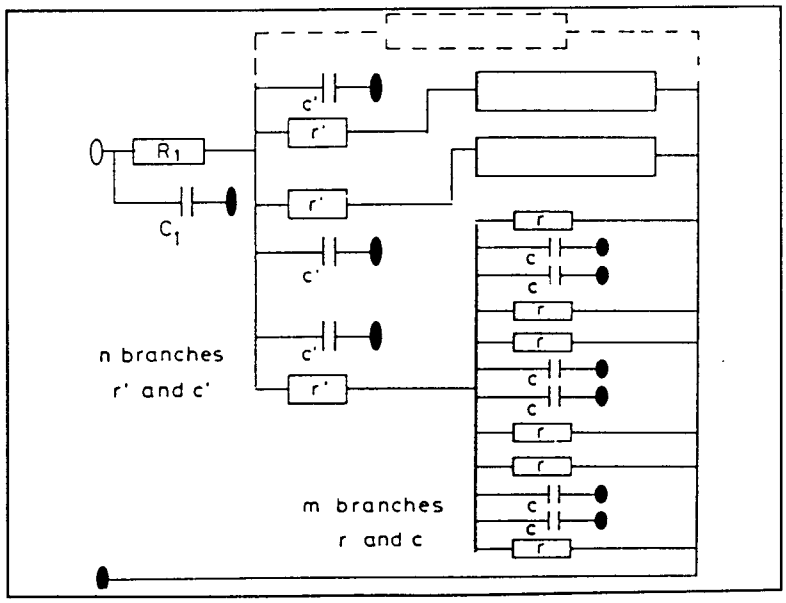

Figure 9.3: Electrical Equivalent Representation of the Umbilical Arteries and Placenta (Thompson and Trudinger 1990)

9.1.4 THE SYSTEM INPUT

The input pressure waveform was pulsatile and was a simple representation of that at the aortic bifurcation. The waveform was an approximation to a half sine wave of amplitude p1 with constant offset p0 (It was not possible to simulate a smooth sine wave, thus a piecewise approximation was used.). The peak ejection pressure was (p1+p0) and was 80 mmHg. The post ejection pressure was p0 and was 50 mmHg. The mean pressure was (p0+p1/π). The mean pressure was thus calculated to be 60 mmHg. The input waveform was split into so called ejection and post ejection components. The ejection component being the component of sinusoidal pressure, and the post ejection component being the constant pressure. The ejection (Et) and post ejection time (PEt) intervals were always equal. Figure 9.4 gives examples of the input waveform for different FHRs. The input simulated a FHR of 100 to 188 bpm and a standard FHR of 133 bpm was assumed.

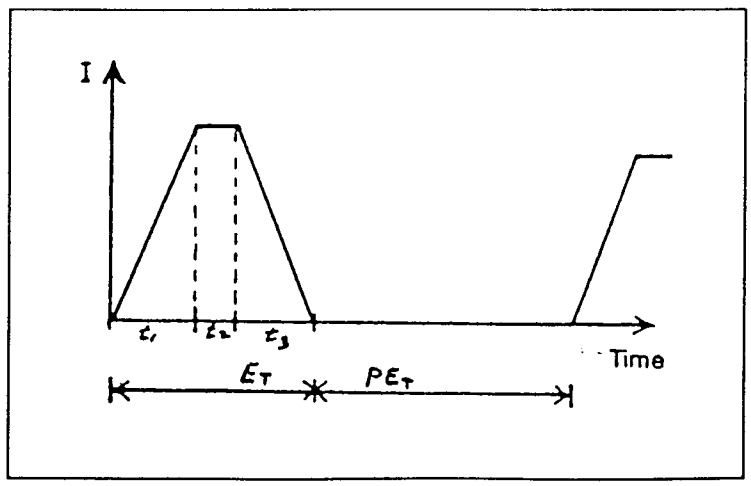

Figure 9.4: Input Waveform
(Et = ejection time
PEt = post ejection time
Et = PEt
t1 = t2 = t3)

9.1.5 THE FLOW MAGNITUDE

The mean umbilical blood flow in a normal foetus is close to 120 ml/min/kg. (This is representative of the 50th centile.) In the model, the average flow was calculated from the mean pressure and the resistance of the placenta. Thompson and Trudinger (1990) reported that the flow in the model was close to 67 ml/min, which was less than the normal value. This value was however within the normal bounds of umbilical flow and was acceptable based on the approximations made in modelling.

9.1.6 THE FINAL MODEL REPRESENTATION

The umbilical and placental circulation was finally modelled by a lumped equivalent circuit. The umbilical and placental resistances were each modelled by a resistor. The compliances of the umbilical artery and the placenta were added and were represented by a single capacitor.

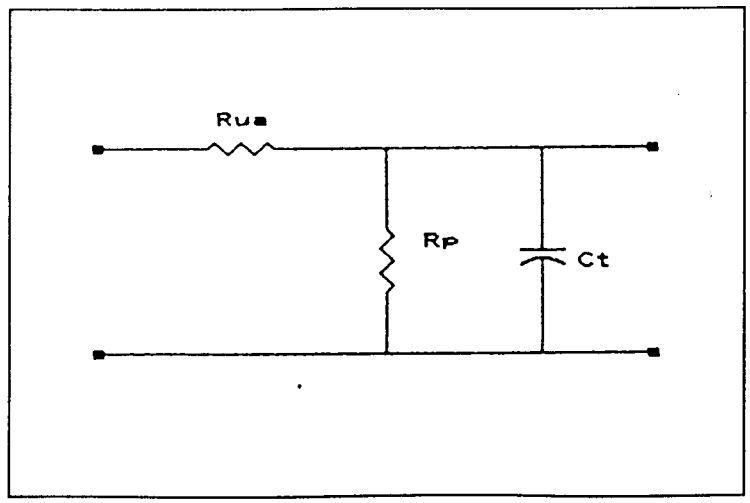

Figure 9.5: A Lumped Representation of the Umbilical Arteries and Placenta

The equivalent resistance of the placenta is given by equation 12.

$$Rp=(R'+R/m)/n \qquad (12)$$

where Rp = placental resistance

R′ = primary and secondary stem villi resistance

R = tertiary stem villi resistance

The equivalent compliance of the placenta is given by equation 13.

$$Cp=nC'+nmC \qquad (13)$$

where Cp = placental compliance

C′ = primary and secondary stem villi compliance

C = tertiary stem villi compliance

The equivalent compliance of the umbilical placental unit is given by equation 14.

$$Ct=Cua+Cp \qquad (14)$$

where Cua = umbilical artery compliance

Ct = total compliance of umbilical placental unit

9.2 THE ASSUMPTIONS OF THE MODEL

The assumptions of this model were:

1) The blood pressure input to the model. The mean blood pressure was 60 mmHg. The systolic to diastolic pressure was 80/50 mmHg and

was maintained for all FHRs. The pressure input consisted of equal ejection and post ejection intervals.

2) The system was expressed in a lumped element circuit model. A transmission line approach was not used thus reflections and transmission line losses experienced in the arteries were not incorporated.

3) The flow profile in all the arteries was parabolic.

4) The viscous forces were less than the frictional forces, thus inertance was not modelled. The inertance was thus negligible compared to the resistance, at the low frequencies simulated.

5) Uniform obliteration occurred in the placenta and was simulated by fractionally reducing the number of placental vessels.

6) The Young's modulus equalled 5×10^{6} dyne/cm^{2} and the viscosity equalled 4×10^{-2} poise (Thompson and Trudinger 1990). These values were constant at all times.

7) The mean venous pressure was 0 mmHg.

CHAPTER TEN

SIMULATIONS OF THE UMBILICAL BLOOD FLOW WAVEFORM USING MODEL 1

10.1 INVESTIGATIONS

The model was used to investigate the following physiological variables on the umbilical flow velocity indices:

10.1.1 Foetal Heart Rate (FHR). The effect of FHR variations, from 100 to 188 bpm, on the indices were examined. This test was done on normal placentas with no disease. A large placenta (n=20, m=200) and a small placenta (n=10, m=50) were used in this analysis. The blood pressure input was maintained at a mean of 60 mmHg and the systolic and diastolic time intervals were equal for all FHRs. RI, PI and HRSI were calculated at each FHR and any variations due to FHR variations were analyzed.

10.1.2 Placental disease. The change in placental resistance and compliance resulting from fractional obliteration of the terminal vessels was examined. Two types of obliteration were implemented. The first was progressive obliteration of the larger placental vessels (primary and secondary villi), and the second, distributed obliteration of the smaller placental vessels (tertiary stem villi). (Fractional obliteration may clinically represent placental embolization or an increase in placental resistance due to hypoxia.) The analysis was done at a fixed FHR of 133 bpm.

The corresponding changes in the indices were calculated from the simulated waveforms and compared with the placental resistance which was calculated according to equations 15 and 16.

$$Rp=(R'm+R)/(1-q)\,nm \qquad (15)$$

(Progressive)

$$Rp=(R'(1-q)\,m+R)/(1-q)\,nm \qquad (16)$$

(Distributed)

q Represented the fraction of placental obliteration. Equation 17 represents the placental compliance. (Appendix A)

$$C=Cua+nC'+nm(1-q)\,C \qquad (17)$$

This section aims to investigate:

a) The effect of placental obliteration on the indices. (At 133 bpm.)

b) The effect of placental size on the indices. (At 133 bpm.)

c) The effect of the type of obliteration on the indices. (At 133 bpm.)

d) The effect of FHR variations on the indices as q increases. (On a Large placenta.)

10.2 RESULTS

Note that reverse flow simulated by the model was negated to absent flow.

10.2.1 Foetal Heart Rate variations. At zero obliteration the HRSI was equal to zero as the FVW had no reduced or absent diastolic flow. Thus only RI and PI were examined in this section.

i) n=20 m=200

The indices were virtually independent of FHR. The RI did not change at all in the range of 100 to 188 bpm. The PI changed by a maximum of 1.69 percent from 0.59 at 133 bpm (table 10.1).

Table 10.1: Index magnitudes vs FHR.

	FHR = 100	FHR = 120	FHR = 133	FHR = 150	FHR = 187.5
HRSI	0	0	0	0	0
RI	0.42	0.42	0.42	0.42	0.42
PI	0.59	0.59	0.59	0.58	0.58

ii) n=10 m=50

The indices were virtually independent of FHR. The RI changed by a maximum of 3.64 percent and the PI changed by a maximum of 2.35

percent in the range of 100 to 188 bpm (table 10.2).

Table 10.2: Index magnitudes vs FHR

	FHR = 100	FHR = 120	FHR = 133	FHR = 150	FHR = 187.5
HRSI	0	0	0	0	0
RI	0.56	0.55	0.55	0.54	0.53
PI	0.87	0.86	0.85	0.84	0.83

10.2.2 Placental resistance.

i) The effect of placental obliteration on the RI, PI and HRSI.

The RI, PI and HRSI all increased with increasing placental obliteration. The calculated placental resistance, using equations 15 and 16, was plotted against the percentage obliteration in figure 10.1.

The placental obliteration was increased from zero to approximately 97 percent at which point the FVW was characterised by a large proportion of absent flow. The placental resistance increased almost linearly until 50 to 60 percent obliteration. Further obliteration lead to an accelerated increase in placental resistance. The capacitance of the placenta decreased with increased obliteration. The fractional decrease in capacitance was

however very small in proportion to the fractional change in resistance.

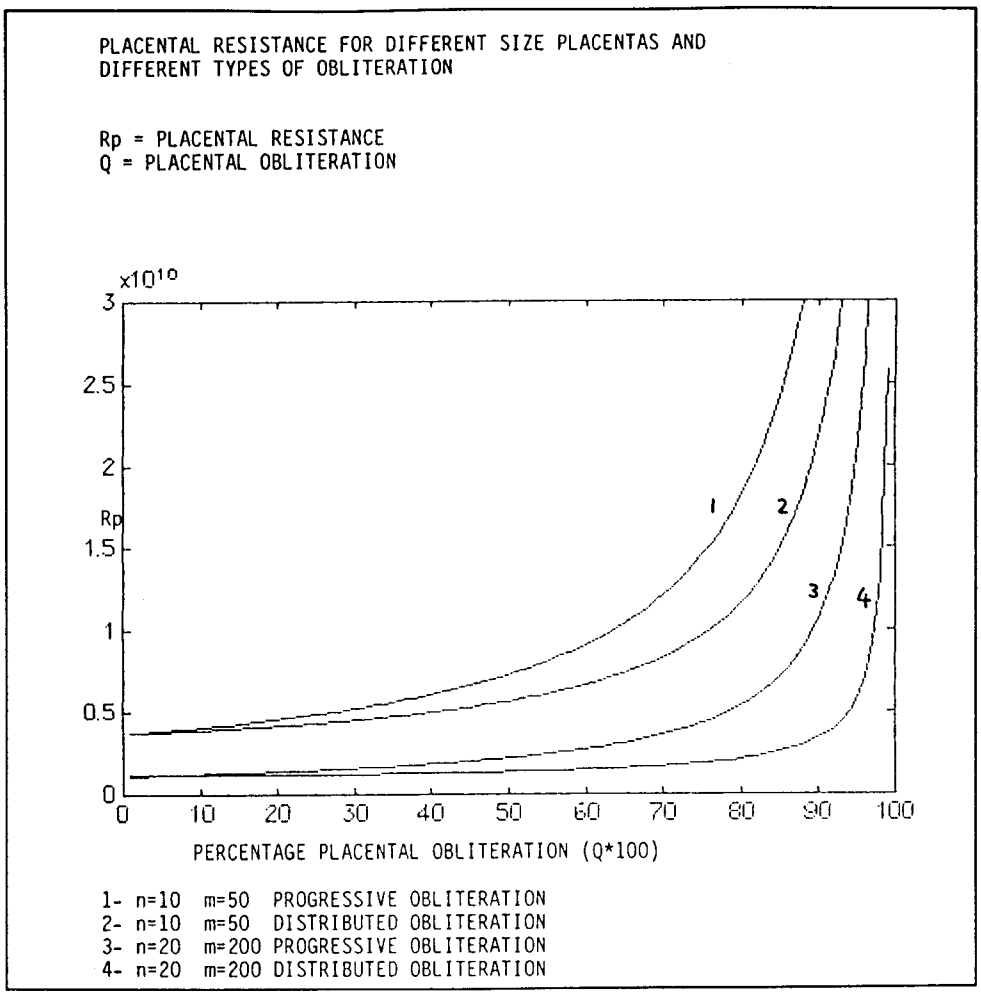

Figure 10.1: Placental Resistance vs Placental Obliteration

The greatest change in placental resistance occurred at large degrees of obliteration. 75 to 100 percent obliteration caused a very large increase in placental resistance. The indices showed a similar trend to the placental resistance as the degree of obliteration was increased. The increase in HRSI was however far more pronounced than in RI or PI. HRSI only began to increase once the FVW had reached a certain degree of reduced flow. Thus due to

its definition, the HRSI was only sensitive to reduced or absent flow and elevated placental resistance. Figures 10.2, 10.3 and 10.4 illustrate the increase in the indices with increasing obliteration.

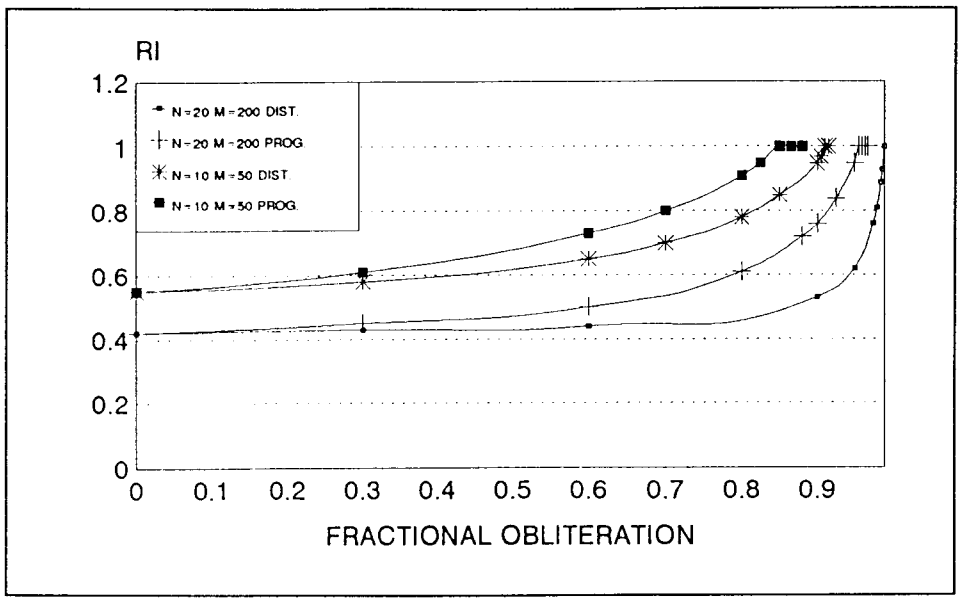

Figure 10.2:
RI vs q

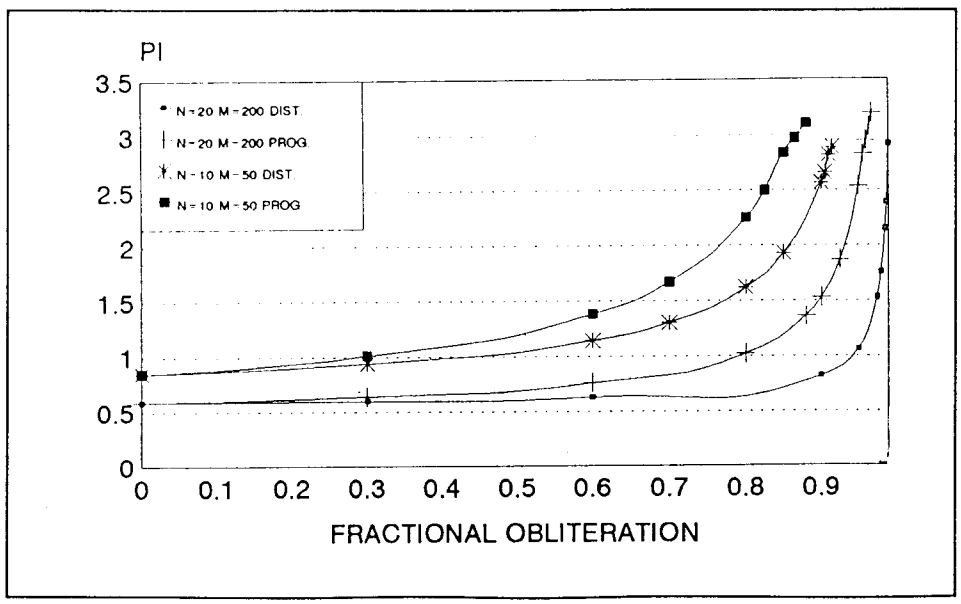

Figure 10.3:
PI vs q

Figure 10.4:

HRSI vs q

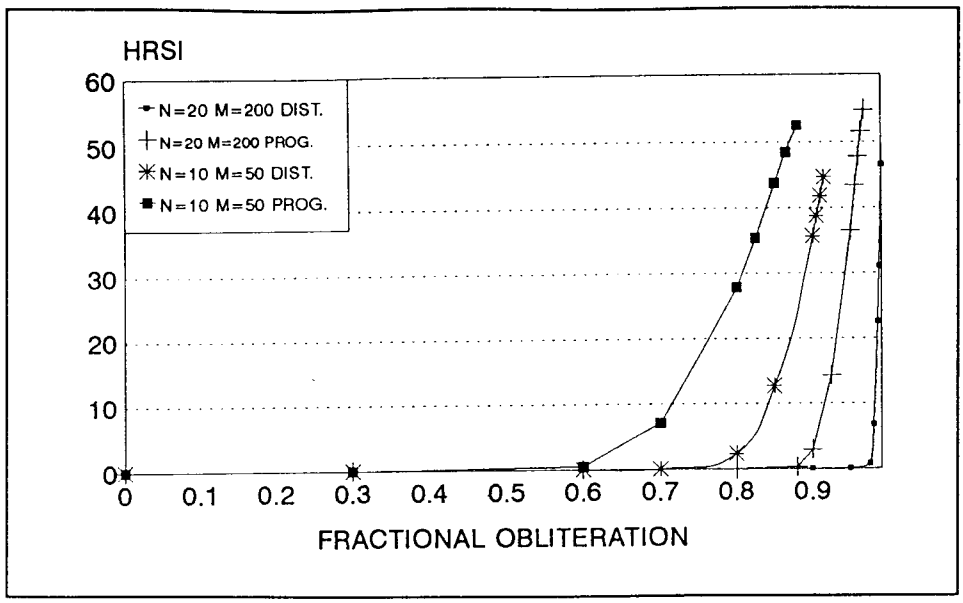

The RI increased with increasing placental resistance yet saturated at unity when absent flow was present. RI first reached unity at approximately 95 percent obliteration. Any further increase in obliteration had no effect on the index.

The PI increased with increasing placental resistance, yet unlike the RI never reached a saturated value. The PI was approximately equal to 2.8 when RI reached unity and absent flow first appeared (95 percent obliteration). PI continued to increase and reached values above 3 for fractional obliteration as high as 97 percent. It was evident that in this region of large placental obliteration, small increases in obliteration cause a large change in the index.

When RI reached unity and absent flow was first established, the HRSI was approximately 40 percent. The HRSI continued to increase

as the placental obliteration was increased and reached a maximum value of approximately 55 percent at a placental obliteration of 97 percent. Larger increases in HRSI, compared to the increases in PI, were present for small increases in placental obliteration. The HRSI increased by a magnitude of 15 percent for a 2 percent increase in obliteration. PI only increased by a magnitude of approximately 0.4 over the same range.

ii) The effect of placental size on the indices

As the fraction of terminal vessels in the placenta was reduced to emulate obliteration, the total placental resistance increased. The placental resistance was also shown to be dependant on the size of the placenta and the type of obliteration.

A smaller placenta (young foetus) has a larger resistance than a large one (older foetus). This is because there was fewer vessels in the smaller placenta. It is expected that with increasing gestational age, the placental size will increase and thus its resistance will decrease (figure 10.1).

Figure 10.1 illustrates the relationship between size of placenta and resistance. As can be seen, the smaller placenta is characterised by a larger resistance, thus the young foetus or the small for gestational age (SGA) foetus with a small placenta has an index higher than that for an older foetus. The young or SGA foetus was thus always characterised by a higher index as its placental

resistance was higher.

There was an initial change (at zero obliteration) in PI from 0.59 to 0.85, and in RI from 0.42 to 0.55 between a small and a large placenta. This was consistent with the clinically observed decrease in RI and PI with advancing gestational age in a normal foetus.

The results of the model support clinical findings in that at a fixed obliteration, decrease with increasing placental size. For example, at 88 percent progressive obliteration, the PI was 0.72 and 3.1 for a large and a small placenta respectively. RI was 0.72 and unity, and HRSI was 0.26 and 52.51 for a large and a small placenta respectively.

The RI reached unity at approximately 85% to 90% progressive and distributed obliteration respectively in the small placenta, yet in the large placenta, 95% to 99% progressive and distributed obliteration respectively, was needed to obtain the same result. The PI reached a value of 2.8, which corresponds to the beginning of absent flow, at approximately 85 to 90 percent obliteration in a small placenta and 95 to 99 percent obliteration in a large one. The HRSI showed the same trends as RI and PI and reached a value of approximately 40 percent when the RI reached unity and the PI reached 2.8.

The early onset of absent flow and elevated indices for a small

placenta, thus indicates that a young or SGA foetus with a small placenta is not able to withstand the same degree of obliteration as well as an older foetus with a larger placenta.

iii) The effect of the type of obliteration on the indices

Progressive obliteration of the lobes required less fractional obliteration to increase the placental resistance than distributed obliteration of the lobules. This can be seen in figure 10.1 where in the same size placenta, progressive obliteration caused a more rapid increase in placental resistance.

iv) The effect of FHR variations on the indices with increasing obliteration (q)

The results of the different types of obliteration and different sized placentas have been described in the sections above. Only the results of a large placenta with distributed obliteration will be examined in this section as the trend was the same for both large and small placentas, as well as for progressive and distributed obliteration.

The RI and PI remain virtually constant at low fractions of obliteration yet are and are thus significantly linearly related to the FHR (Linear Correlation coefficients varied from -0.845 to -0.998, and -0.845 and -0.989 for RI and PI respectively.). Table 10.3 illustrates the average and standard deviation of the indices from the standard value over the FHR range at specific

obliterations.

Table 10.3: Index Mean and Standard Deviation over the FHR Range (the index values are expressed as a mean ± standard deviation. The standard deviation is expressed as a percentage of the mean (in brackets).)

q	RI	PI	HRSI
N=20 M=200			
0	0.42 +- 0.00 (0%)	0.59 +- 0.005 (0.85%)	0.0 +- 0.00 (0%)
0.3	0.45 +- 0.005 (1.1%)	0.64 +- 0.005 (0.78%)	0.0 +- 0.00 (0%)
0.6	0.50 +- 0.007 (1.4%)	0.75 +- 0.012 (1.6%)	0.0 +- 0.00 (0%)
0.8	0.61 +- 0.014 (2.29%)	1.01 +- 0.022 (2.18%)	0.0 +- 0.00 (0%)
0.9	0.76 +- 0.017 (2.24%)	1.52 +- 0.04 (2.63%)	2.78 +- 0.32 (11.51%)
0.925	0.84 +- 0.02 (2.38%)	1.86 +- 0.05 (2.69%)	14.06 +- 0.39 (2.77%)
0.95	0.95 +- 0.02 (2.11%)	2.52 +- 0.072 (2.86%)	36.19 +- 0.45 (1.24%)
0.96	1.0 +- 0.00 (0%)	2.94 +- 0.012 (0.41%)	47.49 +- 0.93 (1.95%)
0.968	1.0 +- 0.00 (0%)	3.17 +- 0.016 (0.505%)	54.69 +- 0.85 (1.55%)
N=10 M=50			
0	0.55 +- 0.01 (1.82%)	0.85 +- 0.014 (1.65%)	0.0 +- 0.00 (0%)
0.3	0.60 +- 0.014 (2.33%)	1.00 +- 0.02 (2%)	0.0 +- 0.00 (0%)
0.6	0.72 +- 0.017 (2.36%)	1.37 +- 0.03 (2.19%)	0.42 +- 0.22 (52.38%)
0.7	0.80 +- 0.017 (2.13%)	1.66 +- 0.044 (2.65%)	6.94 +- 0.095 (1.37%)
0.8	0.91 +- 0.023 (2.53%)	2.24 +- 0.064 (2.86%)	27.58 +- 0.40 (1.45%)
0.825	0.95 +- 0.024 (2.53%)	2.48 +- 0.072 (2.90%)	35.12 +- 0.45 (1.28%)
0.85	0.99 +- 0.02 (2.02%)	2.80 +- 0.069 (2.46%)	43.43 +- 0.72 (1.66%)
0.88	1.0 +- 0.00 (0%)	3.09 +- 0.012 (3.88%)	52.36 +- 0.96 (1.83%)

The variations of RI and PI for FHR variations are thus insignificant. The HRSI is however highly dependant on FHR at very low index magnitudes and is linearly related to FHR (HRSI close to zero. Linear Correlation coefficients varied from -0.971 to -0.986.). As the index increased so it became less dependant on FHR variations and tended towards a constant value. The relationship remains significantly linear. (Linear Correlation coefficients

varied from 0.889 to 0.963). The large dependency on FHR was only seen at low values of HRSI where a small variation in the index gave a large percentage variation of the index. Low values of this index are however not clinically significant as the FVWs have not reached absent flow.

Figures 10.5, 10.6, and 10.7 illustrate the relationships between the indices and placental obliteration at the different FHRs. No significant deviations were visible. RI and PI were seen to decrease with an increase in FHR. HRSI, however, decreased with increasing FHR at low magnitudes yet it increased with increasing FHR at higher magnitudes. This was however insignificant as the standard deviations were small.

Figure 10.5:
RI vs q

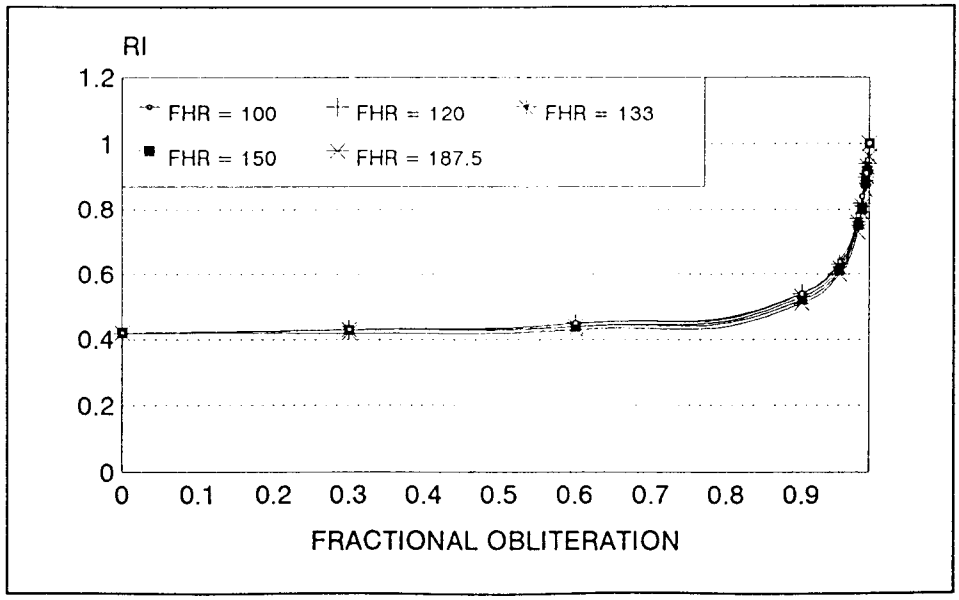

Figure 10.6:

PI vs q

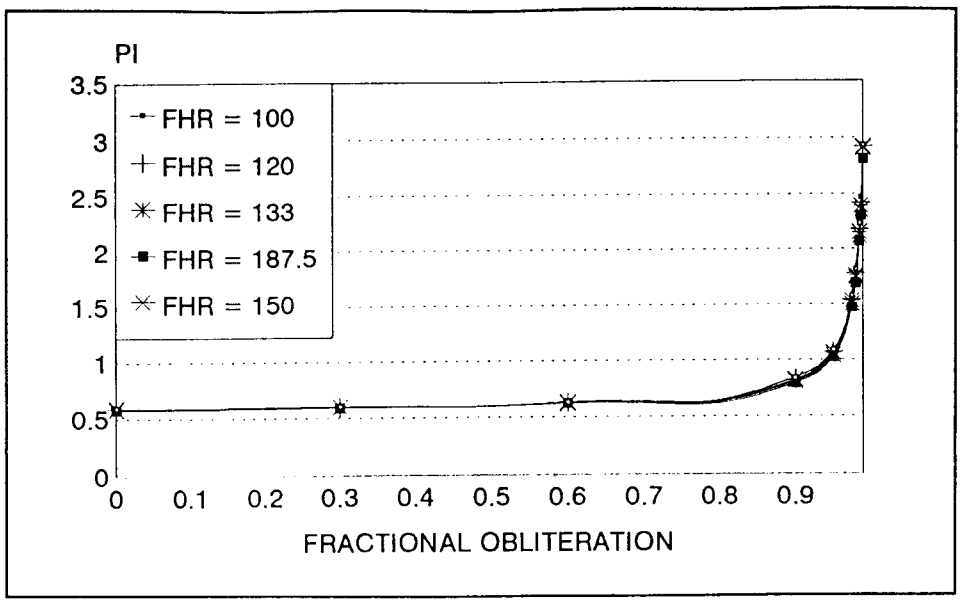

Figure 10.7:

HRSI vs q

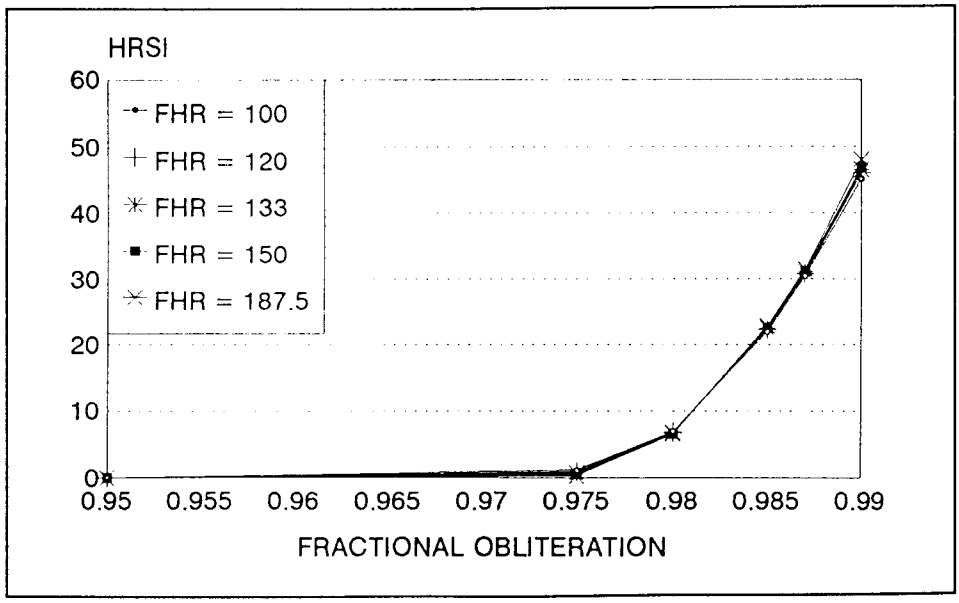

10.3 DISCUSSION

It must be noted that this model was used to examine the effects described above, not to reproduce the FVW exactly, nor to incorporate every physiological condition possible. The model was however able to simulate reverse and reduced flow which is often

present in complicated pregnancies. It is important to note that this model is only an approximation of the umbilical placental circulation as the dimensions are approximations of the real dimensions and the architecture is an approximation of the placenta.

Clinical observations by other authors showed that raised index values were associated with foetal distress, raised placental resistance and reduced umbilical blood flow (Downing et al 1991, Muijsers et al 1991, McCowan et al 1987). This model was useful in theoretically correlating raised index values with raised placental resistance.

It was also shown that the indices are independent of FHR. This was however due to the assumption that the mean umbilical blood pressure, and blood pressure pulsatility were kept constant with varying FHR. In vivo, the blood pressure pulsatility is probably not constant even though the mean blood pressure may be maintained. This may be why clinical investigations have been able to show a definite negative correlation between the RI and PI with FHR (Downing et al 1991). This was more closely investigated in model 2 where the blood pressure and blood pressure pulsatility were dependent on the foetal arterial circulation.

Model 1 clearly showed the difference between the FVW in a small and a large placenta. A large placenta has a lower resistance and

thus a greater blood flow. The indices which described the FVW were lower for a large placenta indicating the lower resistance and larger flow. This is in agreement with the elevated indices for young foetuses found clinically (Pattinson et al 1989). A large placenta thus has a greater reserve and requires large percentages of obliteration to reduce the blood flow to a state where the indices are elevated to a level which is clinically indicative of foetal distress. The increased number of arteries in a large placenta thus reduces the placental resistance and the indices follow the same trend. This is in accordance with the slight decrease in the normal index values as the foetus grows older and is a critical point in stating that the number of arteries in the placenta determine its resistance and that the indices are determined by the placental resistance.

The model also showed the relevance of the site of placental obliteration. Obliterating the larger placental vessels results in a larger increase in placental resistance compared to the obliteration of smaller placental vessels.

The HRSI was shown to follow similar trends as the RI and PI. However, it did not saturate when flow was absent, yet continued to increase with increasing placental resistance. Values of 34 percent and greater occurred with absent and reversed flow. In a clinical setting, any values of this index greater than 34 percent will indicate a high placental resistance and a strong possibility of

foetal distress.

The results on the PI presented by Thompson et al (1990) were similar to those simulated in this equivalent model. The additional results presented by them on the effects of blood pressure pulsatility on the PI have not been validated. It was however interesting to note that they reported that the pulsatility variation of the blood pressure did have a significant effect on the PI. The pulsatility of the blood pressure and mean blood pressure were constant for all FHR's during the experiments, thus explaining why the indices did not vary as the FHR was varied. If the blood pressure pulsatility varied with the FHR, the indices would vary as expected. This is to be investigated in model 2 described in the next section where the blood pressure pulsatility is dependent on the FHR and the physiological response of the foetal circulation to these variations.

CHAPTER ELEVEN

THE TRANSMISSION LINE MODEL (MODEL 2) - A NEW APPROACH

11.1 WHY A NEW MODEL ?

The major problems with model 1 are:

1) The pressure input to the umbilical placental system is not dependent on the foetal circulation and the systolic and diastolic time intervals are always equal regardless of the heart rate. Physiologically this is incorrect. The pressure at the aortic bifurcation is thus independent of the behaviour of the heart and foetal circulation and was unrealistic.

2) The model was a lumped element circuit. The effect of reflections and transmission losses experienced in an artery were thus not included. The system would have to be modelled as a transmission line for this to be implemented.

3) Inertances due to the motion of blood were not included. These would need to be included in order to indicate the effects of wave propagation.

The new model aimed to overcome these problems. New assumptions however needed to be made which also limited the reality of this model.

From this point of view, the new model aimed to:

1) Incorporate the foetal arterial circulation as a system which provided a realistic pressure wave input to the umbilical placental unit. The pressure wave input was dependent on the foetal circulation and the action of the heart.

2) Model the foetal and umbilical circulation in the form of a transmission line. The effects of reflections and transmission losses experienced in arteries were incorporated.

3) Model the umbilical placental circulation based on the previous model yet with the adaptations described above.

11.2 DESCRIPTION OF MODEL 2

The dimensions of the different arteries are listed in the sections 11.3.1 to 11.3.7. The model was based on data obtained from literature and from post mortem measurements.

The effects of non-parabolic flow have been incorporated, consequently, the resistances and compliances are calculated using equations 10 and 4.

As the inertia of the blood affects the phase velocity, inductance was included in the modelling of the systems. Inductance is described by equation 11 and also incorporates the effects of non-parabolic flow.

The phase velocity, calculated using L and C, was used in determining the required dimension of the elements in the lumped parameter transmission line representation of an artery (Appendix G and Appendix D).

The input to the model was a current source which modelled the volume flow output from the heart. The use of a current source simplified the modelling of the heart by assuming that the stroke volume and ejection time of the heart were constant. The current flow into the system set up its own voltages after an initial settling time.

The simulation of umbilical blood flow was done on an electronic circuit simulator package, PSPICE. Reverse flow simulated with the model was negated to absent flow and is in accordance with the clinical measurements, in which reversed flow is obscured by returning blood in the umbilical vein when using a continuous wave ultrasound machine.

Because the umbilical artery was modelled as a transmission line, it was possible to read the FVW at intervals along the artery. In accordance with clinical information, the indices were read at the distal (placental) end of the umbilical artery. Four waveforms were then averaged to give a single index result.

Due to rounding errors and the small errors associated with modelling, variations in results of up to 5 percent were tolerated.

11.3 THE STRUCTURE OF MODEL 2

The model was split into seven stages; as shown in figure 11.1

Figure 11.1: The Structure of Model 2

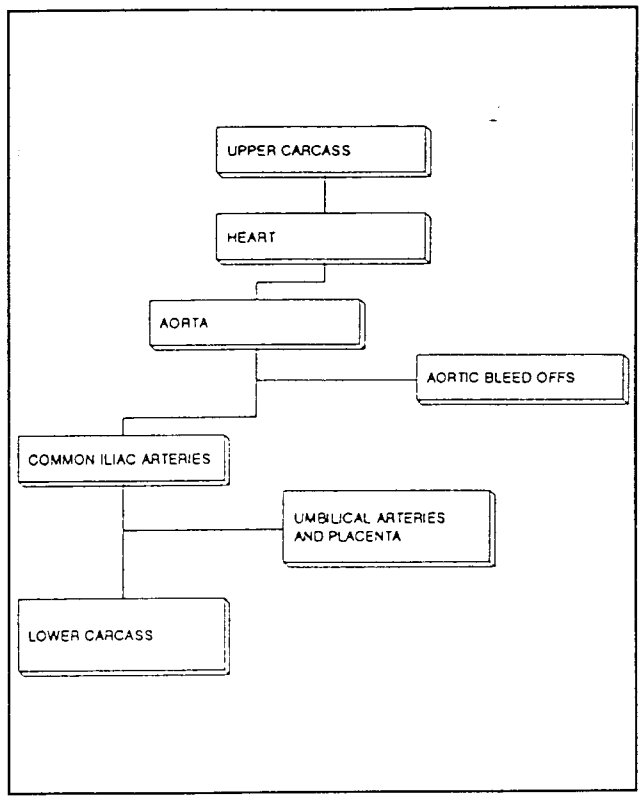

11.3.1 The heart. It is assumed that the two ventricles of the heart have equal volume outputs and mean blood pressures, and can be represented by a single source. The aortic arch and ductus arteriosus were found to be of similar dimensions, which made it possible to simplify the representation of the heart to a single source. The stroke volume was considered to be constant for all normal ranges of FHR which made the modelling of the heart very simple (This was described in section 2.2, page 9). The ejection time (Et) of the heart was set at 180 msec and maintained for all FHRs. Post ejection time (PEt) was thus inversely related to the FHR. Ideally the average placental flow in a normal foetus is approximately 120 ml/min/kg. The placenta receives approximately 41 percent of the cardiac output. Thus the cardiac output must ideally be approximately 291 ml/min/kg. If a standard normal FHR of 140 bpm is assumed, the stroke volume would

be 2.14 ml/kg/stroke.

The input flow waveform is illustrated in figure 11.2. The input waveform had a peak at 53.2 ml (40 mA) and thus gave a stroke volume of 4.84 ml/stroke (FHR =140 bpm; t1=89 msec; t2=2 msec; t3=89 msec). This gave a normalised cardiac output of 263 ml/min/kg and placental flow of 108 ml/min/kg (41.2% of the cardiac output), which were physiologically acceptable.

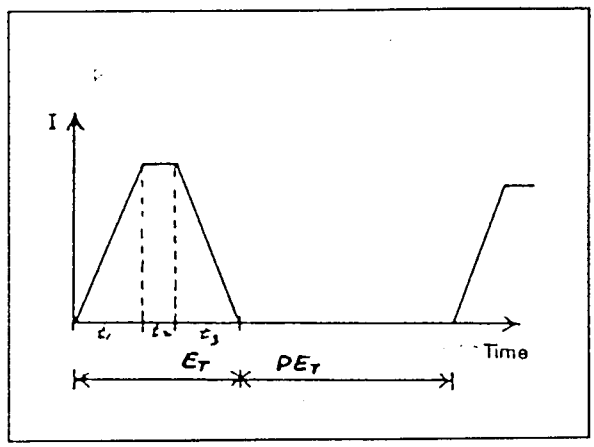

Figure 11.2: The Input Waveform
(Et = Ejection time
PEt = Post Ejection time)

11.3.2 The upper carcass. The mean arterial blood pressure was considered to be 50 mmHg. This was lower than the 60 mmHg used in model 1, however was consistent with human experimental data on foetal blood pressure. (As the thesis was mainly interested in trends in the indices which were dependent on foetal physiological variables, small variations between the models such as this are not important.) The upper carcass was modelled by a single resistance which was dependant on the average flow to it. The upper carcass included the upper limbs, the brain, the adrenals, the heart and the lungs. They were lumped together and modelled as a simple

peripheral bleed off resistor because the flow in this region was not of specific interest to the model.

Table 11.1 (a): Calculated Blood Flow Distribution vs FHR

FHR (bpm)	UMBILICAL ARTERY (%)	UPPER CARCASS (%)	AORTIC BLEED OFFS (%)	LOWER CARCASS (%)
LARGE PLACENTA				
120	46.99	25.51	9.56	17.94
133	42.30	27.77	10.40	19.53
150	37.60	30.03	11.25	21.12
160	35.35	31.16	11.68	21.91
SMALL PLACENTA				
120	23.47	36.83	13.80	25.90
133	21.12	37.96	14.22	26.70
150	18.78	39.09	14.64	27.49
160	17.60	39.66	14.85	27.89
	MEAN PLACENTAL FLOW			
	(ml/min)			
LARGE PLACENTA	281			
SMALL PLACENTA	143			

Table 11.1 (b): Peripheral Resistances vs FHR

FHR (bpm)	UPPER CARCASS (OHMS)	LOWER CARCASS (OHMS)	AORTIC BLEED OFFS (OHMS)
36 WEEK FOETUS			
120	35808	50918	95550
133	29605	42097	79051
150	24335	34601	64957
160	21987	31269	58655
28 WEEK FOETUS			
120	24802	35269	66193
133	21658	30792	57815
150	18695	26583	49916
160	17274	24564	46134

The table of normal flow percentages was calculated as follows: The umbilical volume flow was assumed to be constant at all normal FHRs. Thus, as the cardiac output varied with FHR, so the percentage volume flow to the placenta varied. The remaining blood flow to the periphery was split according to the percentages in table 2.1 which shows normal percentage distribution at a FHR of 140 bpm.

11.3.3 The aorta, aortic arch (AA) and ductus arteriosus (DA). The dimensions of the aorta, aortic arch and ductus arteriosus were taken from human foetal post-mortem specimens (table 5.1). The aortic arch and ductus arteriosus were added in parallel and just like the aorta, were modelled by resistance, compliance and inertance. The AA and DA are approximately 0.9 cm in length and were modelled by one section. The Aorta was broken up into eight equal sections, each section being approximately 0.94 cm long (Appendix G).

The aorta, AA and DA were characterized by plug like flow in a large proportion of the cardiac cycle. This was due to a high value for alpha. Resistances and inertances were thus calculated to accommodate this. Alpha was calculated for these arteries and used in equations 10 and 11 to scale for non-parabolic flow. Table 11.2 present the alpha values, the inductances, resistances and capacitances.

Table 11.2: Arterial Parameters for each FHR

FHR (bpm)	RESISTANCE (ohms)	INDUCTANCE (henry)	CAPACITANCE (farads)	ALPHA
AORTA				
120	90.3	28.66	47u	6.45
133	94.8	28.3	47u	6.96
150	97.01	28.05	47u	7.21
160	99.74	28.03	47u	7.44
ILIACS				
120	226	24.25	0.36u	2.95
133	230	24.16	0.36u	3.18
150	232.5	24.13	0.36u	3.30
160	234	24.07	0.36u	3.40
AA & DA				
120	6.1	1.94	12.7u	6.15
133	6.41	1.91	12.7u	6.48
150	6.55	1.90	12.7u	6.88
160	6.74	1.90	12.7u	7.10

A Young's modulus of 8.5×10^{5} dyne/cm^{2} (Calculated from Struik et al 1992) and a blood viscosity of 3×10^{-2} poise were used for the aorta, AA and DA.

11.3.4 The aortic bleed offs. The aortic bleed offs were represented by four branches radiating from the aorta. The aorta was modelled in eight sections which were combined in T-type formation. Thus four bleed offs representing the aortic bleed off resistances were evenly distributed along the aorta. The mean blood

pressure was 50 mmHg and the resistance was determined by the average volume blood flow through it. The normal percentage of the cardiac output to flow through the aortic bleed offs is given in table 11.1 (a).

11.3.5 The Common Iliac arteries. The dimensions for the common iliac arteries were taken from human foetus post-mortem specimens (table 5.1). The common iliac arteries were combined in parallel and modelled using 4 sections (Appendix G). The reason for this was as follows: the umbilical arteries were modelled in parallel, to form one 'umbilical artery', as they anastomosed just before the placenta. The blood flow down each umbilical artery was considered to be equal, thus combining them in parallel did not alter the amount of blood flow to the placenta. The lower carcass was simply modelled by a single resistance. The common iliac arteries thus pass blood to a single 'umbilical artery' and a single peripheral resistance and were thus simply combined in parallel.

The viscosity of the blood was assumed to remain at 3×10^{-2} Poise in the common iliac arteries, and the Young's modulus of the arterial walls was assumed to be 8.5×10^{6} dyne/cm^2 (Appendix I).

11.3.6 The lower carcass. The lower carcass was represented by a single resistance. The mean pressure was considered to be 50 mmHg and the resistance was determined by the average volume blood flow to it. The normal percentage cardiac output to flow through the

lower carcass is given in table 11.1 (a).

11.3.7 The placental circulation. The model developed by Thompson and Trudinger for the placenta was adapted for this model. The placenta and umbilical arteries were modelled with particular attention to simplifying the branching structure of the system, and each vessel was represented by a resistor, an inductor and a capacitor. The placental resistance was calculated according to equations 15 and 16.

The placenta was modelled as two sets of branches, the first set being the primary and secondary stem villi and the second, the tertiary villi, which branch off each of the vessels of the first set. Vascular changes were modelled as fractional obliteration of the placental bed. The obliteration was either progressive (in which case the larger vessels were obliterated) or distributed (in which case the smaller vessels were obliterated). Obliteration was modelled by fractionally decreasing the number of vessels in each section. Thus the placental resistance increased with increasing obliteration. This was illustrated in model 1 (figure 10.1). Paulick et al (1991) showed that a marked increase in blood pressure was associated with an increased placental resistance. In this model, the blood pressure was thus allowed to vary with variations in placental resistance.

The flow in the umbilical arteries and placenta have already been

shown to be near parabolic and non turbulent, therefore a single alpha value was calculated for a median FHR of 140 bpm and used in equations 10 and 11 to calculate the resistance and the inductance of the arteries. Capacitance was calculated from equation 4 (Table 11.3 illustrates the magnitudes of the resistance, inertance, compliance and alpha at different FHRs.).

The umbilical artery was combined with the radial branching arteries to form one 'umbilical artery'. This was also done in the previous model. The umbilical artery was modelled in the form of a transmission line which incorporated the effects of reflections and transmission line losses experienced in the real artery. The umbilical artery was split into 22 sections. The umbilical artery FVW was shown to comprise of only 3 significant harmonics resulting in the shortest wavelength being at 3 times the maximum frequency, 160 bpm. The length per unit to be used in the transmission line was thus calculated to be 0.869 cm (Appendix G).The magnitudes for resistance, inertance, compliance and alpha are illustrated in table 11.3 and the dimensions of the umbilical artery representing two umbilical arteries and five radially branching arteries are given in table 11.4.

Table 11.3: Placental Arterial Parameters for each FHR (* shows the number of arteries in parallel)

FHR (bpm)	RESISTANCE (per artery)	INDUCTANCE (per artery)	CAPACITANCE (per artery)	ALPHA
UMBILICAL ARTERY (*2)	ohms	henry	farad	
120	10214	1063	4.4u	2.89
133	10406	1052	4.4u	3.15
150	10486	1062	4.4u	3.23
160	10579	1060	4.4u	3.33
RADIAL BRANCH (*5)				
120	31037	865	0.22u	1.44
133	31070	842	0.22u	1.56
150	31111	843	0.22u	1.61
160	31110	852	0.22u	1.65
COMBINED -> UMBILICAL ARTERY (*1)				
120	11314	705	9.9u	-
133	11417	694	9.9u	-
150	11465	700	9.9u	-
160	11511	700	9.9u	-

Table 11.4: Umbilical Artery and Placental Vessel Dimensions (Thompson et al 1990)

UMBILICAL ARTERY	UMBILICAL ARTERIES (2)	RADIAL BRANCHES (5)
RADIUS a (mm) **	1.41	0.705
LENGTH l (mm)	500	100
WALL THICKNESS h (mm)	0.15	0.075
PLACENTA	LARGE BRANCHES	SMALL BRANCHES
RADIUS a (mm)	0.5	0.1
LENGTH l (mm)	100	10
WALL THICKNESS h (mm)	0.1	0.08
RESISTANCE (CGS OHMS)	122230	7639437
CAPACITANCE (CGS FARAD)	58.9n	58.9p
	SMALL PLACENTA	LARGE PLACENTA
No. OF LOBES (n)	10	20
No. OF LOBULES (m)	50	200
YOUNG'S MOD. (Dyne/cm^2)	1E+07	
VISCOSITY (Poise)	0.03	

** OWN ESTIMATION

Table 11.5 illustrates the equivalent dimensions of the arteries once they have been combined in parallel and figure 11.3 illustrates the circuit diagrams designed to represent the foetal placental arterial circulation.

Table 11.5: Equivalent Dimensions for the Simplified Foetal Arterial Circulation

	RADIUS (cm)	LENGTH (cm)	WALL THICKNESS (cm)
AORTA	0.315	7.5	0.0283
COMMON ILIAC ARTERY	0.144	1.2	0.0055
UMBILICAL ARTERY	0.107	19.10	0.0011

The viscosity of the blood in the umbilical artery was 3×10^{-2} Poise and the Young's modulus of the artery walls was 1×10^{7} dyne/cm^2 (Appendix I).

The circuits used to represent the foetal circulation are given below (figure 11.3).

Figure 11.3: Circuit Diagrams of Model 2

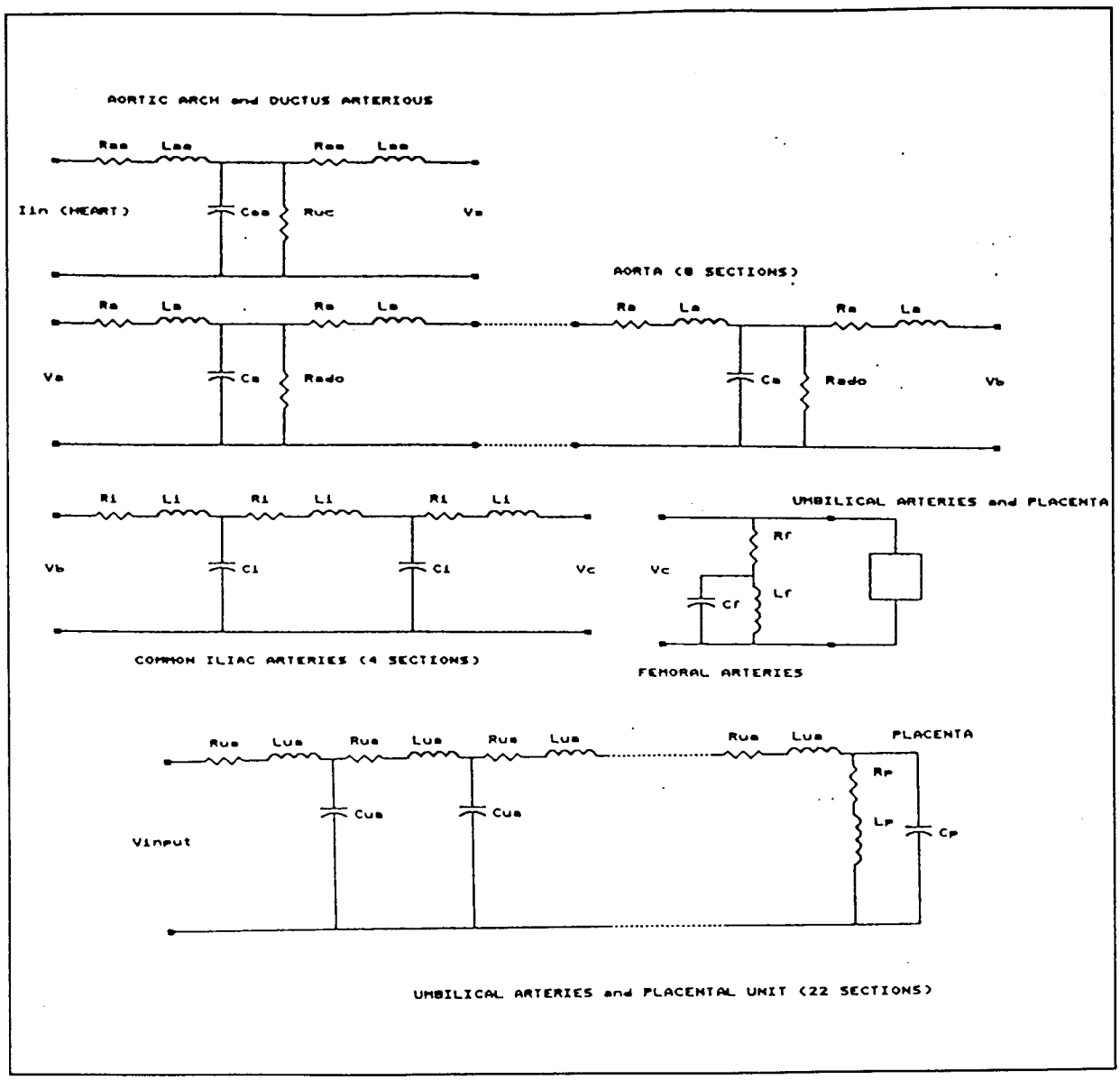

11.4 THE UMBILICAL FVW

Unlike model 1, this model simulated a FVW which was very similar to that present in a live foetus. Reduced flow and eventually reversed flow occurred with increasing placental resistance. This phenomenon has been described by Morrow et al (1989) and Adamson et al (1991) and was evident in the clinical FVWs.

Two examples of the simulated umbilical artery FVWs are given in figure 11.4. Clinical examples are given in figure 11.5. The similarity is evident.

Figure 11.4: Simulated FVW's

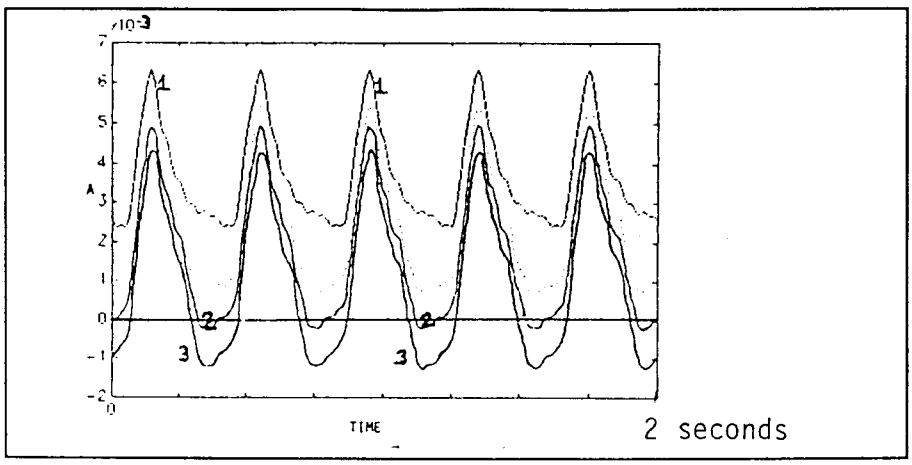

Figure 11.5: Clinical FVW's (Morrow et al 1989)

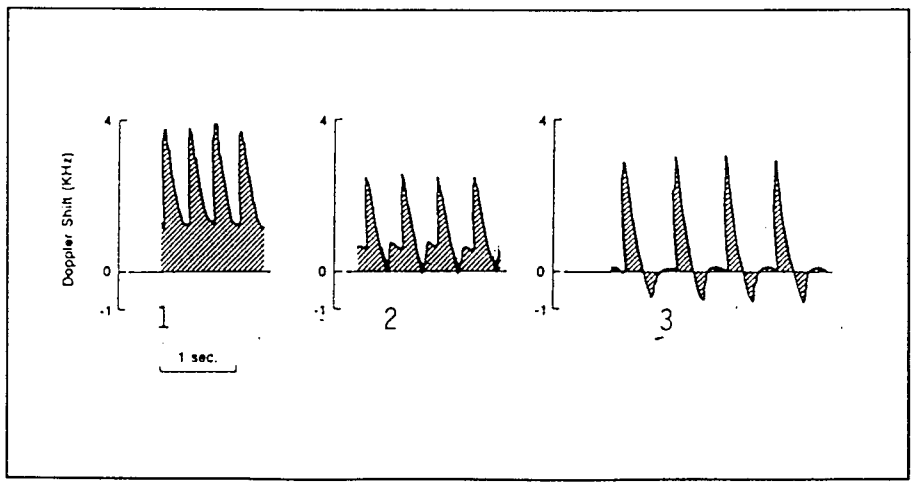

1 - normal flow

2 - absent flow

3 - reversed flow

A - amplitude of flow (Amps)

11.5 THE ASSUMPTIONS OF THE MODEL

The model was based on the following assumptions:

1) The stroke volume and ejection times were constant.

2) The Young's modulus and blood viscosity were 1×10^{7} dyne/cm^{2} and 3×10^{-2} Poise respectively for the umbilical vessels. The Young's modulus for the aorta and common iliac arteries were 8.5×10^{5} dyne/cm^{2} and 8.5×10^{6} dyne/cm^{2} respectively.

3) The mean arterial blood pressure was ideally 50 mmHg.

4) The resistances and inertances were calculated for the fundamental frequency of the FVW.

5) The umbilical blood flow was 41.2 percent of the cardiac output for a 36 week foetus.

6) The umbilical blood flow was 109 ml/min/kg for a 36 week foetus.

7) The aorta was represented by 8 sections, the iliac arteries were combined in parallel and consisted of 4 sections, two umbilical arteries and 5 radial branching arteries were modelled as a single artery consisting of 22 sections.

8) The upper carcass, lower carcass and aortic bleed offs were each represented by a single resistor.

9) The inertance of blood in the umbilical arteries were incorporated into the system to allow the calculation of the phase velocity.

10) Uniform obliteration occurred in the placenta which simulated fractional decrease in the number of vessels in the placenta. Obliteration lead to an increase in blood pressure.

11) The effects of non parabolic flow were implemented by calculating alpha which was used in equations 10 and 11.

12) The umbilical arteries and placenta are not innervated. In a normal foetus the placenta and umbilical arterial resistance was assumed constant and played no role in maintaining blood pressure.

13) The increases in placental resistance due to embolisation overshadowed any small increase in placental and umbilical resistance due to induced hypoxia.

14) Long term FHR variations were associated with a variation in peripheral resistances in an attempt to maintain the mean blood pressure.

15) Short term FHR variations caused variations in the mean blood pressure as the peripheral resistances do not have enough time to respond.

11.6 THE PHYSIOLOGICAL CONDITIONS INCORPORATED IN THE MODEL

Two different physiological systemic adaptations were analyzed. The model did not include a control system to simulate these adaptations. They thus needed to be analyzed individually with the user of the model completing the control loop.

The two physiological adaptations analyzed were:

i) Long term FHR variations. This involved basal FHR variations. In this case the peripheral resistances were adjusted to accommodate the change in cardiac output. The mean arterial blood pressure was

thus theoretically maintained at a constant value for a normal placenta. As the placental resistance was increased so the blood pressure was allowed to increase (figure 11.6).

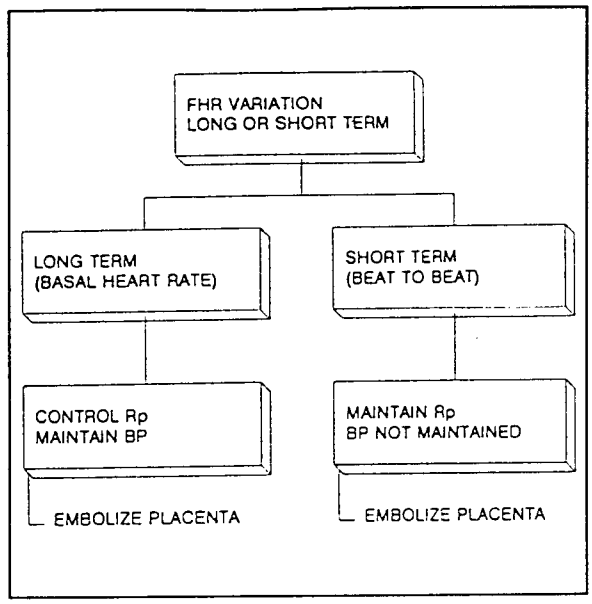

Figure 11.6: Response to FHR Variations

ii) Short term FHR variations. These variations were considered to be the beat to beat variation of the FHR around a basal FHR. In this case the peripheral resistances were not adjusted to accommodate for the change in cardiac output, since, in the case of the foetus, the control systems are too slow to respond. The mean arterial blood pressure variations were thus directly related to the change in cardiac output due to FHR variations (figure 11.6).

11.7 THE NUMERICAL VALUES FOR LONG TERM FHR VARIATIONS

As stated earlier, the percentage distribution of the cardiac output to the periphery varied with a variation in FHR, in order to

maintain a constant blood pressure.

The tables 11.1 (a) and (b) show the percentage blood flow distribution, resistances, inertances and compliances for each vessel or peripheral bleed off for long term FHR variations.

CHAPTER TWELVE

SIMULATIONS OF THE UMBILICAL BLOOD FLOW WAVEFORMS USING MODEL 2

12.1 INVESTIGATIONS

The model was used to investigate the following:

12.1.1 The effect of FHR variations on the RI, PI and HRSI. The effects of both long and short term FHR variations were analyzed. The analysis was done on a normal placenta.

12.1.2 The effect of placental obliteration on the RI, PI and HRSI. Placental obliteration was simulated in the same way as described earlier under the Thompson and Trudinger model (Model 1) and is representative of placental embolization or an increase in placental resistance due to hypoxia.

It is known that an increase in placental resistance causes an increase in mean blood pressure (Paulick et al 1987). In this experiment the peripheral resistances were maintained as the placental resistance was varied. The analogy is that of acute obliteration.

The effect of placental size, type of placental obliteration, the mean umbilical blood pressure and blood pressure pulsatility were analyzed for both responses to FHR variations.

12.1.3 The effect of site of measurement (along the umbilical artery) on the FVW. The FVW was simulated at four different sites along the umbilical artery and the RI and PI calculated. The simulation was done on a normal large placenta, resulting in a HRSI value of zero.

12.2 RESULTS

12.2.1 FHR variations in a normal placenta. The FHR was varied over the normal range of 120 bpm to 160 bpm.

i) LONG TERM EFFECTS

a) n=20 m=200 (large placenta)

The HRSI was constant at zero over this range of FHRs. The RI was approximately 0.54 and PI was approximately 0.82. Both RI and PI decreased slightly with increasing FHR, RI decreased by a maximum of 3.7 %, and PI by a maximum of 4.9 % (table 12.1). The mean blood pressure and blood pressure pulsatility are illustrated in table 12.5 and are both constant for this simulation.

Table 12.1: Index magnitudes vs FHR (large placenta with no obliteration)

	FHR = 120	FHR = 133	FHR = 150	FHR = 160
HRSI	0	0	0	0
RI	0.55	0.54	0.53	0.52
PI	0.85	0.82	0.79	0.78

b) n=10 m=50 (small placenta)

The HRSI, RI and PI all increased with increasing FHR. HRSI varied from 0.77 to 6.09, RI and PI were approximately 0.76 and 1.71 respectively but increased by a maximum of 5.3 % and 3.5 % respectively (table 12.2).

Table 12.2: Index magnitudes vs FHR (small placenta with no obliteration)

	FHR = 120	FHR = 133	FHR = 150	FHR = 160
HRSI	0.77	1.30	4.35	6.09
RI	0.74	0.76	0.78	0.80
PI	1.72	1.71	1.75	1.77

ii) SHORT TERM EFFECTS

a) n=20 m=200 (large placenta)

HRSI was constant at zero over this range of FHR. At a FHR of 133 bpm the RI equalled 0.56 and PI equalled 0.87 but these decreased by 14.3 % and 20.69 % respectively over the range of FHR's (table 12.3). The mean blood pressure (BP) and blood pressure pulsatility (BPPI) are illustrated in table 12.6. The BP increased with increasing FHR and the BPPI decreased with increasing FHR. The percentage blood distribution was maintained at a constant value as the FHR was varied. This was due to the fact that the peripheral resistances were maintained at constant values.

Table 12.3: Index magnitudes vs FHR (large placenta with no obliteration)

	FHR = 120	FHR = 133	FHR = 150	FHR = 160
HRSI	0	0	0	0
RI	0.61	0.59	0.54	0.51
PI	1.0	0.87	0.76	0.69

b) n=10 m=50 (small placenta)

HRSI was not zero in the small normal placenta. All the indices were elevated reflecting the elevated placental resistance in the small placenta. The indices all decreased with increasing FHR. The HRSI decreased from 8.23 to 1.33 with a standard value at 133 bpm of 4.8. The RI varied by 2.56% from 0.76 to 0.80. The PI varied by 13.2% from 2.03 to 1.58 with a standard value at 133 bpm of 1.82 (table 12.4). The percentage blood distribution was maintained at a nearly constant value for all values of normal FHR.

Table 12.4: Index magnitudes vs FHR (small placenta with no obliteration)

	FHR = 120	FHR = 133	FHR = 150	FHR = 160
HRSI	8.23	4.08	1.85	1.33
RI	0.80	0.78	0.77	0.76
PI	2.03	1.82	1.66	1.58

Table 12.5: BP and BPPI vs FHR and Obliteration (long term)

q	FHR = 120 BP BPPI	FHR = 133 BP BPPI	FHR = 150 BP BPPI	FHR = 160 BP BPPI	PERCENTAGE VARIATION FROM THE MEAN
0	49 (0.673)	49 (0.673)	49 (0.653)	50 (0.62)	0.9 (3.0)
0.3	53 (0.654)	53 (0.65)	52 (0.596)	52 (0.577)	0.95 (4.8)
0.6	60 (0.55)	59 (0.552)	57 (0.526)	57 (0.526)	2.2 (1.9)
0.8	69 (0.478)	67 (0.485)	64 (0.484)	63 (0.492)	3.6 (1.0)
0.85	72 (0.472)	70 (0.464)	66 (0.469)	66 (0.469)	3.8 (0.6)
0.9	76 (0.447)	73 (0.438)	69 (0.449)	68 (0.441)	4.5 (0.9)
0.915	78 (0.436)	74 (0.432)	70 (0.443)	69 (0.435)	4.9 (0.9)
0.93	79 (0.430)	75 (0.427)	71 (0.437)	70 (0.429)	4.8 (0.9)
0.945	81 (0.432)	77 (0.429)	73 (0.411)	71 (0.423)	5.1 (1.9)

Table 12.6: BP and BPPI vs FHR and Obliteration (short term)

q	FHR = 120 BP BPPI	FHR = 133 BP BPPI	FHR = 150 BP BPPI	FHR = 160 BP BPPI	PERCENTAGE VARIATION FROM THE MEAN
0	42 (0.81)	46 (0.717)	52 (0.577)	56 (0.536)	11 (16.7)
0.3	44 (0.75)	49 (0.653)	55 (0.564)	60 (0.517)	11.6 (14.4)
0.6	49 (0.673)	55 (0.582)	62 (0.5)	66 (0.469)	11.2 (14.4)
0.7	52 (0.635)	58 (0.552)	65 (0.462)	70 (0.429)	11.1 (14.4)
0.75	54 (0.611)	59 (0.542)	67 (0.449)	72 (0.431)	11 (13.7)
0.9	61 (0.541)	68 (0.471)	76 (0.408)	82 (0.366)	11.1 (15.7)
0.92	63 (0.524)	69 (0.464)	78 (0.384)	84 (0.369)	11 (13.8)
0.95	65 (0.508)	72 (0.444)	81 (0.37)	87 (0.356)	11 (14.3)

12.2.2 The effect of placental vascular resistance on the HRSI, RI and PI.

The fraction of vessels obliterated was denoted by q (Thompson and Trudinger 1990). As q increased, the total resistance of the placental bed increased and the total capacitance decreased. The increase in resistance was dependant on the type of obliteration simulated. The relationships between fractional obliteration, size of placenta, type of obliteration and placental resistance are illustrated in figure 12.1.

Figure 12.1: Placental Resistance vs q

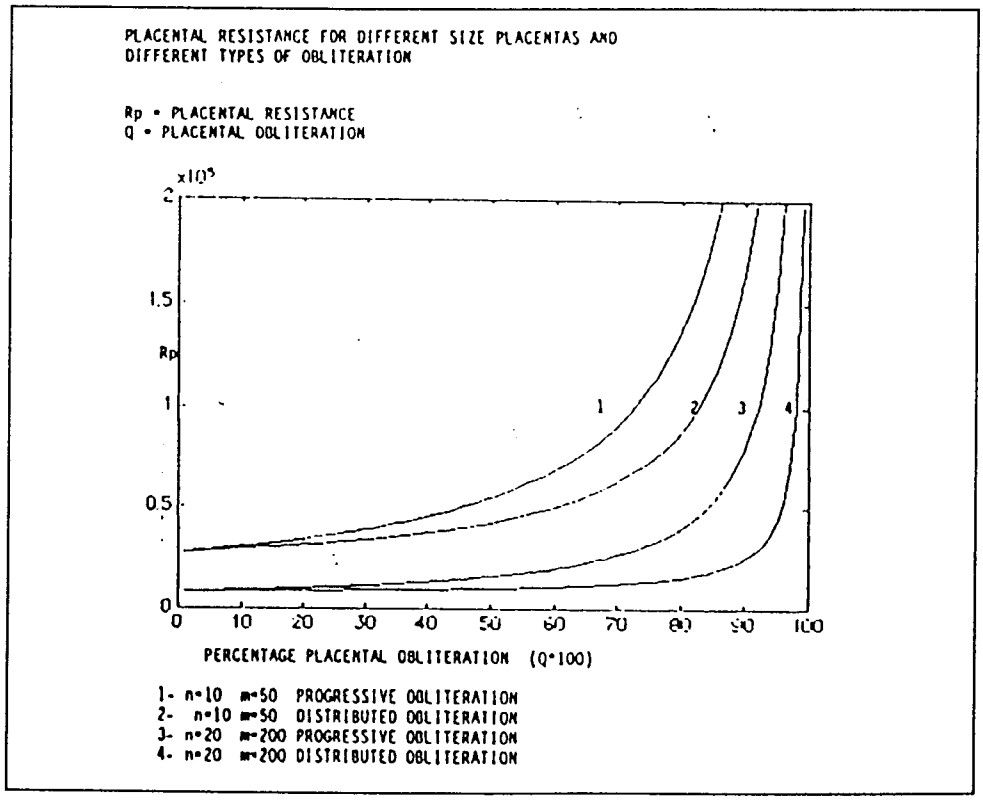

The effects of these variables were analyzed in this section.

i) LONG TERM EFFECTS ON A LARGE AND A SMALL PLACENTA

a) THE EFFECT OF INCREASING PLACENTAL OBLITERATION ON THE INDICES

The increase in placental obliteration (q) resulted in increases in the HRSI, RI and PI (figures 12.2, 12.3 and 12.4 respectively).

The increases in the indices were exponential. At 133 bpm the correlation coefficients were 0.929, 0.908 and 0.888 for RI, PI and HRSI respectively, for a large placenta with progressive obliteration. A linear correlation on the same results revealed lower correlation coefficients of 0.907, 0.831 and 0.707 respectively, revealing a more significant exponential relationship between the placental obliteration and the indices.

Figure 12.2:
RI vs q

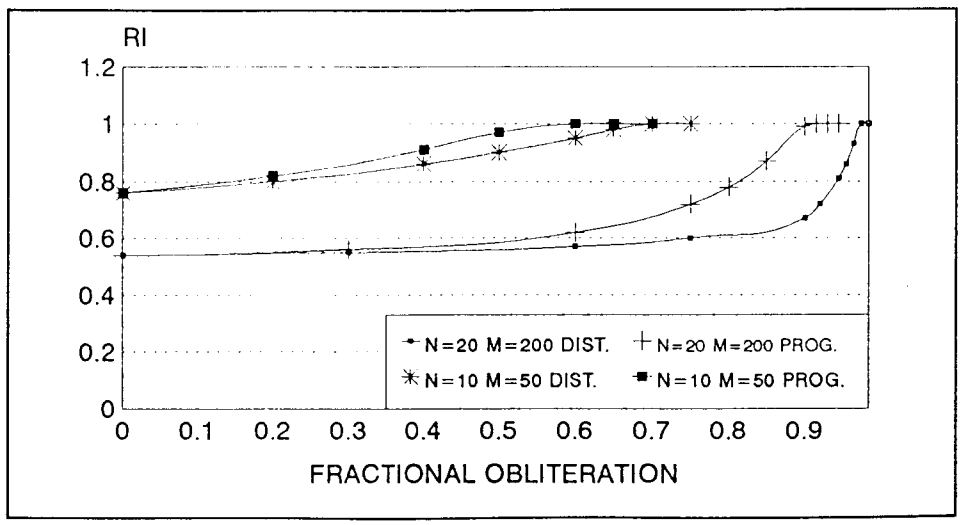

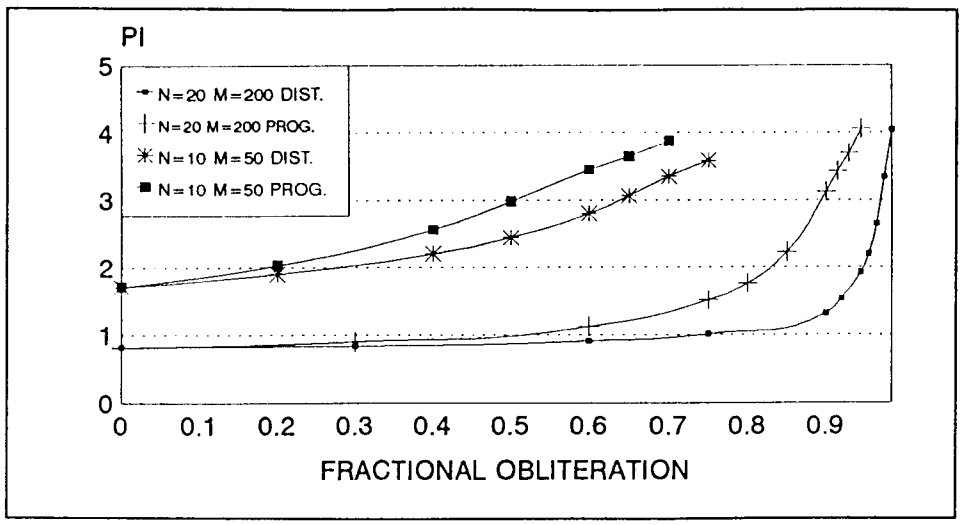

Figure 12.3:

PI vs q

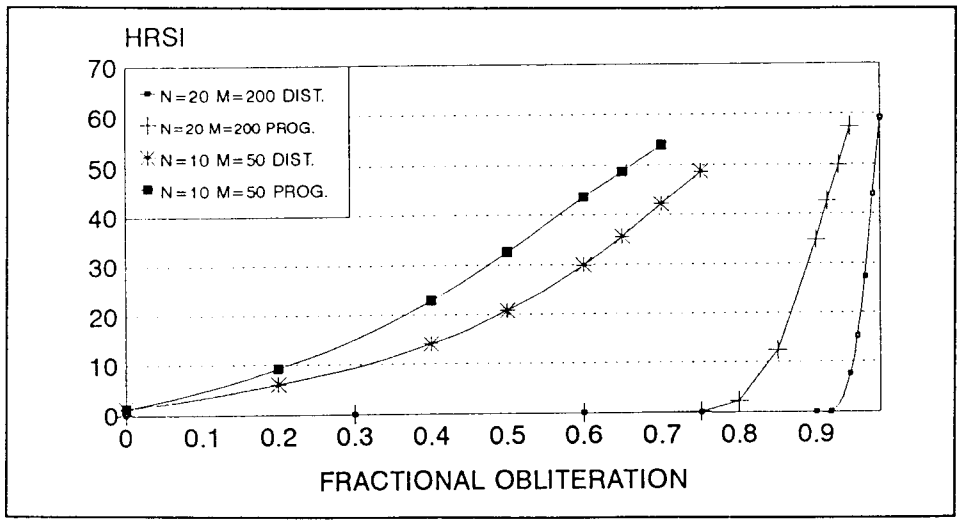

Figure 12.4:

HRSI vs q

RI saturated at unity at large degrees of obliteration (90 (progressive) to 97 (distributed) percent obliteration for a large placenta and 50 (progressive) to 65 (distributed) for a small placenta). At this stage the PI reached a value approximately equal to 3.2, the HRSI reached a value of approximately 40 percent.

These two indices continued to increase for additional increases in placental obliteration.

b) THE EFFECT OF THE TYPE OF OBLITERATION ON THE INDICES

The relationship between the placental resistance and the type of obliteration is illustrated in figure 12.1. The indices which describe the FVW are dependent on the placental resistance and are thus also affected by the type of placental obliteration as the type of placental obliteration is simply a mode of increasing the placental resistance.

c) THE EFFECT OF FHR VARIATIONS DURING OBLITERATION

The analysis is done for progressive obliteration. The effects of the FHR variations were analyzed on the indices once absent flow was established. The RI was saturated at unity at this stage and was thus unaffected by FHR variations. The PI decreased with increasing FHR by minimal amounts (Table 12.7). The HRSI increased with increasing FHR by significant amounts as the FHR increased from 120 to 160 bpm. The variation of the index however decreased as the duration of absent flow became longer. HRSI was thus more affected by FHR variations at the point when absent flow was first established than large degrees of absent flow was present. Thus, as the obliteration increased so the dependence of the HRSI on FHR variations decreased (Table 12.7).

Placental obliteration between zero and the first sign of absent flow yielded an inconsistent behaviour of the indices with FHR variations. The mean, standard deviations and percentage variation are represented in table 12.7.

Table 12.7: Index Mean, Standard Deviations and Percentage Variation over the FHR Range (120 to 160 bpm) (long term)

q	RI	PI	HRSI
N=20 M=200			
0	0.54 +- 0.01 (1.85%)	0.81 +- 0.027 (3.33%)	0.0 +- 0.00 (0%)
0.3	0.56 +- 0.004 (0.71%)	0.90 +- 0.02 (2.22%)	0.0 +- 0.00 (0%)
0.6	0.63 +- 0.009 (1.43%)	1.13 +- 0.01 (0.88%)	0.0 +- 0.00 (0%)
0.75	0.74 +- 0.03 (4.05%)	1.56 +- 0.06 (3.85%)	1.16 +- 1.16 (100%)
0.8	0.80 +- 0.03 (3.75%)	1.83 +- 0.078 (4.26%)	4.59 +- 3.25 (70.8%)
0.85	0.89 +- 0.03 (3.37%)	2.30 +- 0.108 (4.7%)	16.14 +- 6.28 (38.9%)
0.9	0.99 +- 0.012 (1.21%)	3.16 +- 0.06 (1.9%)	37.78 +- 5.97 (15.8%)
0.915	1.0 +- 0.00 (0%)	3.45 +- 0.018 (0.52%)	44.89 +- 4.86 (10.8%)
0.93	1.0 +- 0.00 (0%)	3.74 +- 0.06 (1.6%)	51.88 +- 3.91 (7.5%)
0.945	1.0 +- 0.00 (0%)	4.04 +- 0.14 (3.47%)	57.94 +- 2.02 (3.49%)
N=10 M=50			
0	0.77 +- 0.022 (2.86%)	1.74 +- 0.024 (1.38%)	3.12 +- 2.19 (70.2%)
0.2	0.84 +- 0.024 (2.86%)	2.07 +- 0.038 (1.84%)	11.02 +- 3.15 (28.6%)
0.4	0.93 +- 0.027 (2.9%)	2.61 +- 0.044 (1.69%)	25.19 +- 4.08 (16.2%)
0.5	0.98 +- 0.019 (1.94%)	3.03 +- 0.043 (1.42%)	34.94 +- 4.28 (12.25)
0.6	1.0 +- 0.00 (0%)	3.45 +- 0.072 (2.09%)	45.12 +- 3.07 (6.8%)
0.65	1.0 +- 0.00 (0%)	3.65 +- 0.097 (2.66%)	50.07 +- 2.60 (5.19%)
0.7	1.0 +- 0.00 (0%)	3.87 +- 0.131 (3.38%)	54.89 +- 2.06 (3.75%)

LONG TERM FHR VARIATIONS

The index magnitudes for RI, PI and HRSI for varying FHR and placental obliteration are illustrated in table 12.8. The pulsatility of the umbilical artery blood pressure (BPPI) and the

mean umbilical blood pressure (BP) at different FHRs are illustrated in table 12.5.

Figures 12.5, 12.6, 12.7, and 12.8 illustrate the relationship between RI, PI, HRSI, BP, BPPI and FHR variations at absent flow.

Table 12.8: Index Magnitudes vs q at Different FHRs (long term)

	HRSI	RI	PI	HRSI	RI	PI
q	FHR=120	FHR=120	FHR=120	FHR=133	FHR=133	FHR=133
0	0	0.55	0.85	0	0.54	0.82
0.3	0	0.57	0.93	0	0.56	0.90
0.6	0	0.62	1.14	0	0.62	1.12
0.8	0.93	0.76	1.75	2.21	0.78	1.76
0.85	8.02	0.85	2.18	12.41	0.87	2.22
0.9	29.64	0.97	3.08	34.73	0.99	3.12
0.915	38.15	1	3.47	42.64	1	3.43
0.93	46.53	1	3.84	49.85	1	3.70
0.945	54.85	1	4.26	57.45	1	4.06
q	FHR=150	FHR=150	FHR=150	FHR=160	FHR=160	FHR=160
0	0	0.53	0.79	0	0.52	0.78
0.3	0	0.56	0.88	0	0.56	0.88
0.6	0	0.62	1.12	0	0.64	1.14
0.8	6.07	0.81	1.86	9.16	0.84	1.94
0.85	20.06	0.91	2.36	24.05	0.93	2.45
0.9	41.89	1	3.20	44.87	1	3.23
0.915	48.13	1	3.43	50.67	1	3.46
0.93	54.76	1	3.70	56.38	1	3.70
0.945	59.54	1	3.96	59.93	1	3.89

N=20 M=200 PROGRESSIVE OBLITERATION

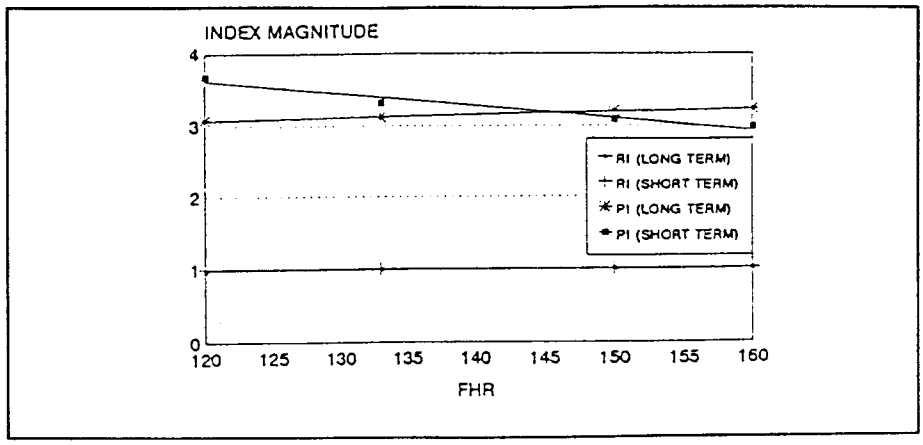

Figure 12.5:

RI and PI vs FHR

(at absent flow)

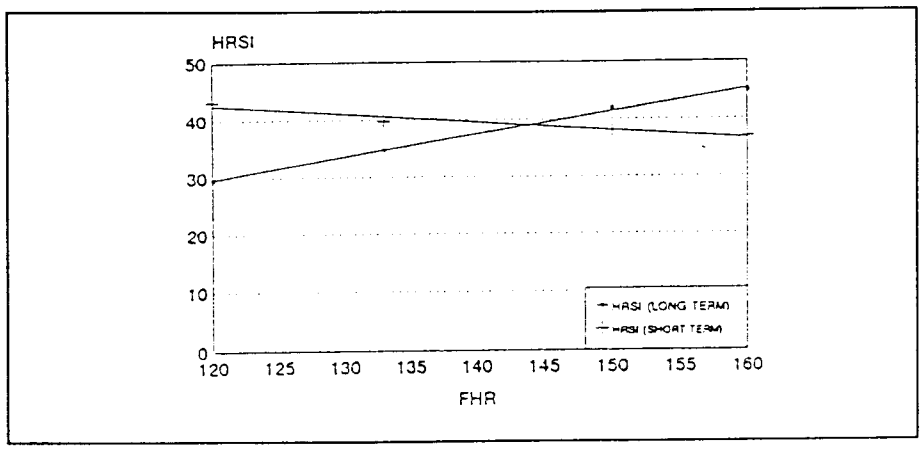

Figure 12.6:

HRSI vs FHR

(at absent flow)

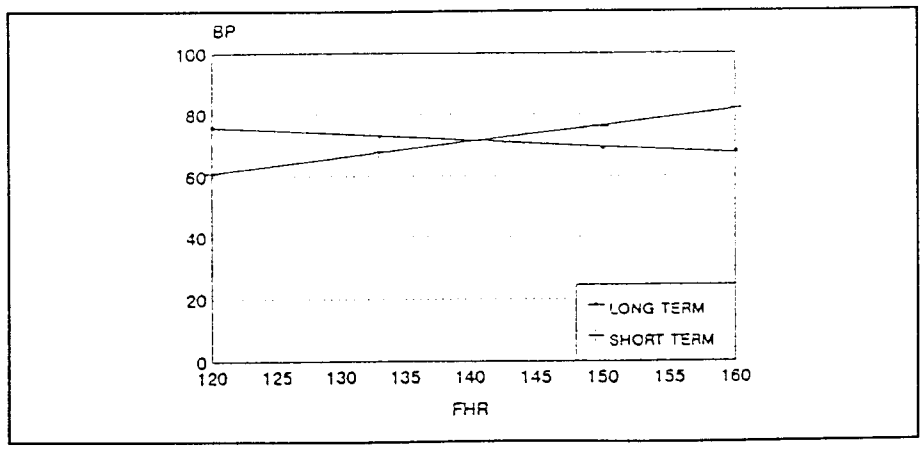

Figure 12.7:

BP vs FHR

(at absent flow)

Figure 12.8:

BPPI vs FHR

(at absent flow)

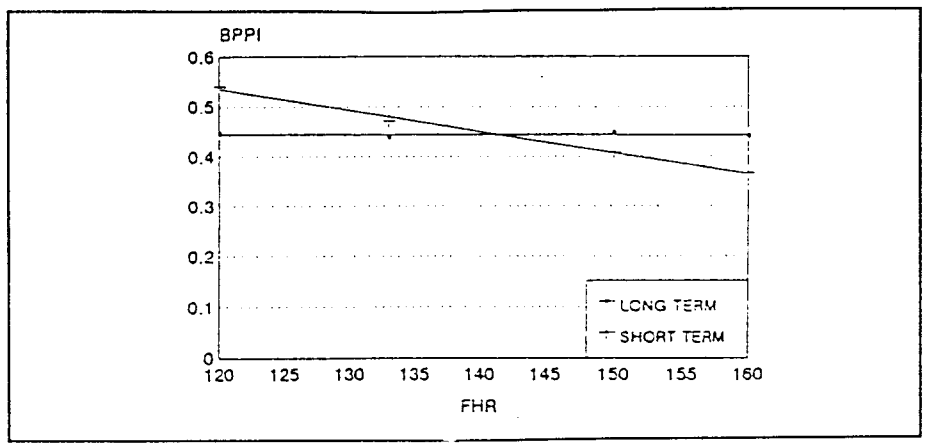

d) BLOOD FLOW DISTRIBUTION

Blood flow increased to the periphery with increasing placental obliteration. This was because of the increased placental resistance and reduced placental flow. The umbilical flow decreased from 41.57 percent of the cardiac output to between 9 and 7 percent as the number of vessels in a large placenta were obliterated from zero to 94.5% (progressive) and 98.8% (distributed) (figures 12.9 and 12.10).

Figure 12.9: Percentage Umbilical Flow vs q (large and small placenta)

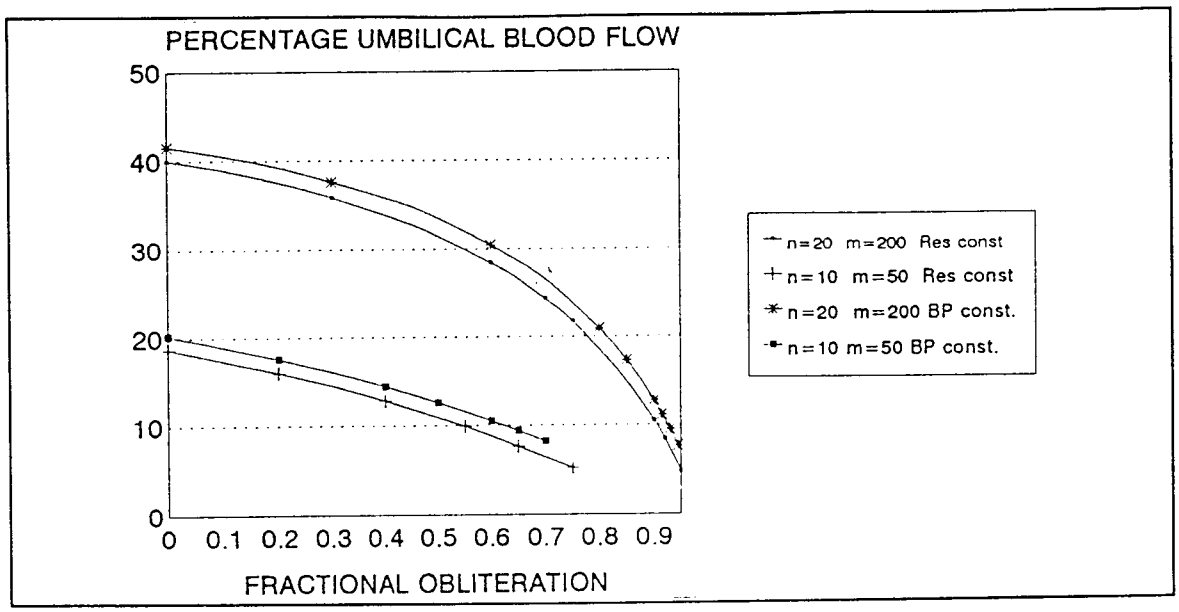

Figure 12.10: Percentage Blood Flow vs q (large placenta)

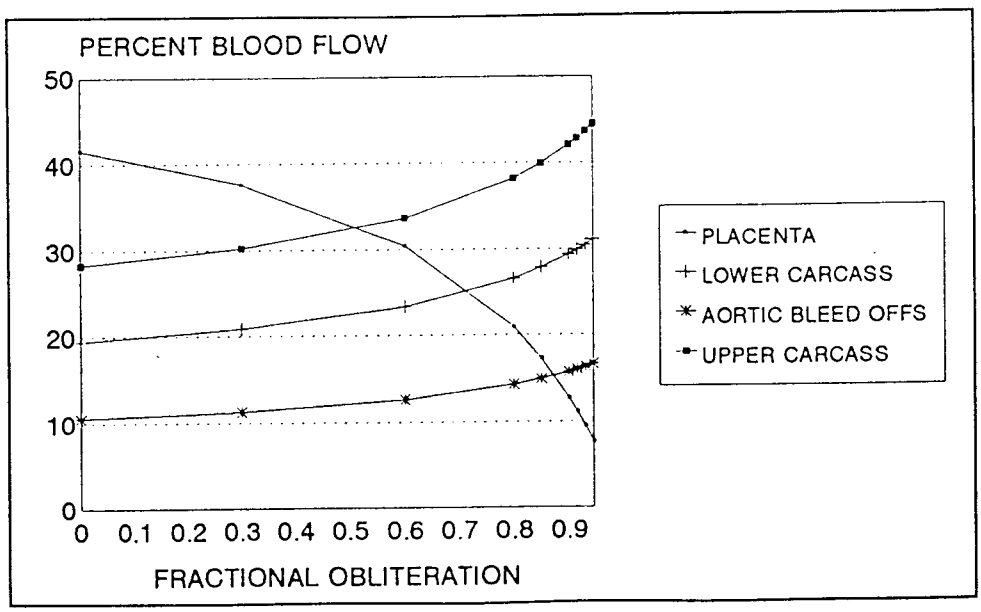

In the case of a small placenta, the umbilical flow decreased from 20.24 percent of the cardiac output to between 10 and 8 percent as it was obliterated as above (figure 12.11).

Figure 12.11: Percentage Blood Flow vs q (small placenta)

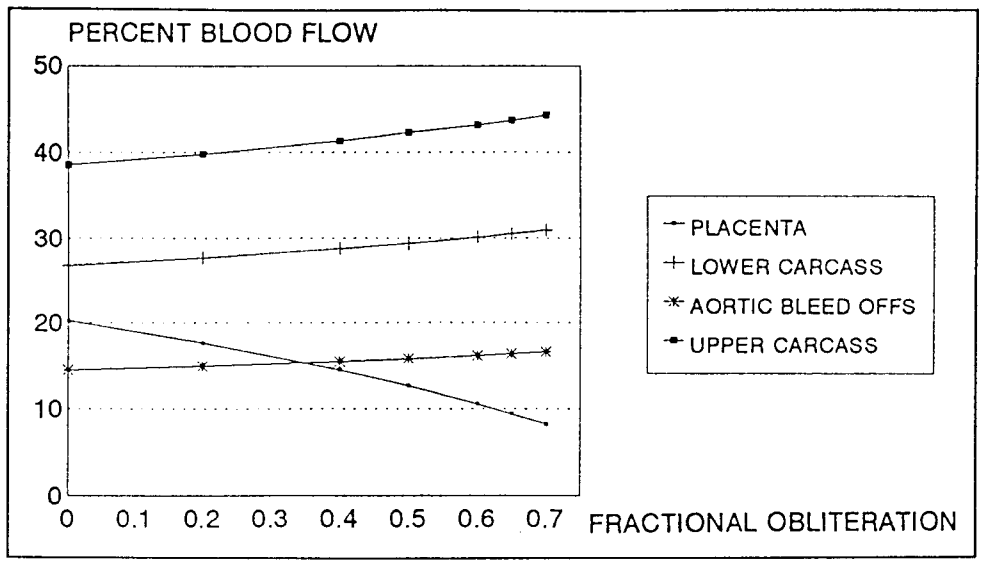

ii) SHORT TERM EFFECTS ON A LARGE AND SMALL PLACENTA

Excluding the umbilical and placenta resistance which were altered in cases of obliteration, the peripheral resistances were maintained at constant values and the blood pressure was allowed to vary with variations in FHR.

a) THE EFFECT OF INCREASING PLACENTAL OBLITERATION ON THE INDICES

Increasing placental obliteration (q) resulted in exponential increases in HRSI, RI and PI (At 133 bpm the correlation coefficients were 0.894, 0.876 and 0.775 for RI, PI and HRSI respectively.). A linear correlation revealed lower correlation

coefficients of 0.865, 0.799 and 0.695 respectively indicating an exponential relationship between placental obliteration and the indices. The RI saturated at unity at large degrees of obliteration (90 to 98 percent obliteration in a large placenta and between 55 and 65 percent obliteration in a small placenta). At this stage the PI reached a value approximately equal to 3.3, and the HRSI reached a value of approximately 40 percent. These two indices continued to increase for additional increases in placental obliteration (figures 12.12, 12.13 and 12.14).

Figure 12.12:

RI vs q

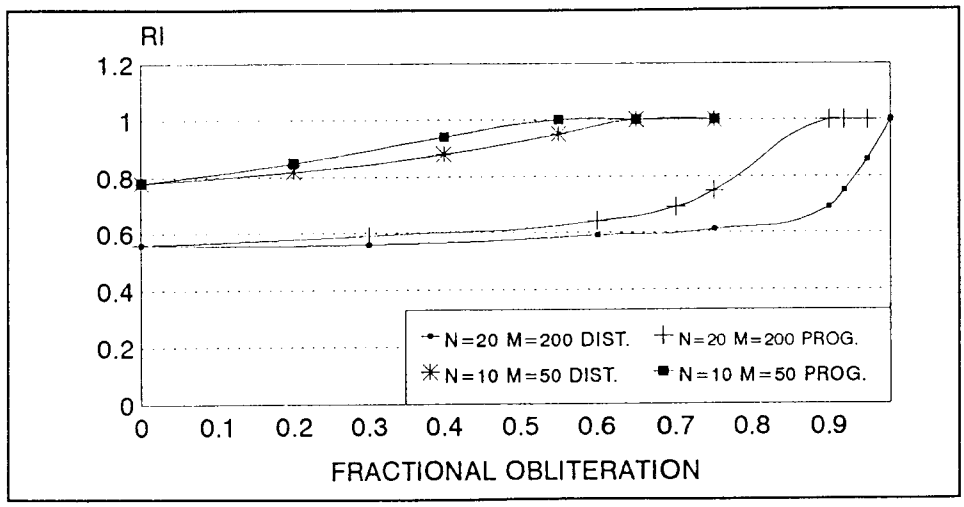

Figure 12.13:

PI vs q

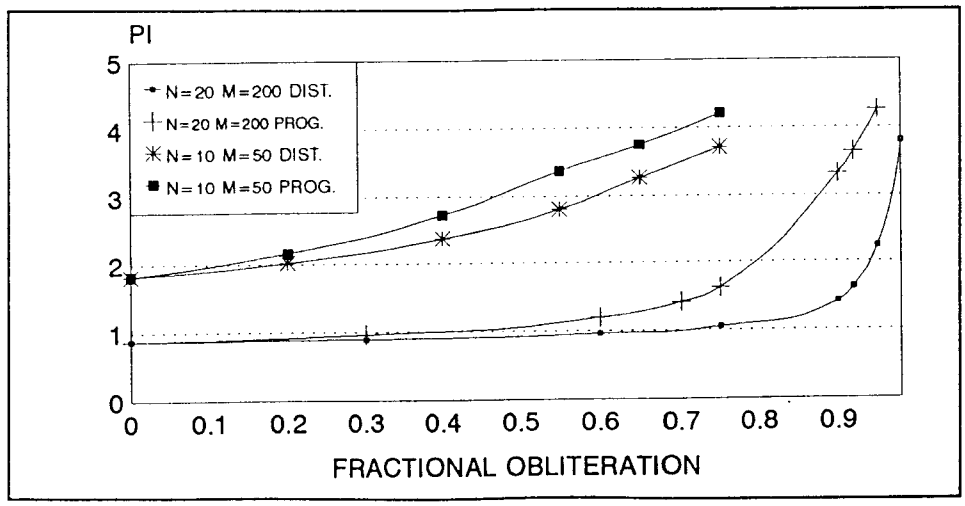

Figure 12.14:

HRSI vs q

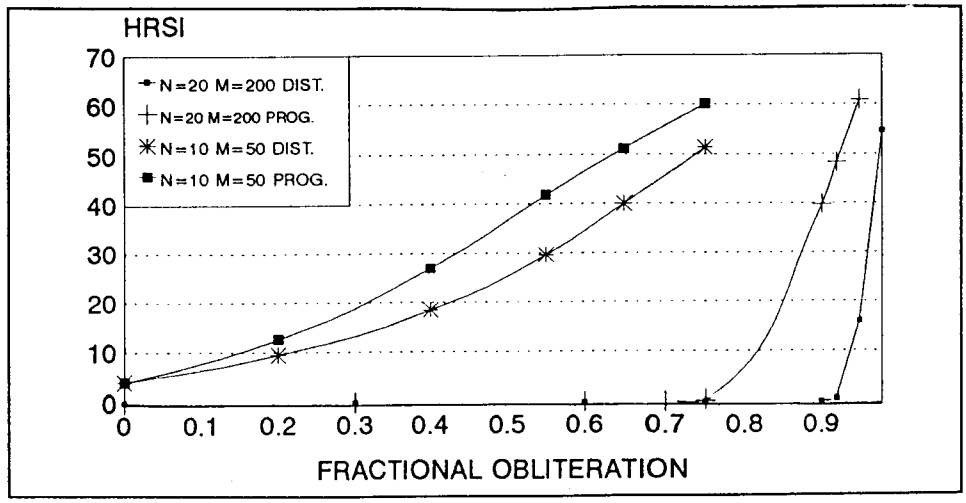

The dependence of the indices on the type of obliteration and the reduction of blood flow to the placenta with increased placental resistance followed similar trends to that in long term FHR variation simulations. The results are presented in figures 12.12, 12.13, 12.14, 12.15 and 12.16 and will not be described in detail.

Figure 12.15: Percentage Blood Flow vs q (large placenta)

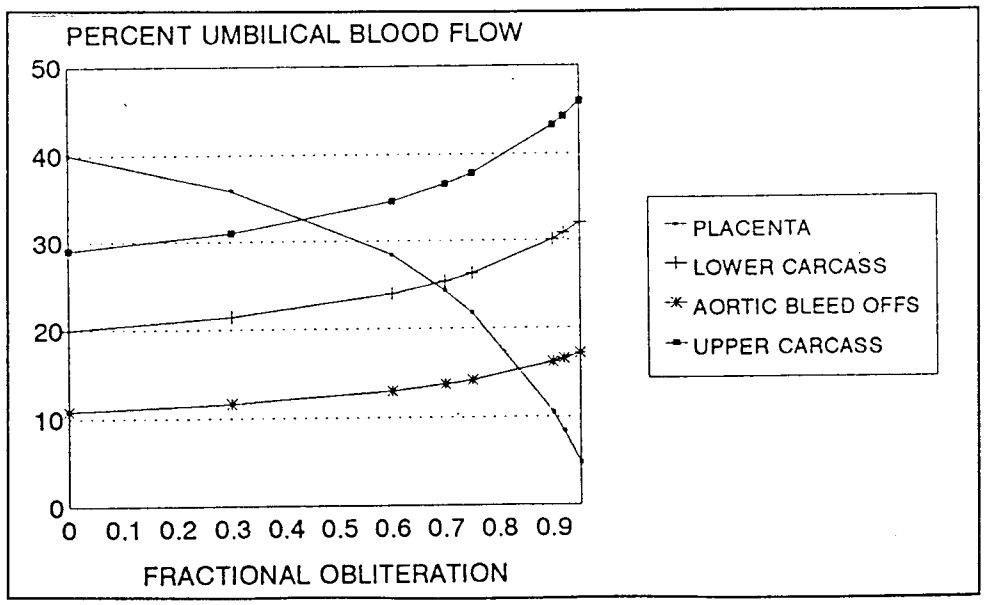

Figure 12.16: Percentage Blood Flow vs q (small placenta)

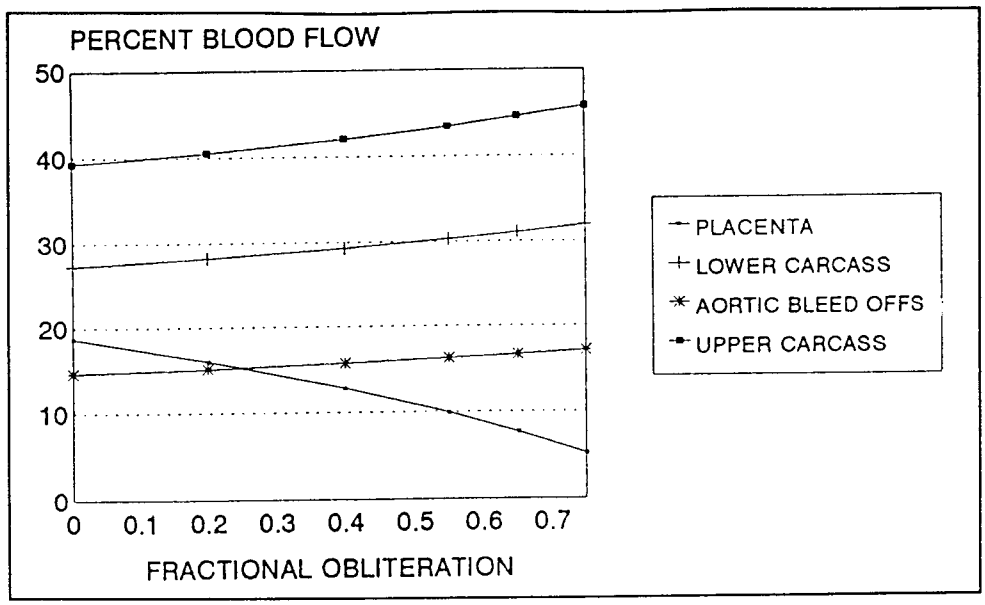

b) THE EFFECT OF FHR VARIATIONS DURING OBLITERATION

The effects of FHR were analyzed on the indices once absent flow had been established. The RI was saturated at unity at this stage and was thus unaffected by FHR variations. The PI decreased with increasing FHR by significant amounts (Table 12.9). This was evident for all magnitudes of elevated index values.

The HRSI, however, was not greatly affected by FHR variations as absent and further reductions in flow were obtained (Table 12.9). This is evident if one observes the variation of HRSI at 90% obliteration in a large placenta and at 55% obliteration in a small placenta. The index variation is as low as 6 %.

Placental obliteration between zero and the first sign of absent

flow, yielded a consistent decrease in all the indices with increasing FHR. The relationship between the index variation and FHR variations at different degrees of obliteration are illustrated in table 12.9. The mean, the standard deviation and percentage deviations are given in this table. The magnitudes for RI, PI and HRSI are illustrated in table 12.10.

The blood pressure was noted to always increase with increasing FHR yet the blood pressure pulsatility of the umbilical artery blood pressure always decreased with increasing FHR (table 12.6).

Table 12.9: Index Mean, Standard Deviation and Percentage Variation over the FHR Range (120 to 160 bpm) (short term)

q	RI	PI	HRSI
N=20 M=200			
0	0.54 +- 0.05 (9.26%)	0.83 +- 0.12 (14.45%)	0.0 +- 0.00 (0%)
0.3	0.57 +- 0.05 (8.77%)	0.92 +- 0.13 (14.13%)	0.0 +- 0.00 (0%)
0.6	0.63 +- 0.04 (6.35%)	1.15 +- 0.14 (12.17%)	0.0 +- 0.00 (0%)
0.7	0.68 +- 0.02 (2.94%)	1.37 +- 0.13 (9.49%)	0.06 +- 0.06 (100%)
0.75	0.74 +- 0.02 (2.7%)	1.57 +- 0.16 (10.19%)	0.59 +- 0.57 (96.6%)
0.9	1.0 +- 0.00 (0%)	3.27 +- 0.27 (8.26%)	39.47 +- 2.38 (6.02%)
0.92	1.0 +- 0.00 (0%)	3.58 +- 0.30 (8.38%)	48.09 +- 1.97 (4.10%)
0.95	1.0 +- 0.00 (0%)	4.22 +- 0.40 (9.48%)	60.60 +- 2.15 (3.55%)
N=10 M=50			
0	0.78 +- 0.015 (1.92%)	1.78 +- 0.17 (9.55%)	3.87 +- 2.72 (70.28%)
0.2	0.84 +- 0.019 (2.26%)	2.11 +- 0.21 (9.95%)	12.01 +- 3.35 (27.89%)
0.4	0.93 +- 0.016 (1.72%)	2.66 +- 0.27 (10.15%)	26.17 +- 3.51 (13.41%)
0.55	1.0 +- 0.00 (0%)	3.31 +- 0.29 (8.76%)	41.22 +- 2.71 (6.57%)
0.65	1.0 +- 0.00 (0%)	3.68 +- 0.33 (8.97%)	50.62 +- 2.28 (4.5%)
0.75	1.0 +- 0.00 (0%)	4.15 +- 0.38 (9.16%)	59.70 +_ 2.14 (3.58%)

SHORT TERM FHR VARIATIONS

Table 12.10: Index Magnitudes vs q at different FHRs (short term)

q	HRSI FHR=120	RI FHR=120	PI FHR=120	HRSI FHR=133	RI FHR=133	PI FHR=133
0	0	0.61	1.0	0	0.56	0.87
0.3	0	0.63	1.11	0	0.59	0.96
0.6	0	0.68	1.37	0	0.64	1.19
0.7	0.012	0.71	1.56	0	0.69	1.41
0.75	1.35	0.77	1.80	0.4	0.75	1.62
0.9	43.17	1	3.68	39.80	1	3.32
0.92	51.17	1	4.04	48.37	1	3.64
0.95	63.98	1	4.86	60.87	1	4.26
q	FHR=150	FHR=150	FHR=150	FHR=160	FHR=160	FHR=160
0	0	0.51	0.76	0	0.48	0.69
0.3	0	0.54	0.83	0	0.51	0.77
0.6	0	0.60	1.05	0	0.59	1.0
0.7	0	0.67	1.28	0	0.66	1.22
0.75	0.01	0.72	1.46	0	0.71	1.40
0.9	38.02	1	3.08	36.87	1	2.98
0.92	46.85	1	3.38	45.97	1	3.26
0.95	59.23	1	3.95	58.32	1	3.82

N=20 M=200 PROGRESSIVE OBLITERATION

Figures 12.5, 12.6, 12.7, and 12.8 illustrate the relationship between RI, PI, HRSI, BP, BPPI and FHR variations at absent flow.

12.2.3 THE EFFECT OF UMBILICAL ARTERY SITE OF MEASUREMENT ON RI AND PI

The pulsatility of the FVW was greatest at the proximal (aortic) end of the umbilical artery. The RI decreased from 0.66 to 0.55 as site of measurement moved from the proximal end to the distal end of the umbilical artery. The PI decreased from 1.20 to 0.84 from the proximal to the distal end.

The lowest value was obtained at the most distal end, thus all clinical ultrasound readings should ideally be taken at this end to

ensure that the worst scenario is obtained. Since it is not possible to choose the position using continuous wave Doppler ultrasound units, this would be a source of clinical uncertainty (figure 12.17).

Figure 12.17: PI and RI vs Position of Measurement on the Umbilical Artery (U.A.)

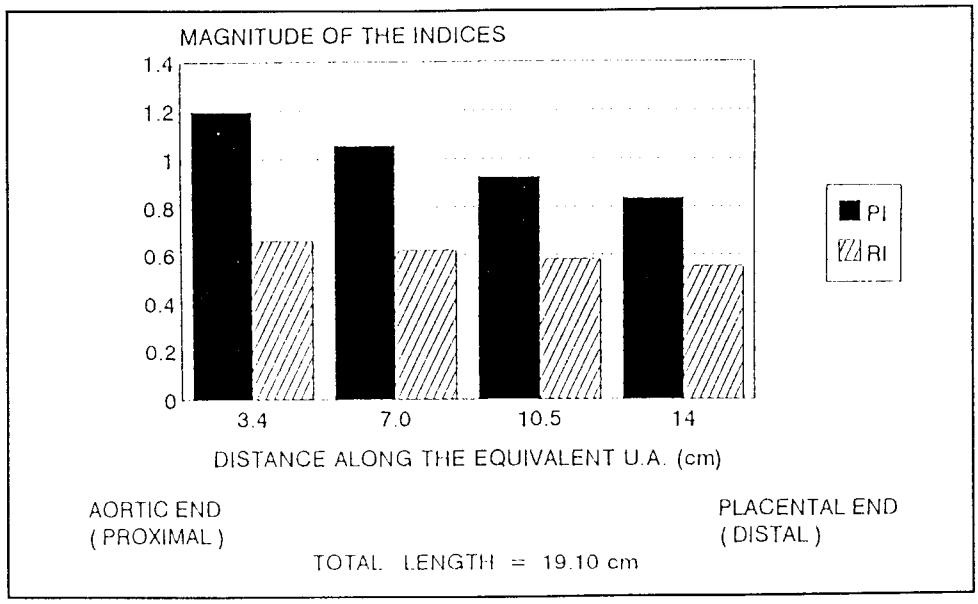

12.3 DISCUSSION

A transmission line model of the foetal arterial circulation has been developed with specific interest in simulating the blood flow in the umbilical arteries. The umbilical blood flow velocity waveform is empirically described by the pulsatility index, the resistance index and the HRSI. This thesis aimed to demonstrate the effects of placental resistance, placental size, FHR, BP, BPPI and the site of measurement of the FVW on the PI, the RI and the HRSI,

with a specific focus on the HRSI.

It must be added that the RI and PI calculated on normal umbilical FVW simulations correlated well with the normally accepted values for clinical results.

The RI, PI and HRSI have been shown to be dependent on the size of the placenta and the type of obliteration occurring. The trends are however similar. The increase in the indices with increasing placental obliteration (increasing placental resistance) was exponential and were shown to be significant as the correlation coefficients were fairly large. The rate of increase of the indices depended on the size of the placenta and the type of obliteration and was independent of physiological variables such as FHR.

The indices were thus demonstrated to be dependent on the placental resistance. This was clinically also demonstrated by Downing et al (1991), Muijsers et al (1991) and McCowan et al (1987). The simulations also showed that smaller placentas have a larger normal placental resistance which gives rise to elevated indices. These elevated values are also seen clinically in normal young foetuses, and are reported to decrease with increasing gestational age (Pattinson et al 1989).

The obliteration of the larger vessels in the placenta resulted in a greater increase in the placental resistance as shown by figure

12.1. Progressive obliteration of the larger vessels resulted in a greater rise in the umbilical FVW indices than distributed obliteration of the smaller vessels. This indicates the importance of the patency of the larger vessels in order to supply blood to the smaller vessels where the exchange of nutrients and gases occurs with the maternal blood.

Distributed obliteration of a large placenta required as much as 97 percent obliteration before absent flow was established during diastole. In the same placenta, progressive obliteration only needed to be extended to 90 percent to obtain the same result. It is clinically unlikely that as much as 97 percent of a placenta is obliterated before absent flow is presented. A combination of progressive obliteration and distributed obliteration must be present in vivo. This would theoretically reduce the percentage obliteration required to produce absent flow. However, this still showed the incredible reserve of the placenta to continue functioning well, even when there was a large degree of obliteration.

Similar simulations revealed that small placentas required less obliteration to present an absent flow. A young or SGA foetus only needed just over half its placenta embolised before absent flow appeared. Clinically this indicates that the young or SGA foetus does not have the ability to cope with large percentage placental embolisation. The older foetus with a larger placenta is able to

cope a lot better.

The effect of FHR variations :

In the case of simulations of long term FHR variations, a constant mean umbilical artery blood pressure and blood pressure pulsatility was maintained over the normal FHR range for a normal placenta. The RI, PI and HRSI were not significantly effected by these simulations thus demonstrating the insignificant effect of long term FHR variations on a normal FVW. At large degrees of placental obliteration the mean blood pressure however decreased with increasing FHR. The blood pressure pulsatility was however maintained. (The scaling of the resistance and inertance of the aorta and common iliac artery for flow profile variations over the normal FHR range resulted in unpredicted decreases in the mean umbilical artery blood pressure (Appendix H).) The discussion to follow has thus taken into account the fact that the mean blood pressure was decreased and the blood pressure pulsatility was constant for simulations of long term variations in FHR at increased placental resistances.

The results indicated that the RI and PI did not vary by more than 4 to 5 percent. The indices were thus not affected by the large variations in mean blood pressure yet may be dependent on blood pressure pulsatility which was relatively unchanged. The HRSI was however largely affected by these FHR variations. When absent flow was established, which is the area of interest, the index was shown

to vary by a maximum of 15 percent (Large placenta). This indicated the dependency of this index on the mean blood pressure rather than the blood pressure pulsatility. The HRSI however becomes less dependent on the FHR variations as it increases in magnitude and once absent flow is established, the index becomes insignificantly effected by the FHR variations.

Figure 12.5 and 12.6 illustrate the variations of HRSI and BP with FHR variations. It is evident that the HRSI and BP are inversely related. The relationship is significantly linear as the correlation coefficients for HRSI and BP versus FHR vary between 0.974 and 0.998, and -0.97 and -0.99 respectively.

Short term FHR variations (beat to beat variations) demonstrated a consistent decrease in the magnitudes of the RI, PI and HRSI as the FHR was increased (Downing et al (1991) showed a similar result for RI and PI obtained clinically.). The maximum deviation of RI was approximately 10 percent. However, at reduced or absent flow, the deviations were small enough to ignore the effects of FHR variations.

The PI however varied by significant amounts with short term FHR variations. The standard deviations were a minimum of approximately 10 percent. Even when reduced or absent flow was present, the index showed a large standard deviation and was thus greatly affected by short term FHR variations.

In order to determine the correlation between RI, PI and BPPI with FHR, it was necessary to examine these variables for all degrees of obliteration and obtain a range of correlations. For a large placenta the correlation coefficients for RI and PI versus FHR vary between -0.987 and -0.999, and -0.979 and -0.995 respectively. The correlation coefficient of BPPI versus FHR varies between -0.986 and -0.997. This demonstrates a significant linear relationship between RI, PI and BPPI versus FHR. The RI and PI are thus significantly related to BPPI in the same way.

For short term FHR variations, the HRSI showed a standard deviation equal to the magnitude of the index at low magnitudes. The standard deviation however decreased in proportion to the index as larger magnitudes were reached. The HRSI is however intended for use only for severely reduced or absent flow in which case elevated values close to 40 percent are obtained. In these cases the standard deviations were as small as 8 percent with an insignificant effect from the short term FHR variations.

For a large placenta, analyzing the entire range of obliterations, the correlation coefficients for HRSI and BP versus FHR vary between -0.779 and -0.975, and 0.998 and 0.999 respectively. HRSI and BP thus demonstrate a significant linear relationship with FHR. The HRSI and BP are thus significantly related in the same manner.

The inability of the foetus to maintain a constant blood pressure

pulsatility for short term heart rate fluctuations caused these large fluctuations in the RI and PI. Thus, the clinically significant fluctuations in the FVW indices (presented by Downing et al 1991) are due to the short term fluctuations of the FHR around the basal heart rate and variations in blood pressure pulsatility. This is illustrated by figures 12.5 and 12.8 where the RI and PI, and BPPI are represented versus FHR variation. It is evident that the indices are directly related to the BPPI.

The tables below summarise the effects of long and short term FHR variations on the indices ((a) Before absent flow is reached. (b) Once absent flow has been established.).

(a)

	RI	PI	HRSI	BP	BPPI
LTV'S	INSIG	INSIG	SIG (+)	SIG (-)	INSIG
STV'S	INSIG	SIG (-)	SIG (-)	SIG (+)	SIG (-)

(b)

	RI	PI	HRSI	BP	BPPI
LTV'S	N/A (RI = UNITY)	INSIG	INSIG	SIG (-)	INSIG
STV'S	N/A (RI = UNITY)	SIG (-)	INSIG	SIG (+)	SIG (-)

N/A = NOT APPLICABLE SIG = SIGNIFICANTLY LARGE VARIATION
INSIG = INSIGNIFICANTLY SMALL VARIATION
(-) = NEGATIVE CORRELATION (+) = POSITIVE CORRELATION

The behaviour of the RI and PI with FHR variation were simply attributed to the blood pressure pulsatility. Consequently, for

long term FHR variations, the RI and PI did not vary by large amounts as the blood pressure pulsatility was relatively constant. Short term FHR variations however caused large variations in the umbilical artery blood pressure pulsatility. This in turn resulted in the variation of the RI and PI (table 12.9). The RI and PI were thus dependent on the physiological response to FHR variations which in turn determined the blood pressure pulsatility.

Mulders et al (1986) state, "The PI is dependent on the placental resistance and blood pressure pulsatility, and that biological PI variations should be mainly determined by short term variations in blood pressure. With the assumption that the placental resistance does not vary much in a healthy near term foetus, this blood pressure pulsatility can play a major role in the relationship between FHR and PI." This model has also shown the relationship between placental resistance and short term blood pressure variations on the RI and PI which supports the work by Mulders et al (1986).

The behaviour of the HRSI is not related to the BPPI but rather to the BP. The HRSI increased with increasing FHR for "long term" responses yet decreased with increasing FHR for short term responses. The mean blood pressure increased with increasing FHR for long term responses yet decreased with increasing FHR for short term responses. The HRSI thus appeared to be inversely dependent on the mean blood pressure and was not affected by the blood pressure

pulsatility. The exact relationship has not been investigated.

Disregarding the effects of FHR variations, the HRSI was found to behave in a similar way to RI and PI. It was dependent on the placental resistance, placental size and type of placental obliteration. The HRSI however was designed to increase in magnitude only once the FVW had reached an advanced stage of reduced diastolic flow. It did not saturate for absent flow yet continued to increase exponentially. Small changes in placental obliteration, once reduced flow was established, resulted in large changes in HRSI. The index is thus particularly sensitive to the length of absent flow during diastole.

The HRSI may be more useful than RI as it did not saturate at a fixed value once absent flow was established and it remained dependent on the degree of absent flow. The HRSI however did not appear to be a better predictor of placental resistance than PI. However for an identical degree of precision, the range of PI values was considerably smaller than the range of HRSI values. Small variations in the placental resistance thus caused large changes in the HRSI yet small changes in the PI. HRSI is less sensitive to short term changes in FHR than PI when the placental resistance is high and absent flow is present. HRSI is also not greatly effected during long term changes in FHR once absent is established.

Based on the findings of this investigation, it is concluded that the HRSI, just like the PI, is a useful predictor of elevated placental resistance and thus of severely reduced, absent and reversed flow.

The effect of the site of measurement along the umbilical artery was also analyzed and was found to affect the PI and RI. Clinically it is advised that the umbilical FVW is read at the placental end of the umbilical artery as this is where the FVW is least pulsatile (Mehalek et al 1989). Model 2 analysis of the blood flow along the umbilical artery yielded the same results thus supporting the clinical findings.

It is clear from the results of this thesis that model 1 provides a very simple approximation to the foetal placental circulation. It is useful in investigating the effects of placental resistance on the indices but falls short when investigating the effects of FHR variations on the indices. Physiologically, the BP and BPPI are varying parameters, dependent on the foetal circulation. Model 1 is unable to simulate this dynamic property and can only serve as a very simple approximation to the foetal placental circulation. Model 2 has however been very useful in indicating the effects of placental resistance, varying blood pressure pulsatility and mean blood pressure on the indices concerned as it dynamically simulates variations in the foetal placental circulation.

CHAPTER THIRTEEN

CONCLUSIONS

Based on the findings of this report, I am able to draw the following conclusions:

1) The indices which describe the umbilical blood flow are a function of placental resistance. They are thus able to predict reduced umbilical blood flow due to increased placental resistance. The indices are exponentially related to the placental resistance and the relationship is significant.

2) The indices are also dependent on the type of placental obliteration, and are very sensitive to the obliteration of the larger primary and secondary villi. The indices are dependent on the size of the placenta and indicate that a large placenta is able to withstand large degrees of obliteration.

3) The adaptations of the foetal circulation for various physiological variations plays a major role in the variation of the blood pressure pulsatility (BPPI) and the indices. This is conclusively demonstrated by the different results in index variations obtained for FHR variations in model 1 and the two simulations of FHR variations in model 2.

4) Blood pressure pulsatility (BPPI) variation plays an important role in the variation of the RI and PI as the FHR is varied. The analysis on a normal placenta yields conclusive results on this. Model 1 and the response to long term FHR variations in model 2 yield similar results in that small variations in BPPI cause small variations in these indices. Short term FHR variations however induce large variations in BPPI and a significant decrease in the RI and PI as the FHR is increased. This is very similar to the results presented by Downing et al (1991) where it was demonstrated that these indices are inversely related to FHR. The relationship in both cases is linear.

5) Mean blood pressure variations result in large variations in the HRSI at its lower magnitudes. Once absent flow is established and the HRSI reaches its upper magnitudes, it is not significantly effected by variations in blood pressure. The HRSI is thus not significantly effected by FHR variations once absent flow has been established in the umbilical FVW. Unlike the RI and PI, the blood pressure pulsatility does not have a great effect on the HRSI.

6) The pulsatility of the umbilical FVW is largest at the proximal (aortic) end of the umbilical artery.

CHAPTER FOURTEEN

RECOMMENDATIONS

Based on the conclusions the following recommendations are made:

1) Elevated index magnitudes should be used as an indication of an increased placental resistance

2) When using the RI, PI and HRSI clinically, standard deviations of 3 to 4 percent should be allowed for the RI, and 10 percent for the PI. A HRSI value of 34 percent should be taken to indicate the possible beginning of absent flow. The scaling for RI and PI only applies to elevated values which do not fall into an acceptably normal range.

3) The umbilical FVW should be read at the placental end of the umbilical artery.

CHAPTER FIFTEEN

POSSIBLE FUTURE IMPROVEMENTS

This thesis is not a perfect approximation to the Foetal arterial circulation. The following improvements may be attended to in order to improve the approximation:

1) Increase the number of segments used to represent the aorta and umbilical arteries in transmission line format.
2) Obtain more post mortem specimens in order to obtain a more comprehensive data list of arterial dimensions.
3) Use ultrasound techniques to obtain values for the Young's modulus for the arteries concerned. A more precise estimation of this magnitude is required.
4) Correlate the mean blood pressure and blood pressure pulsatility with the indices.

APPENDIX A PLACENTAL RESISTANCE AND COMPLIANCE

The aim of this appendix is to derive the equations of resistance and compliance of the placental unit.

The placenta is split into two levels. The first level is the lobes (n), the second level is the lobules (m).
The placenta consists of n lobes and m lobules. Each branch consists of a resistor and a capacitor.

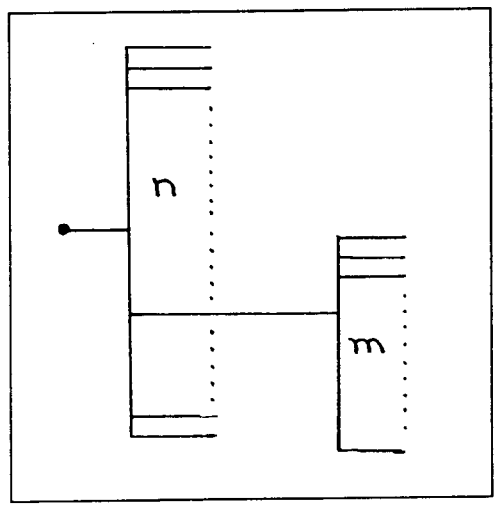

Figure A1: A Schematic Representation of the Lobes and Lobules

Equivalent resistance of m lobules in parallel

$$Rm = R(lobule)/m \qquad (A1)$$

A single lobe contains m lobules. Thus the resistance of a lobe is

$$R = [R(lobe) + Rm] \qquad (A2)$$

(R(lobule) is the resistance of a single lobule, and R(lobe) is the resistance of a single lobe.)

n lobes in parallel gives a total resistance of

$$Rt = R/n = [R(lobe) + R(lobule)/m]/n \qquad (A3)$$

Equivalent capacitance:

m number of lobules in parallel $Cm = m*C(lobule)$ (A4)

n number of lobes in parallel $Cn = [C(lobe) + Cm]*n$ (A5)

$= C(lobe)*n + C(lobule)*n*m$

Obliteration:

Obliteration involves the fractional reduction of the number of vessels in the placenta. q Denotes the fractional obliteration. If q vessels are obliterated then (1-q) vessels remain.

Progressive obliteration:

This involves the obliteration of n lobes.

Number of vessels remaining after obliteration = $n(1-q)$ (A6)

$Rt = [R(lobe) + R(lobule)/m]/n(1-q)$ (A7)

therefore $Rt = [R(lobe)m + R(lobule)]/[nm(1-q)]$ (A8)

$Ct = C(lobe)n(1-q) + C(lobule)nm(1-q)$ (A9)

distributed obliteration:

This involves the obliteration of the lobules. (m)

Number of vessels remaining after obliteration = $m(1-q)$ (A10)

$Rt = [R(lobe) + R(lobule)/m(1-q)]/n$ (A11)

therefore $Rt = [R(lobe)m(1-q) + R(lobule)]/[nm(1-q)]$ (A12)

$Ct = C(lobe)n + C(lobule)nm(1-q)$ (A13)

APPENDIX B EQUIVALENT ANALYSIS

The aim of this appendix is to show that the simple equations represented by equations 12, 13 and 14 in the chapter 9 give equivalent results to the more complex equations representing the overall conductance and compliance of the placental unit.

1) m BRANCHES :

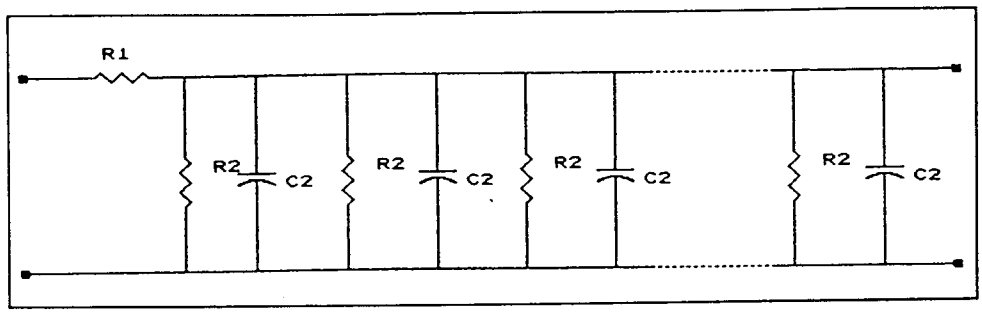

Figure B1: The Circuit Diagram of the LOBULES

$$Zm=1/G2+jwC2 \qquad \text{(B1)}$$

WHERE Zm = Impedance of the m branches

j = imaginary component

$$G2=m/R2 \qquad \text{(B2)}$$

AND

$$C2=m*Cm \qquad \text{(B3)}$$

2) n BRANCHES :

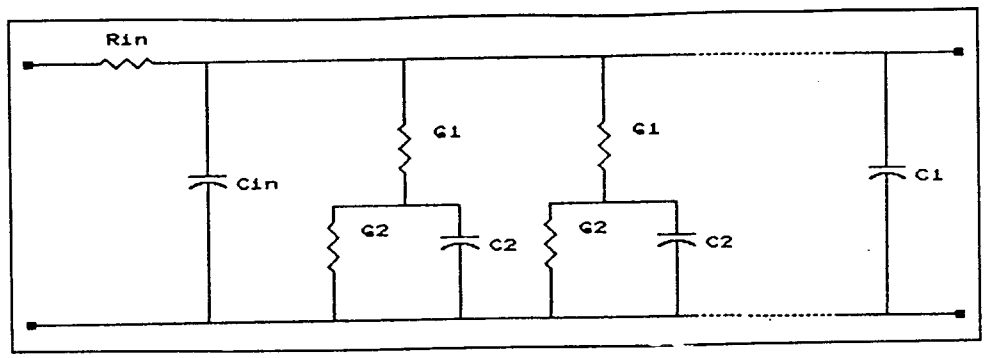

Figure B2: The Circuit Diagram of the Placental Unit.

$$Z=1/(G2+jwC2)+1/G1 \qquad (B4)$$

$$Z=((G2+G1)+jwC2)/(G1G2+jwC2G1) \qquad (B5)$$

$$Z=1/(Geq+jwCeq) \qquad (B6)$$

WHERE Z = the impedance of a lobe and its lobules

$$G1=1/R1 \qquad (B7)$$

$$Geq+jwCeq=(G1G2+jwC2G1)/((G1+G2)+jwC2) \qquad (B8)$$

$$= ((G1G2^2+G1^2G2+w^2C2^2G1)+jwC2G1^2)/((G1+G2)^2+w^2C2^2) \quad (B9)$$

THEREFORE

$$Geq=(G1G2^2+G1^2G2+w^2C2^2G1)/((G2+G1)^2+w^2C2^2) \quad (B10)$$

AND

$$Ceq=C2G1^2/((G1+G2)^2+w^2C2^2) \quad (B11)$$

$$Ct=n(Ceq+C1)+Cin) \quad (B12)$$

Where C1 = compliance of the lobes

Cin = compliance of the umbilical arteries

$$Gt=nGeq \quad (B13)$$

$$Ct=n((C2G1^2/((G1G2)^2+w^2C2^2)+C1)+Cin \quad (B14)$$

$$Gt=n(G1G2^2+G1^2G2+w^2C2^2G1)/((G1+G2)^2+w^2C2^2) \quad (B14)$$

R1 = 1.63×10^{10} Ohms == umbilical artery

R2 = 102×10^{10} Ohms == placenta

$C1 = 11.8\times10^{-13}$ F == primary and secondary stem villi

$C2 = 0.012\times10^{-13}$ F == tertiary stem villi

$Cin = 710\times10^{-13}$ F == umbilical artery

N=20 M=200 THEREFORE $Ct = 9.487\times10^{-11}$ F

AND $Rt = 106.99\times10^{7}$ Ohms AT 140 bpm.

If the simple equations given by Thompson, Trudinger and Stevens (1989) (12, 13 and 14) are used to represent the placental resistance and compliance, the following results are obtained :

$Rt = 107\times10^{7}$ Ohms

$Ct = 9.94\times10^{-11}$ F (5% error from the actual value)

The simple representations given by Thompson, Trudinger and Stevens are accurate representations of the equivalent resistances and compliances of the umbilical placental unit.

APPENDIX C HARMONICS

Nine normal umbilical FVWs, which all contained diastolic flow, from clinical trials were used to identify the frequency content of normal FVW's. Table C1 illustrates the magnitudes of the harmonics from each umbilical FVW represented as a percentage of the magnitude of the fundamental.

Table C1: Harmonic magnitudes of FVWs

FVW No.	1st	2nd	3rd
1	12	0	0
2	15	0	0
3	20	8	0
4	42	16	4
5	20	13	0
6	20	7	0
7	20	4	3
8	22	6	0
9	23	6	0

The normal umbilical FVW thus comprises of at most 3 harmonics. Mo et al (1988) did a similar analysis on the uterine blood flow waveform which is very similar to the umbilical FVW. He found that

the 4th harmonic was only 2.6% of the amplitude of the fundamental.

The same umbilical FVWs were used to estimate the ratio of mean amplitude to maximum amplitude.

Table C2: Mean and maximum amplitudes of the FVWs.

FVW No.	maximum	mean	max/mean
1	35	19.5	1.8
2	38	20	1.9
3	47	27.9	1.7
4	33	10.7	3.1
5	44	20	2.2
6	54	31.6	1.7
7	50	24.5	2.0
8	63	33.8	1.9
9	42	23	1.8

The magnitudes of the maximum and mean are not absolute values as the magnitude of the umbilical FVW is dependent on the angle of ultrasound insonation. These values have not been scaled according to the individual angle of insonation.

Four abnormal umbilical FVWs, which all contained absent flow, were analyzed to estimate their frequency composition. The results are

also expressed as a percentage of the fundamental and are represented in the table below.

Table C3: Harmonic magnitudes for abnormal FVWs

FVW No.	1st	2nd	3rd	4th	5th
1	57	29	7	11	1
2	67	29	8	1	1
3	57	17	3	2	1
4	43	8	5	2	1

There is more energy in the higher harmonics with abnormal FVW's. However, the assumption that the umbilical FVW comprises of at most 3 significant harmonics thus also holds true for abnormal FVWs.

APPENDIX D PHASE VELOCITY AND WAVELENGTH

The transmission line model of an artery includes the capacitance of the artery wall, the inertance of the fluid, the resistance to flow and any leakage conductance. Additional variables such as the compliance of the fluid and the inertance of the artery wall are not included in the analogous model (The theory is based on work done by Bunn 1980.).

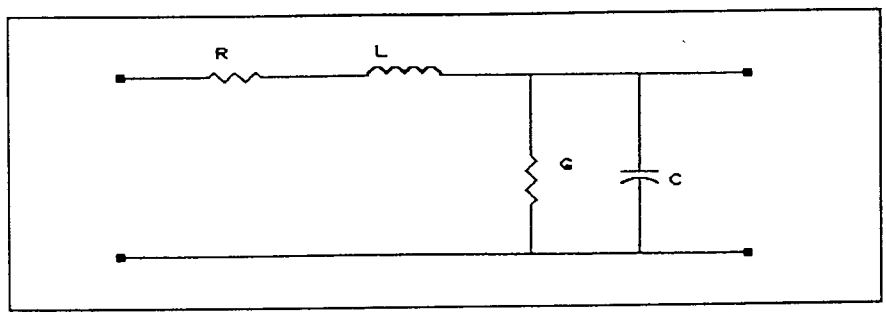

Figure D1: A typical transmission line segment

A transmission line is made up of a certain number of segments which each represent a certain length of the line. The phase velocity and wavelength of the wave travelling in the artery must be calculated in order to determine the length of a segment and the number of segments required to model the artery as a transmission line. Each segment must be less than the minimum wavelength present in the signal passing down the line. As a rule of thumb, the segment dimension must be approximately

$$\lambda/10 \qquad \text{(D1)}$$

If there are no losses in a transmission line, the phase velocity is simply described by

$$Vp=1/\sqrt{(LC)} \qquad \text{(D2)}$$

where L = inductance

C = compliance

Every artery has a resistance to flow and in some cases a leakage conductance which affect the phase velocity.

Transmission line equations of the AC line yield a propagation factor which is related to the attenuation factor and phase factor. The propagation factor is described by

$$\gamma=\sqrt{((R+j\omega L)(G+j\omega C))} \qquad \text{(D3)}$$

where R = resistance

L = inductance

C = compliance

G = conductance

It is equated to the attenuation and phase factor by

$$\gamma=\alpha+j\beta \qquad \text{(D4)}$$

The phase factor can be calculated to be equal to (Bunn 1980)

$$\beta=\sqrt{(0.5(\sqrt{((R^2+\omega^2L^2)(G^2+\omega^2C^2))}-\omega^2LC+RG))} \quad (D5)$$

The phase velocity is simply equal to

$$Vp=\omega/\beta \quad (D6)$$

The phase velocity can thus be calculated for a transmission line with losses. As the wavelength of a wave with a certain phase velocity is equal to

$$\lambda=Vp/f \quad (D7)$$

it is simply a matter of determining the maximum frequency present in order to calculate the minimum wavelength.

The effects of fluid compliance and wall inertance can be added into the system. The equivalent circuit will thus be (Bunn 1980)

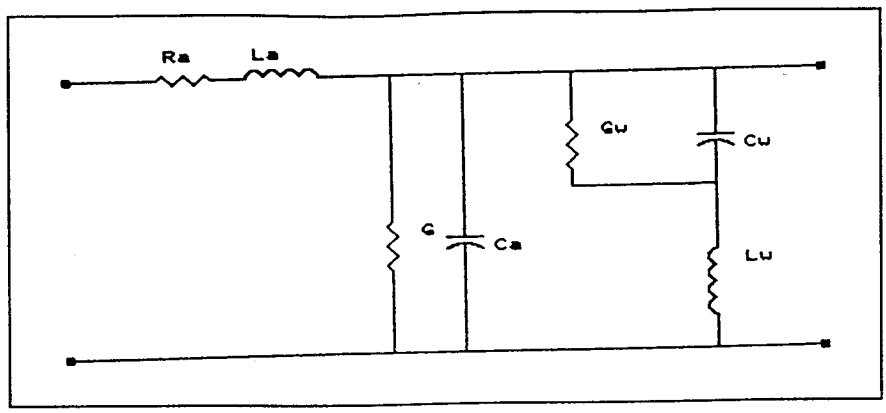

Figure D2: The circuit diagram of an artery including fluid compliance and wall inertance.

The wall inertance is calculated from

$$Lw=(\rho h/2\pi r l)+\rho/8\pi \qquad (D8)$$

Lw is a representation of the wall inertance plus the transverse inertance of the fluid. Model 1 and model 2 do however not incorporate Lw as it is far smaller than the total inertance of the fluid.

The fluid compliance is described by

$$Ca=(\pi r^2)\,l/Kb \qquad (D9)$$

Kb is simply the bulk modulus of the fluid.

(Kb = 8×10^4 kg/cm^2)

The circuit must be simplified to a single equivalent conductance and an equivalent compliance. The equations for these equivalent

magnitudes are described by (Bunn 1980)

$$Geq=G/\left((1-\omega^2 LwCw)^2+G^2\omega^2 Lw^2\right) \qquad (D10)$$

$$Ceq=\left(Cw(1-\omega^2 LwCw)-G^2 Lw\right)/\left((1-\omega^2 LwCw)^2+G^2\omega^2 Lw^2\right)+Ca \qquad (D11)$$

Ca can be ignored if the fluid is assumed to be incompressible. The equations for the equivalent conductance and compliance, the phase factor and the phase velocity are written into a MATLAB program and used to calculate the phase velocity at a particular frequency. The wavelengths are calculated once the phase velocities have been calculated and are used as a guide in determining the dimensions of the transmission line.

It is considered that the maximum frequency in the umbilical and foetal artery FVWs is at the 3rd harmonic (Appendix C). The maximum frequency to be analyzed is at a FHR of 160 bpm. The maximum frequency is thus 8 Hz.

The phase velocities for lossless conditions are calculated for the aorta, the common iliac artery and the umbilical artery. The MATLAB program is used to calculate the phase velocities under lossy conditions. The wavelengths are also calculated up to and including the 3rd harmonic. The results are shown below for the dimensions illustrated in the table.

At the low frequencies, the phase velocities are nearly equal to the phase velocities under lossless conditions.

$$\sqrt{(1/LC)} \tag{D12}$$

Thus, when calculating the phase velocity for a certain artery at low frequencies, the phase velocity can easily be calculated by

$$\sqrt{(1/LCeq)} \tag{D13}$$

Table D1: Phase Velocity and Wavelength Magnitudes

PHASE VELOCITY AND WAVELENGTH MAGNITUDES

160 bpm

	Vp (cm/sec)	WAVELENGTH (cm)	Vp (cm/sec) (lossless)	WAVELENGTH (cm) @ 160 bpm
AORTA				
n=1	27.37	10.32	27.42	10.28
n=2	27.25	5.09	27.42	5.14
n=3	27.03	3.38	27.42	3.43
ILIACS				
n=1	148.7	62.73	340	127.5
n=2	181.3	37.28	340	63.75
n=3	205.3	28.06	340	42.45
UMB. ARTERY				
n=1	11.97	4.52	12.01	4.5
n=2	11.99	2.24	12.01	2.25
n=3	11.99	1.5	12.01	1.5

APPENDIX E POISEULLE EQUATIONS

J.L Poiseulle determined how the flow rate of an incompressible fluid undergoing laminar flow in a cylindrical tube is affected by the properties of the fluid and the dimensions of the tube. His result is known as the Poiseulle's equation and is defined as follows

$$Q=(\pi r^4(P1-P2))/8l\mu \qquad \text{(E1)}$$

where r = radius , l = length , P1-P2 = pressure difference between the ends of the tube , μ = viscosity of the fluid and
Q = volume flow rate of the fluid.

The resistance to flow is defined as pressure divided by the flow rate.

$$R=(8l\mu)/\pi r^4 \qquad \text{(E2)}$$

This is the well known formula for resistance to flow for laminar flow in a cylindrical tube.

Womersley produced a solution to the flow and pressure gradient for an oscillating pressure gradient. He found the flow to be

$$Q=(\pi r^4 M' M \sin(wt-\Phi+\epsilon))/(\mu\alpha^2) \quad \text{(E3)}$$

The pressure gradient is

$$(P1-P2)/l=M\cos(wt-\Phi) \quad \text{(E4)}$$

$$Z=R+jwL \quad \text{(E5)}$$

The impedance to flow (pressure divided by flow) can be calculated from these two equations giving a solution to the resistance to flow and the inertance of the fluid under different flow conditions.

$$R=(\mu\alpha^2\sin(\epsilon))/(\pi r^4 M') \quad \text{(E6)}$$

$$L=(\rho\cos(\epsilon))/(\pi r^2 M') \quad \text{(E7)}$$

APPENDIX F TABLE OF ALPHA MAGNITUDES

The values for

$$M'/\alpha^2 \qquad \text{(F1)}$$

and

$$\epsilon \qquad \text{(F2)}$$

for values of alpha from 0 to 10 are given in the table below McDonald 1974).

$\epsilon = \epsilon_{10}$

$M' = M_{10}$

α	M'_{10}/α^2	ϵ_{10}	α	M'_{10}/α^2	ϵ_{10}	α	M'_{10}/α^2	ϵ_{10}	α	M'_{10}/α^2	ϵ_{10}
0·00	0·1250	90·00	2·50	0·0855	44·93	5·00	0·0302	18·65	7·50	0·0147	11·87
0·05	0·1250	89·98	2·55	0·0837	43·88	5·05	0·0297	18·43	7·55	0·0146	11·78
0·10	0·1250	89·90	2·60	0·0819	42·86	5·10	0·0292	18·23	7·60	0·0144	11·70
0·15	0·1250	89·79	2·65	0·0802	41·86	5·15	0·0287	18·02	7·65	0·0142	11·61
0·20	0·1250	89·62	2·70	0·0784	40·90	5·20	0·0282	17·83	7·70	0·0140	11·53
0·25	0·1250	89·40	2·75	0·0767	39·96	5·25	0·0278	17·63	7·75	0·0139	11·45
0·30	0·1250	89·14	2·80	0·0750	39·05	5·30	0·0273	17·44	7·80	0·0137	11·37
0·35	0·1250	88·83	2·85	0·0734	38·17	5·35	0·0269	17·26	8·85	0·0136	11·29
0·40	0·1250	88·47	2·90	0·0717	37·32	5·40	0·0264	17·08	7·90	0·0134	11·21
0·45	0·1249	88·07	2·95	0·0701	36·50	5·45	0·0260	16·90	7·95	0·0133	11·14
0·50	0·1249	87·61	3·00	0·0685	35·70	5·50	0·0256	16·73	8·00	0·0131	11·06
0·55	0·1248	87·11	3·05	0·0670	34·93	5·55	0·0252	16·56	8·05	0·0130	10·98
0·60	0·1248	86·57	3·10	0·0655	34·18	5·60	0·0248	16·39	8·10	0·0128	10·91
0·65	0·1247	85·97	3·15	0·0640	33·46	5·65	0·0244	16·23	8·15	0·0127	10·84
0·70	0·1246	85·33	3·20	0·0626	32·77	5·70	0·0240	16·07	8·20	0·0125	10·77
0·75	0·1244	84·65	3·25	0·0612	32·09	5·75	0·0237	15·91	8·25	0·0124	10·70
0·80	0·1243	83·91	3·30	0·0598	31·45	5·80	0·0233	15·76	8·30	0·0122	10·63
0·85	0·1240	83·14	3·35	0·0585	30·82	5·85	0·0230	15·61	8·35	0·0121	10·56
0·90	0·1238	83·32	3·40	0·0572	30·22	5·90	0·0226	15·46	8·40	0·0120	10·49
0·95	0·1235	81·45	3·45	0·0559	29·64	5·95	0·0223	15·32	8·45	0·0119	10·42
1·00	0·1232	80·55	3·50	0·0547	29·08	6·00	0·0220	15·18	8·50	0·0117	10·36
1·05	0·1228	79·60	3·55	0·0535	28·53	6·05	0·0216	15·04	8·55	0·0116	10·29
1·10	0·1224	78·61	3·60	0·0523	28·01	6·10	0·0213	14·90	8·60	0·0115	10·22
1·15	0·1219	77·59	3·65	0·0512	27·51	6·15	0·0210	14·77	8·65	0·0114	10·16
1·20	0·1213	76·53	3·70	0·0501	27·02	6·20	0·0207	14·63	8·70	0·0112	10·10
1·25	0·1207	75·44	3·75	0·0490	26·55	6·25	0·0204	14·50	8·75	0·0111	10·04
1·30	0·1200	74·31	3·80	0·0480	26·10	6·30	0·0201	14·38	8·80	0·0110	9·97
1·35	0·1193	73·16	3·85	0·0470	25·66	6·35	0·0199	14·25	8·85	0·0109	9·91
1·40	0·1185	71·98	3·90	0·0460	25·24	6·40	0·0196	14·13	8·90	0·0108	9·85
1·45	0·1176	70·77	3·95	0·0451	24·83	6·45	0·0193	14·01	8·95	0·0107	9·79
1·50	0·1166	69·54	4·00	0·0441	24·43	6·50	0·0191	13·89	9·00	0·0106	9·73
1·55	0·1156	68·30	4·05	0·0432	24·05	6·55	0·0188	13·77	9·05	0·0104	9·68
1·60	0·1144	67·03	4·10	0·0424	23·68	6·60	0·0185	13·66	9·10	0·0103	9·62
1·65	0·1133	65·76	4·15	0·0415	23·32	6·65	0·0183	13·54	9·15	0·0102	9·56
1·70	0·1120	64·47	4·20	0·0407	22·98	6·70	0·0181	13·43	9·20	0·0101	9·51
1·75	0·1107	63·18	4·25	0·0399	22·64	6·75	0·0178	13·32	9·25	0·0100	9·45
1·80	0·1093	61·89	4·30	0·0391	22·32	6·80	0·0176	13·21	9·30	0·0099	9·40
1·85	0·1078	60·59	4·35	0·0384	22·00	6·85	0·0173	13·11	9·35	0·0098	9·34
1·90	0·1063	59·30	4·40	0·0376	21·70	6·90	0·0171	13·00	9·40	0·0097	9·29
1·95	0·1047	58·02	4·45	0·0369	21·40	6·95	0·0169	12·90	9·45	0·0096	9·24
2·00	0·1031	56·74	4·50	0·0362	21·11	7·00	0·0167	12·80	9·50	0·0096	9·18
2·05	0·1015	55·47	4·55	0·0355	20·84	7·05	0·0165	12·70	9·55	0·0095	9·13
2·10	0·0998	54·22	4·60	0·0349	20·56	7·10	0·0163	12·60	9·60	0·0094	9·08
2·15	0·0980	52·98	4·65	0·0342	20·30	7·15	0·0161	12·50	9·65	0·0093	9·03
2·20	0·0963	51·77	4·70	0·0336	20·05	7·20	0·0159	12·41	9·70	0·0092	8·98
2·25	0·0945	50·57	4·75	0·0330	19·80	7·25	0·0157	12·31	9·75	0·0091	8·93
2·30	0·0927	49·39	4·80	0·0324	19·55	7·30	0·0155	12·22	9·80	0·0090	8·88
2·35	0·0909	48·24	4·85	0·0319	19·32	7·35	0·0153	12·13	9·85	0·0089	8·84
2·40	0·0891	47·11	4·90	0·0313	19·09	7·40	0·0151	12·04	9·90	0·0088	8·79
2·45	0·0873	46·01	4·95	0·0308	18·86	7·45	0·0149	11·95	9·95	0·0088	8·74
2·50	0·0855	44·93	5·00	0·0302	18·65	7·50	0·0147	11·87	10·00	0·0087	8·69

APPENDIX G SEGMENT LENGTHS

UMBILICAL ARTERY:

The umbilical artery in the model was a combination of the 2 umbilical arteries and the 5 radial branches. The equivalent dimensions are : length = 19.11 cm, radius = 0.107 cm, wall thickness = 1.12×10^{-3} cm.

L = 694 H (36.31 H/cm)

C = 9.9 uF (0.518 uF/cm)

therefore c = 12.1 cm/sec

The maximum frequency was 2.6666667 Hz (160 bpm)

The maximum frequency component was at the third harmonic, therefore fmax = 3 * 2.6666667 = 8 Hz

wavelength = 12.1/8

= 1.51 cm

length per segment = 1.51 cm

The umbilical artery was represented by 22 sections of 0.868 cm each. The dimension of a section was less than the minimum wavelength. Each segment was 1.74 times smaller than the minimum wavelength. This was not an ideal representation of a transmission line as each segment is not 10 times smaller than the minimum wavelength (Ideally 84 segments). Due to the memory limitations imposed on a circuit file in PSPICE, very long transmission lines

are not able to be implemented. The system was checked for an umbilical artery of 40 segments. This produced no difference in the representation of the FVW and thus a model with more segments was not necessary. The approximation to a transmission line using 22 segments was thus used.

AORTA:

L = 28.3 H

C = 47 uF

wavelength = 27.42/8

= 3.42 cm

The total length of the aorta was 7.5 cm and was made up of 8 segments in the model. The length per segment was thus 0.9375 cm which was less than the minimum wavelength. Each segment was 3.65 times smaller than the minimum wavelength. This was not an ideal representation for a transmission line as each segment should be approximately 10 times smaller than the minimum wavelength (22 segments).

COMMON ILIAC ARTERY:

L = 24.16

C = 0.36 uF

therefore c = 339 cm/sec

wavelength = 339/8

= 42.38 cm

The total length of the iliac arteries was 2.4 cm, and was modelled by 4 sections. Each segment was thus 0.6 cm in length which was 70.64 times smaller than the minimum wavelength. An ideal transmission line was thus represented in the common iliac artery and provided an accurate pressure waveform as an input to the umbilical placental unit.

The transmission line was thus set up as an average approximation to the foetal arterial circulation. The most realistic transmission line approximation was for the Common Iliac artery. This was where the pressure wave input to the umbilical artery was simulated. An accurate representation was thus felt to be of most importance. The Aorta and Umbilical arteries were also approximations to a transmission line. Modelling with more segments was not possible with the PSPICE simulator used. Small extensions were possible yet produced the same waveforms, thus they were felt to be unnecessary and the existing dimensions were implemented.

	Ra	La	Ca	G	Lw	Cw
AORTA						
	94.8	28.3	1E-10	1.22E-04	2.360E-01	4.7E-05
ILIACS						
	230	24.16	1E-10	7.52E-05	1.450E-01	3.60E-07
UMB. ARTERY						
	11417	700	1E-10	1.24E-04	7.16E-02	9.9E-06

Table G1: Foetal Artery Transmission Line Dimensions

G = leakage conductance

placenta: G = 1/Rp (Rp = placental resistance)

aorta: G = 1/Rabo (Rabo = Aortic bleed off resistance)

iliacs: G = 1/Rlc (Rlc = lower carcass resistance)

APPENDIX H TIME CONSTANTS

The blood pressure waveform decays from its systolic maximum to a diastolic minimum. The TIME CONSTANT is defined as being the time required to reduce the amplitude to 36.8 percent of it initial value.

The blood pressure (voltage) and the time constant simulated by the PSpice circuit representing the Foetal Arterial Circulation are dependent on the magnitudes of the Resistance to flow, the inertance of the fluid and the compliance of the vessels.

A simple LRCR circuit was analyzed in order to determine the response of the circuit used to simulate foetal arterial blood flow. The natural response of the circuit was calculated in order to calculate the poles of the system. The transfer function calculated was a representation of input to output voltage and provided an equation from which the time constants of the system were calculated for the different magnitudes of the parameters of interest.

R1 = flow resistance in major artery

R2 = peripheral resistance to blood flow

L = inertance of the blood

C = compliance of artery walls

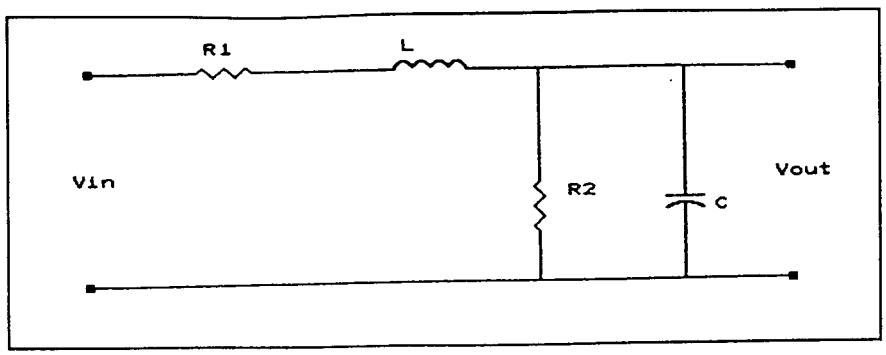

Figure H1: A Simple RLCR circuit

$$Z1=R1+sL \quad \text{(H1)}$$

$$Z2=R2/(1+sR2C) \quad \text{(H2)}$$

Table H2: A circuit diagram of the equivalent impedances.

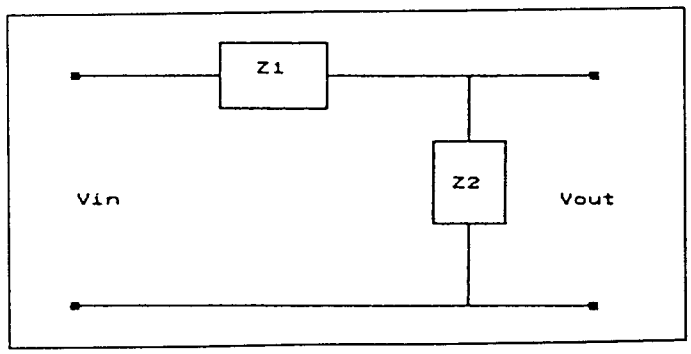

The equivalent impedance of the system was calculated as follows.

$$Vout=(Z2/(Z1+Z2))\,Vin \quad \text{(H3)}$$

$$Zt=Z1+Z2 \quad \text{(H4)}$$

$$Zt=R1+sL+R2/(1+sR2C) \tag{H5}$$

$$Zt=(s^2(R2LC)+s(R1R2C+L)+(R1+R2))/(1+sR2C) \tag{H6}$$

$$V2/V1=Z2/Zt \tag{H7}$$

$$V2/V1=R2/(s^2(R2LC)+s(R1R2C+L)+(R1+R2)) \tag{H8}$$

The poles of the system occurred when

$$s^2(R2LC)+s(R1R2C+L)+(R1+R2)=0 \tag{H9}$$

The poles of the system occur at $S_{1,2}$

$$S_{1,2}=-b/2a\pm\sqrt{(b^2-4ac)}/2a \tag{H10}$$

WHERE

$$a=R2LC \tag{H11}$$

$$b=R1R2C+L \tag{H12}$$

$$c=R1+R2 \tag{H13}$$

A Matlab program was written in which the real and imaginary parts of the poles were calculated depending on the magnitude of the parameters R1, R2, L and C.

The natural response was plotted as

$$Vn=A(\exp(Ret))(\sin(Imt+\theta)) \tag{H14}$$

WHERE Re = THE REAL COMPONENT

Im = THE IMAGINARY COMPONENT

It was not necessary to calculate A (amplitude scaling factor) or theta as only the time constant or time of decay was of importance.

A plot of

$$Vn=\exp(Ret) \tag{H15}$$

was run for a length of time. By varying the parameters and plotting this function enables the assessment of the effect of parameter variation on the decay of the voltage signal.

The analysis reveals that the real component (Re) decreased with increasing peripheral resistance. The time of decay thus increased in this case.

Scaling for different flow profiles at different heart rates results in a variation in the time constant. The decay time decreased with increasing heart rate which resulted in a slightly reduced voltage at large FHRs if the peripheral resistance and the compliance were maintained and the other parameters scaled according to the flow profile.

The major contributor to the time constant of decay was however the peripheral resistance which included the resistance of the upper carcass, the lower carcass, the aortic bleed offs and the placenta.

The response to short and long term FHR variations were examined.

LONG TERM FHR VARIATIONS:

The aim was to model the blood pressure as a constant magnitude for all FHRs. This was done by simply adjusting the peripheral

resistance as the heart rate was varied. Simulations revealed that for elevated placental resistances, the mean blood pressure was not maintained for all FHR's. The resistance and inertance of the aorta and common iliac artery were scaled according to the flow profile determined for each FHR. This scaling for flow profile variations plus an elevated placental resistance resulted in a decrease in the time constant of the system and lower "diastolic voltage" which in turn resulted in lower "systolic voltages". Lower mean voltages thus occurred.

SHORT TERM FHR VARIATIONS:

The peripheral resistances were maintained in these simulations. The time constant of the system was thus maintained which logically resulted in a larger blood pressure (voltage) at higher FHRs. This was simply due to the fact that at a large FHR the onset of the next heart beat occurred higher up on the decay slope of the stabilizing voltage.

APPENDIX I YOUNG'S MODULUS

The Young's modulus of an artery was needed in calculating the compliance of the artery wall. The Young's modulus is defined as

$$E=\Delta P r^2/h\Delta r \qquad (I1)$$

Knowledge of the radius of the artery during diastolic flow, the maximum radius of the artery during peak systolic flow, the wall thickness of the artery and the pulse pressure amplitude of the blood pressure waveform were required in order to determine this quantity. Δr is the change in radius due to a change in pressure.

Experimental data on these quantities for the foetal aorta was published by Struik et al (1992). No data was available for the umbilical arteries or the common iliac arteries. Radius and wall thickness for these arteries was thus measured from post mortem specimens.

Model 2, described in chapter 11, assumed that the mean blood pressure in the major arteries was constant. The blood pressure pulsatility required to calculate the Young's modulus was thus assumed to be the same for the aorta, the common iliac arteries and the umbilical arteries.

The change in the radius of the umbilical arteries and common iliac

arteries is unknown and depends on the elasticity of the artery walls. The change in radius was however assumed to be identical for these two arteries as their biological composition and their radii were similar. In order to estimate the range of Young's moduli magnitudes possible for these arteries, the change in radius was assumed to be a quarter that of the aorta as these arteries were approximately half the radius of the aorta. This was based on the following analysis :

$$C=\Delta Volume/\Delta Pressure=2\pi r^3 l(1-\sigma^2)/Eh \tag{I2}$$

$$Kr^3=\Delta V/\Delta P \tag{I3}$$

Area is defined as

$$A=\pi r^2 \tag{I4}$$

$$dA/dr=2\pi r \tag{I5}$$

Thus

$$\Delta A=\Delta R2\pi r \tag{I6}$$

Now

$$C=Kr^3=\Delta Al/\Delta P \tag{I7}$$

Thus

$$Kr^3=\Delta r 2\pi r l/\Delta P \tag{I8}$$

And

$$r^2 \propto \Delta r \tag{I9}$$

Thus if the radius of the aorta is twice the radius of the common iliac artery, the difference in the change in radius is 4 times.

As can be seen in the table, the Young's Moduli for the Aorta and Common Iliac arteries are arbitrarily chosen and fall within the maximum and minimum bounds. The Young's modulus for the umbilical arteries is chosen to be slightly less than the minimum value. This value produced accurate representations of the Umbilical FVW and is acceptable as far as modelling of the system is concerned. It has been shown that the pulsatility of a blood pressure waveform decreases as it moves away from to the heart. Physiologically this reduction in blood pressure pulsatility in these distal regions will result in a lower value for the Young's modulus. The selection of this lower value is thus acceptable.

Figure I1: Young's modulus estimations

YOUNG'S MODULUS ESTIMATES

FROM RESULTS PUBLISHED BY STRUIK ET AL 1992

AGE (weeks)	YOUNGS MODULUS (MINIMUM) dyne/cm^2	YOUNGS MODULUS (MAXIMUM) dyne/cm^2	YOUNGS MODULUS (SELECTED) dyne/cm^2
AORTA			
30	559000	1360000	850000
37	1170000	2300000	850000
38	689000	1700000	850000
40	487000	1380000	850000
COMMON ILIAC			
37	6060000	1.8E+07	8500000
UMBILICAL ARTERY			
36	1.674E+07	5E+07	1E+07

REFERENCES

ADAMSON SL, MORROW RJ, BULL SB, LANGILLE BL.

1989

Vasomotor responses of the umbilical circulation in fetal sheep.

American journal of physiology, 256:R1056-R1062.

ADAMSON SL, WHITELY KJ, LANGILLE BL.

1992

Pulsatile pressure-flow relations and pulse-wave propagation in the umbilical circulation of fetal sheep.

Circulation research, 70(4):761-772.

ALONSO JG, OKAI T, LONGO LD, GILBERT RD

1989

Cardiac function during long-term hypoxemia in fetal sheep.

American journal of physiology, 257:H581-589.

ASSALI NS, BEKEY GA, MORRISON LW.

1968

Fetal and neonatal circulation.

N.S.ASSALI, Acad. Press, New York and London.

BARNES AC.

1968

Intra-uterine development.

Lea and Feliger, Philadelphia.

BEARD RW. AND NATHANIELSZ PW.

1976

Fetal physiology and medicine.

2nd Edition. WB Saunders Company LTD. New York.

BRAR HS, PLATT LD.

1989

Antepartum improvement of abnormal umbilical artery velocimetry: does it occur ?

American journal of obstetrics and gynaecology, 160(1):36-39.

BUNN A.E.

1980

Theory and physiological applications of pressure waves in compliant tubes.

Doctorate thesis. Faculty of Medicine, University of Stellenbosch.

CAMPBELL S, VYAS S, NICOLAIDES KH.

1991

Doppler investigation of the fetal circulation.

Journal of perinatal medicine, 19:21-26.

CHEN HY, CHANG FM, HUANG HC, HSEIH FJ, LU CC.

1988

Antenatal fetal blood flow in the descending aorta and in the umbilical vein and their ratio in normal pregnancy.

Ultrasound in medicine and biology, 14(14):263-268.

CHUDLEIGH P AND PEARCE MJ.

1986

Obstetric ultrasound, how, why, when ?

Edinburgh : Churchill Livingstone.

COHN HE, PIASECKI GJ, JACKSON BT.

1980

The effect of fetal heart rate on cardiovascular function during hypoxemia.

American journal of obstetrics and gynaecology, 138(8):1190-1199.

CREASY RK AND RESNIK R.

1989

Maternal-fetal medicine.

2nd Edition. Philadelphia, Saunders.

DANFORTH D.

1977

Obstetrics and gynaecology.

3rd Edition, Harper and Row, New York.

DAWES GS.

1968

Fetal and neonatal physiology.

Year Book Medical Publishers, Inc., Chicago.

DAWES GS, DUNCAN SL, LEWIS BV, MERLET CL, OWEN-THOMAS TB, REEVES JT.

1969a

Hypoxaemia and aortic chemoreceptor function in fetal lambs.

Journal of physiology, 201(1):105-116.

DAWES GS, DUNCAN SL, LEWIS BV, MERLET CL, OWEN-THOMAS TB, REEVES JT.

1969b

Cyanide stimulation of the systemic arterial chemoreceptors in fetal lambs.

Journal of physiology, 201(1):117-128.

DEMULDER X, FOWAN JC, BARD H, RIOPEL L, LERFER H.

1984

The difference between the systolic time intervals of the left and right ventricles during fetal life.

American journal of obstetrics and gynaecology, 149(7):737-40.

DOWNING GJ, YARLAGADDA P, MAULIK D.

1991

Effects of acute hypoxaemia on umbilical arterial doppler indices in a fetal ovine model.

Early human development, 25:1-10.

GILES WB, LANGMAN G, MARSAL K, TRUDINGER BJ.

1986

Fetal volume blood flow and umbilical artery flow velocity waveform analysis : A comparison.

British journal of obstetrics and gynaecology, 93(5):461-465.

GILL RW, TRUDINGER BJ, GARRETT WJ, KOSSOFF G, WARREN PS.

1981

Fetal umbilical venous flow measured in utero by pulsed doppler and b-mode ultrasound.

American journal of obstetrics and gynaecology, 130(6):720-725.

GOODLIN RC, GIRARD J, HOLLMEN A.

1972

Systolic time intervals in the fetus and neonate.

Obstetrics and gynaecology, 39(2):295-303.

HIBBARD BM.

1988

Principles of obstetrics.

London, Butterworths.

HOSKINS PR, LOUPAS T, McDICKEN WN.

1991

An investigation of the simulated umbilical artery doppler waveforms.

Ultrasound in medicine and biology, parts 1-3, 17(1):7-22,23-30,703-708.

HOWARD RB, HOSKOWAWA T, MAGUIRE MH.

1987

Hypoxia-induced fetoplacental vasoconstriction in perfused human placental cotyledons.

American journal of obstetrics and gynaecology, 157(5):1261-1266.

HYTTEN F, CHAMBERLAIN G.

1991

Clinical physiology in obstetrics

2nd Edition. Blackwell Scientific Publications. London

JENSEN A, ROMAN C, RUDOLPH AM.

1991

Effects of reducing uterine blood flow on fetal blood flow distribution and oxygen delivery.

Journal of developmental physiology, 15:309-323.

JENSEN A, BERGER R.

1992

Fetal circulatory responses to oxygen lack.

Journal of developmental physiology, 16:181-207.

JOHNSTONE FD, HADDAD NG, HOSKINS P, McDICKEN W, CHAMBERS S, MUIR B.

1988

Umbilical artery doppler velocity waveform: the outcome of pregnancies with absent end diastolic flow.

European journal of obstetrics and gynaecology and reproductive biology, 28:171-178.

KALUZYNSKI K, PALKO T.

1993

Effect of method and parameters of spectral analysis on selected indices of simulated doppler spectra.

Medicine and biological engineering and computing, 31:249-256.

KITANAKA T, ALONSO JG, GILBERT RD, SIU BL, CLEMONS GK, LONGO LD.

1989

Fetal responses to long-term hypoxemia in sheep.

American journal of physiology, 256:R1348-R1354.

KOOS BJ, SAMESHIMA H, POWER GG.

1987

Fetal breathing, sleep state, and cardiovascular responses to graded hypoxia in sheep.

Journal of applied physiology, 62(3):1033-1039.

KUNZEL W.

1986

Fetal shock syndrome.

Z Geburtshilfe perinatol, 190(5):177-184.

LAMPE LG, VOJCEK L, PRINCZKEL E, CSOMAR S.

1988

Blood flow redistribution during isocapnic hypoxia in fetal lamb.

Acta physio hung, 71:529-34.

LIEDTKE AJ, URSCHEL CW, KIRK ES.

1973

Total systemic autoregulation in the dog and its inhibition by baroreceptor reflex.

Circulation research, 32:465-470.

LOW JA.

1991

The current status of maternal and fetal blood flow velocimetry.

American journal of obstetrics and gynaecology, 164:1049-1063.

MAKOWSKI EL, MESCHIA G, DROEGEMUELLER W, BATTAGLIA FC.

1968

Measurements of umbilical arterial blood flow to the sheep placenta and fetus in utero.

Circulation research, 23:623-631.

MASSEY BS.

1976

Mechanics of fluids.

3rd Edition. William Clowes and Sons LTD. London.

MAULIK D.

1989

Basic principles of doppler ultrasound as applied in obstetrics.

Clinical obstetrics and gynaecology, 32(4):628-643.

McCOWAN LM, MULLEN BM, RITCHIE K.

1987

Umbilical artery flow velocity waveforms and the placental vascular bed.

American journal of obstetrics and gynaecology, 157(4):900-902.

McDONALD DA.

1974

Blood flow in arteries.

2nd Edition. The Camelot Press LTD., Southampton.

MEHALEK KE, ROSENBERG J, BERKOWITZ GS, CHITKARA U, BERKOWITZ RL.

1989

Umbilical and uterine artery flow velocity waveforms.

Journal of ultrasound in medicine, 8:171-176.

MO LY, BASCOM PAJ, RITCHIE K, McCOWAN LME.

1988

A transmission line modelling approach to the interpretation of uterine doppler waveforms.

Ultrasound in medicine and biology, 14(5):365-376.

MORROW RJ, ADAMSON SL, SHELLEY BB, RITCHIE K.

1989

Effect of placental embolization on the umbilical arterial velocity waveform in fetal sheep.

American journal of obstetrics and gynaecology, 161:1055-1060.

MUIJSERS GJ, HASAART TH, VAN HUISSELING H, DE HAAN J.

1990a

The response of the umbilical artery pulsatility index in the fetal sheep to acute and prolonged hypoxemia and acidemia induced by embolization of the uterine microcirculation.

Journal of developmental physiology, 13(4):231-236.

MUIJSERS GJ, HASAART TH, RUISSEN CJ, VAN HUISSELING H, PEETERS LL.

1990b

The response of the umbilical and femoral artery pulsatility indices in fetal sheep to progressively reduced uteroplacental blood flow.

Journal of developmental physiology, 13(4):215-221.

MUIJSERS GJ, VAN HUISSELING H, HASAART THM.

1991

The effect of selective umbilical embolization on the common umbilical artery pulsatility index and umbilical vascular resistance in fetal sheep.

Journal of developmental physiology, 15:259-267.

MUIJSERS GJ, VAN HUISSELING H, HASAART TH.

1993

The effect of maternal hypoxaemia on the umbilical and femoral artery blood flow velocity waveforms and the relationship with mean arterial pressure in fetal sheep.

Gynaecological and obstetric investigation, 35(1):1-6.

MULDERS LG, MUIJERS GJ, JONGSMA HW, NIJHUIS JG, HEIN PR.

1986

The umbilical artery blood flow velocity waveform in relation to fetal breathing movement, fetal heart rate and fetal behavioral states in normal pregnancy at 37 to 39 weeks.

Early human development, 14:283-93.

MURATA Y, MARTIN CB.

1974

Systolic time intervals of the fetal cardiac cycle.

Obstetrics and gynaecology, 44(2):224-232.

NEWNHAM J, PETTERSON L, JAMES I, REID S.

1990

The effect of heart rate on doppler flow velocity systolic-diastolic ratios in the umbilical and uteroplacental arterial waveforms.

Early human development, 21:21-29.

OUNSTED C.

1973

On fetal growth rate.

London, Heinemann.

PARER JT.

1983

The influence of beta-adrenergic activity on fetal heart rate and the umbilical circulation during hypoxia in fetal sheep.

American journal of obstetrics and gynaecology, 147(5):592-597.

PATTINSON RC, THERON GB, THOMPSON ML, LAI TUNG M.

1989

Doppler ultrasonography of the fetoplacental circulation - normal reference values.

South African medical journal, 76:623-625.

PATTINSON RC, BRINK AL, DE WET PE, ODENDAAL HJ.

1991

Early detection of poor fetal prognosis by serial doppler velocimetry in high risk pregnancies.

South African medical journal, 80:428-430.

PAULICK RP, KASTENDIECK E, WETH B, WERNZE H.

1987

Metabolic, cardiovascular and sympathoadrenal reactions of the fetus to progressive hypoxia-animal experiment studies.

Z Geburtshilfe perinatol, 191(4):130-139.

PAULICK RP, MEYERS RL, RUDOLPH AM.

1991

Vascular responses of umbilical-placental circulation to vasodilators in fetal lambs.

American journal of physiology, 261:h9-h14.

POLIN RA AND FOX WW.

1992

Fetal and neonatal physiology.

WB Saunders Company. London.

PURVES JT, BISCOE TJ.

1966

Development of chemoreceptor activity.

British medical bulletin, 22(1):56

REED KL, MEIJBOOM EJ, SAHN DJ, SCAGNELLI SA, VALDES-CRUZ LM, SHENKER L.

1986

Cardiac doppler flow velocities in human fetuses.

CIRCULATION, 73(1):41-46.

RICHARDSON BS.

1992

The effect of behavioral state on fetal metabolism and blood flow circulation.

Seminars in perinatology, 16(4):227-233.

ROCHELSON B.

1989

The clinical significance of absent end-diastolic velocity in the umbilical artery waveforms.

Clinical obstetrics and gynaecology, 32(4):692-701.

RUDOLPH AM, HEYMANN MA.

1967

The circulation of the fetus in utero: methods for studying distribution of blood flow , cardiac output and organ blood flow.

Circulation research, 21(2):163-184.

RUDOLPH AM.

1970a

The changes in the circulation after birth.

Circulation, 41:343-359.

RUDOLPH AM, HEYMANN MA.

1970b

Circulatory changes during growth in the fetal lamb.

Circulation research, xxvi:289-299.

SAGAWA K, EISNER A.

1975

Static pressure-flow relation in the total systemic vascular bed of the dog and its modification by the baroreceptor reflex.

Circulation research, 36:406-413.

STRUIK PC, WLADIMIROFF JW, HOP WCJ, SIMONAZZI E.

1992

Pulse pressure assessment in the human fetal descending aorta.

Ultrasound in medicine and biology, 18(1):39-43.

SZENTKUTI A, CAPPER WL, NORMAN K, WRIGHT AW, ODENDAAL H.

1993

The high resistance state index: a new method to assess foetal compromise in absent diastolic umbilical arterial flow.

Journal of maternal-foetal investigation, 3(3):177.

THOMPSON RS, TRUDINGER BJ, COOK CM.

1986

A comparison of doppler ultrasound waveform indices in the umbilical artery - indices derived from the maximum velocity waveform.

Ultrasound in medicine and biology, 12(11):835-844.

THOMPSON RS.

1987

Blood flow velocity waveforms.

Seminars in perinatology, 11(4):300-310.

THOMPSON RS, STEVENS RJ.

1989

Mathematical model for interpretation of doppler velocity waveform indices.

Medicine and biological engineering and computing, 27:269-276.

THOMPSON RS, TRUDINGER BJ.

1990

Doppler waveform pulsatility index and resistance, pressure and flow in the umbilical placental circulation: an investigation using a mathematical model.

Ultrasound in medicine and biology, 16(5):449-458.

TRUDINGER BJ, STEVENS D, CONNELLY A, HALES JRS, ALEXANDER G, BRADLEY L, FAWCETT A, THOMPSON RS.

1987a

Umbilical artery flow velocity waveforms and placental resistance: the effects of embolization of the umbilical circulation.

American journal of obstetrics and gynaecology, 157:1443-1448.

TRUDINGER BJ.

1987b

The umbilical circulation.

Seminars in perinatology, 11(4):311-321.

VETH AFL.

1976

Modelling the foetal circulation.

Institute of Medical Physics Tno. Netherlands.